Advanced drug delivery systems to enhance topical oromucosal administration of therapeutic agents

Tyagi, Vasundhara

UNIVERSITÉ DE GENÈVE
Section de Sciences Pharmaceutiques
Laboratoire de Biochimie Pharmaceutique

FACULTÉ DES SCIENCES
Professeur Yogeshvar N. Kalia

Advanced drug delivery systems to enhance topical oromucosal administration of therapeutic agents

THÈSE

présentée à la Faculté des sciences de l'Université de Genève pour obtenir le grade de
Docteur ès sciences, mention sciences pharmaceutiques

par

Vasundhara Tyagi
de
Delhi (INDE)

These N°: 5418

Genève
Atelier de reproduction Repromail
2019

UNIVERSITÉ
DE GENÈVE
FACULTÉ DES SCIENCES

DOCTORAT ÈS SCIENCES
MENTION SCIENCES PHARMACEUTIQUES

Thèse de Madame Vasundhara TYAGI

intitulée :

«Advanced Drug Delivery Systems to Enhance Topical Oromucosal Administration of Therapeutic Agents»

La Faculté des sciences, sur le préavis de Monsieur Y. KALIA, professeur associé et directeur de thèse (Section des sciences pharmaceutiques), Monsieur O. JORDAN, docteur (Section des sciences pharmaceutiques), Madame S. NICOLI, professeure (Department of Food and Drug Sciences, University of Parma, Italia), Madame V. SUTER, docteure (Station für Zahnärztliche Radiologie und Stomatologie, Klinik für Oralchirurgie und Stomatologie, Bern, Schweiz), autorise l'impression de la présente thèse, sans exprimer d'opinion sur les propositions qui y sont énoncées.

Genève, le 12 décembre 2019

Thèse - 5418 -

Le Décanat

N.B. - La thèse doit porter la déclaration précédente et remplir les conditions énumérées dans les "Informations relatives aux thèses de doctorat à l'Université de Genève".

If it's both terrifying and amazing then you should definitely pursue it
-Erada

Yesterday I was clever, so I wanted to change the world. Today I am wise, so I am changing myself
-Rumi

Dedicated to my loving parents – my father, Ramavtar Singh Tyagi, and my mother, Sunita Tyagi

Contents

Résumé

L'administration topique de médicaments sur la muqueuse buccale pour les maladies locales offre l'avantage d'augmenter la biodisponibilité du médicament sur la cible par rapport à une administration systémique. Par conséquent, atteindre la bonne concentration thérapeutique améliorerait la réponse thérapeutique résultante. Cependant, la fonction protectrice de la muqueuse buccale pose un défi important à une administration topique efficace. Des techniques d'administration telles que l'iontophorèse et une nouvelle formulation pourraient aider à surmonter cette barrière et à améliorer la pharmacothérapie.

Le but de cette thèse est d'étudier l'administration ciblé dans la muqueuse buccale de (i) petites molécules hydrophiles et d'un anticorps en utilisant l'iontophorèse (ii) de médicaments faiblement solubles dans l'eau utilisant des nanovecteurs polymères.

Le chapitre 1 commence par une introduction à la structure et à la composition de la formidable barrière muqueuse buccale et à une discussion sur l'état actuel des recherches sur la technique d'amélioration physique (iontophorèse) et chimique (micelles polymériques). Le chapitre 2 étudie l'effet de l'iontophorèse à courant constant sur l'administration et la biodistribution d'une petite molécule, le chlorhydrate de buflomédil (BUF) dans la muqueuse buccale, dans le cadre du traitement de la fibrose sous-muqueuse buccale. La quantification de BUF a été réalisée par UHPLC-MS / MS; en plus de la libération totale, les quantités présentes dans les épithéliums et dans la lamina propria (le tissu cible) ont également été déterminées. Des cellules de diffusion verticale à deux compartiments ont été utilisées pour étudier les effets de la densité de courant (0,5, 1 et 2 mA / cm^2), du temps d'application (5, 10 et 20 min) et de la concentration (5, 10 et 20 mM) sur la libération par iontophorèse de BUF de solutions aqueuses. Contrairement à la délivrance passive, une iontophorèse de 10 minutes à 1 mA / cm2 a entraîné un transport statistiquement équivalent d'une solution à 20 mM et d'un hydrogel HEC à 2% (avec une charge équivalente en BUF; 20 µmol). La livraison de BUF à partir de l'hydrogel à l'aide de cellules de diffusion et une nouvelle configuration coplanaire «côte à côte» étaient statistiquement équivalentes (304,2 ± 28,9 et 278,2 ± 40,3

µg/cm^2) - la délivrance passive était également similaire. L'ionophorèse (10 min à 1 mA/cm^2) avec un film mince (20 µmol de BUF) était supérieure au contrôle passif (323,3 ± 5,9 et 24,8 ± 5,9 µg/cm^2). Les concentrations dans la LP étaient environ 700 fois supérieures à la CI50 pour bloquer la production de collagène, offrant potentiellement une nouvelle stratégie thérapeutique pour la fibrose sous-muqueuse buccale.

Suite à ces résultats prometteurs, au chapitre 2, l'administration simultanée par iontophorèse de BUF et d'un corticostéroïde, le phosphate de dexaméthasone (Dex-P) a été étudiée pour le traitement de la fibrose sous-muqueuse buccale. Une nouvelle installation pour étudier l'administration par iontophorèse des deux médicaments à charges opposées a été conçue en interne. Les compartiments donneurs ont été conçus de manière concentrique et les médicaments administrés ont été quantifiées séparément dans tous les compartiments en utilisant les méthodes UHPLC-MS / MS et UHPLC-UV. Un courant constant de 3,0 mA (0,6 mA/cm^2 pour le BUF et 1,95 mA/cm^2 pour le Dex-P) a été appliqué sur la muqueuse œsophagienne de porc pendant 5, 10 et 20 minutes. Par rapport au contrôle passif, 5 minutes d'électrotransport ont augmenté le débit total de i) BUF de 29,8 ± 5,1 nmol/cm^2 à 194,3 ± 23,8 nmol/cm^2 ii) et de Dex-P de 29,4 ± 1,2 nmol / cm2 à 193,3 ± 19,8 nmol/cm^2. Les données de biodistribution fournies par la mise en place ont révélées que l'iontophorèse augmentait les quantités de médicaments administrés ainsi que leur degré de migration. En l'absence de courant, Dex-P n'a pas pu migrer latéralement vers une zone voisine et n'a été détecté que sous sa propre zone d'application. 5 minutes d'application de courant électrique ont augmenté la distribution de Dex-P de plus de 5 fois dans sa propre zone d'application et de 8 fois dans la zone voisine. De même, l'administration de BUF a été améliorée d'environ 6,8 fois sous la zone où elle a été appliquée et d'environ 12,8 fois dans la zone d'application de Dex-P. En raison de la nature permsélective de la membrane muqueuse au pH physiologique, l'efficacité de l'administration iontophorétique d'un cation (BUF) était meilleure que celle de l'anion (Dex-P). L'iontophorèse globale a permis l'administration des deux médicaments à une concentration thérapeutiquement pertinente en un temps d'application rapide de 5 min. De plus, l'iontophorèse offrait la possibilité d'administrer des agents thérapeutiques par voie régiosélective

et de contrôler leur cinétique de d'administration. Une administration iontophorétique de courte durée de plusieurs agents thérapeutiques simultanément à la muqueuse peut augmenter leur biodisponibilité dans la région et constituer une option de traitement adaptée aux patients pour la fibrose sous-muqueuse buccale.

L'objectif du chapitre 3 était d'étudier la possibilité d'utiliser l'iontophorèse pour administrer le rituximab (RTX), un anticorps chimérique monoclonal (poids moléculaire: 145 kDa) à la muqueuse pour le traitement du pemphigus vulgaris par voie orale. L'administration topique d'anticorps pour les maladies localisées est une alternative efficace aux injections intraveineuses invasives, car elles sont peu chères et peuvent minimiser les risque d'effets secondaires. Les deux cibles locales et régionales pour la diffusion thématique de RTX ont été reconnues comme étant la lamina propria où l'infiltration immunitaire suggérée se produit et les ganglions lymphatiques sous-maxillaires où le flux lymphatique de la muqueuse buccale est drainé. La technique ELISA en sandwich a été développée pour quantifier RTX dans des échantillons de muqueuse après des études de d'administration in vitro. Après la fin des expériences, la muqueuse a été sectionnée finement en lamelles de 40 microns pour étudier le degré de pénétration et la distribution de l'anticorps dans la muqueuse. Après l'application passive de RTX à 1 mg / ml (dans un tampon MES, pH = 7) pendant 10 minutes, la déposition d'anticorps était médiocre; 0,47 ± 0,05 $\mu g/cm^2$ de RTX s'est déposé dans la muqueuse. La RTX ne pouvait pas pénétrer à travers la muqueuse. L'application d'une densité de courant de 1,5 mA/cm^2 pendant 10 minutes a permis d'améliorer les quantités de RTX déposées dans la muqueuse plus de 5 fois (2,2 ± 0,1 $\mu g/cm^2$). Les quantités de RTX administrées et son degré de pénétration dans les couches ultérieures de la muqueuse ont augmenté linéairement avec l'augmentation de la durée de l'application en cours. Les données de biodistribution de RTX ont confirmé que des concentrations supérieures à la CE_{50} de RTX avaient été atteintes en moins de 10 minutes dans la lamina propria. Comparée au transport passif où la déposition était superficielle, l'iontophorèse était capable de déposer RTX à travers la muqueuse. Après 2 h de transport iontophorétique, 1,5 ± 0,6 $\mu g/cm^2$ de RTX pourrait traverser la muqueuse, atteignant potentiellement la cible régionale. Le mécanisme de l'électrotransport s'est révélé être l'électroosmose. On s'attendait à ce que les anticorps de très haut poids moléculaire ne puissent rivaliser

pour porter la charge électrique, ils agissent alors comme des molécules neutres dont la déposition est fonction de la nature anionique de la muqueuse. Une corrélation a été trouvée entre la distribution de charge en surface de l'anticorps et son électrotransport. Il a été conclu que l'iontophorèse pouvait améliorer avec succès la cinétique de l'administration de RTX. En moins de 10 minutes, l'iontophorèse permettait l'administration de RTX à la cible locale et en 2 heures à la cible régionale à des concentrations thérapeutiquement pertinentes.

La dernière partie de la thèse aborde un nouveau défi: la distribution de médicaments peu solubles dans l'eau. Le chapitre 4 visait à mettre au point des formulations de micelles polymères de solutions aqueuses / hydrogel à base de copolymère di-séquencé de succinate de poly (éthylèneglycol) D-α-tocophérol et d'acétonide de triamcinolone (TA) et de fluocinonide (FLU), et à étudier leur capacité à administrer du TA / FLU à la jonction épithélium-lamina propria de la muqueuse et la comparer aux produits commercialisés. La solubilité aqueuse de TA et de FLU a été augmentée de 35 fois et 26 fois, respectivement. Dans une comparaison comparative directe, l'apport total en AT après application de Kenacort® A Orabase® (0,1%) et d'hydrogel micellaire (0,1%) pendant 60 minutes était de 242,1 ± 68,5 et de 5936,7 ± 1269,6 ng/cm^2, respectivement. La libération totale de FLU après application de Novoter (0,05%) et d'hydrogel micellaire (0,05%) pendant 60 min était respectivement de 617,1 ± 126,5 et 2580,0 ± 285,5 ng/cm^2. L'étude de biodistribution a révélé que l'application d'hydrogel micellaire occlus TA / FLU pendant 30 minutes avait entraîné un dépôt de 117,0 ± 15,6 ng/cm^2 et de 225,6 ± 36,7 ng/cm^2 de TA et de FLU, respectivement, dans la zone thérapeutique ciblée. Les quantités de TA et de FLU déposées après l'application de Kenacort® A Orabase® et de Novoter étaient inférieures à la limite de quantification. Les résultats indiquent que les micelles de copolymère TPGS sont des nanoporteurs très efficaces pour l'administration topique de TA et de FLU par la muqueuse et peuvent améliorer le traitement des PLO.

Summary

Topical drug delivery to the buccal mucosa for locally occurring diseases offers the advantage of increasing drug bioavailability at the target site over systemic administration. Consequently, attaining the right therapeutic concentration would improve the resulting therapeutic response. However, the protective function of buccal mucosa poses a significant challenge to an efficient topical delivery. Delivery techniques like iontophoresis and novel formulation could assist to overcome this barrier and improve the pharmacotherapy.

The aim of this thesis was to investigate the targeted buccal mucosal delivery of (i) hydrophilic small molecules and an antibody by using iontophoresis (ii) poorly water-soluble drugs using polymeric nanocarriers.

Chapter 1 begins with an introduction to the structure and composition of the formidable barrier – buccal mucosa and a discussion into the current state of research of the physical (iontophoresis) and chemical (polymeric micelles) enhancement technique. **Chapter 2** investigates the effect of constant current iontophoresis on the delivery and biodistribution of a small molecule, buflomedil hydrochloride (BUF) in the buccal mucosa for the management of oral submucous fibrosis. Quantification of BUF was performed by UHPLC-MS/MS; in addition to total delivery, the amounts present in the epithelia and the lamina propria (the target tissue) were also determined. Two-compartment vertical diffusion cells were used to investigate the effect of current density (0.5, 1 and 2 mA/cm^2), application time (5, 10 and 20 min) and concentration (5, 10 and 20 mM) on iontophoretic delivery of BUF from aqueous solutions. In contrast to passive delivery, iontophoresis for 10 min at 1 mA/cm^2 resulted in statistically equivalent transport from a 20 mM solution and a 2% HEC hydrogel (with equivalent BUF loading; 20 µmol). BUF delivery from the hydrogel using diffusion cells and a new coplanar "side-by-side" set-up was statistically equivalent (304.2 ± 28.9 and 278.2 ± 40.3 µg/cm^2) - passive delivery was also similar. Iontophoresis (10 min at 1 mA/cm^2) using a thin film (20 µmol BUF) was superior to the passive control (323.3 ± 5.9 and 24.8 ± 5.9 µg/cm^2). Concentrations

in the LP were ~700-fold > IC_{50} to block collagen production, potentially providing a new therapeutic strategy for oral submucous fibrosis.

Following these promising results, in **Chapter 2** simultaneous iontophoretic delivery of BUF and a corticosteroid, dexamethasone phosphate (Dex-P) was studied for the management of oral submucous fibrosis. A novel set-up for studying iontophoretic delivery of the two oppositely charged drugs was designed in house. The donor compartments were devised concentrically and deliveries of the drugs were quantified in all the different compartments separately using UHPLC-MS/MS and UHPLC-UV methods. A constant current of 3.0 mA (0.6 mA/cm^2 for BUF and 1.95 mA/cm^2 for Dex-P) was applied to porcine esophageal mucosa for 5, 10 and 20 minutes. Compared to passive control, 5 mins of electrotransport increased the total delivery of i) BUF from 29.8 ± 5.1 nmol/cm^2 to 194.3 ± 23.8 nmol/cm^2 ii) and Dex-P from 29.4 ± 1.2 nmol/cm^2 to 193.3 ± 19.8 nmol/cm^2. The biodistribution data offered by the set-up revealed that iontophoresis enhanced the amounts of drugs delivered as well as their extent of migration. In the absence of current, Dex-P was unable to migrate laterally to any neighbouring area and was found only under its own application area. 5 minutes of current application increased the delivery of Dex-P by over 5 folds in its own application area and over 8 folds in the neighbouring area. Similarly, the delivery of BUF was enhanced ~ 6.8 folds under the area where it was applied and ~ 12.8 folds in the area where Dex-P was applied. Due to the permselective nature of the mucosal membrane at physiological pH, iontophoretic delivery efficiency of a cation (BUF) was better than the anion (Dex-P). Overall iontophoresis afforded the delivery of the two drugs at therapeutically relevant concentration in a rapid application time of 5 min. Moreover, iontophoresis provided a possibility to regioselectively deliver therapeutic agents and control their delivery kinetics. Short duration iontophoretic delivery of multiple therapeutic agents simultaneously to the mucosa may increase their bioavailability in the area and present a patient friendly treatment option for oral submucous fibrosis.

The objective of **Chapter 3** was to investigate the feasibility of using iontophoresis to deliver rituximab (RTX), a monoclonal chimeric antibody (molecular weight: 145 kDa) to the mucosa for the management

of oral pemphigus vulgaris. Topical delivery of antibody for localized diseases is an effective alternative to invasive intravenous injections because they are cost effective and can minimize the risk of side effects. The two local and regional targets for the topical delivery of RTX were recognized as the lamina propria where the suggested immune infiltration occurs, and the submandibular lymph nodes, where the lymphatic flow from buccal mucosa is drained, respectively. Sandwich ELISA technique was developed to quantify RTX in mucosal samples after in vitro delivery studies. After the end of the experiments, mucosa was finely sectioned in 40 microns lamellae to study the extent of penetration and distribution of the antibody in the mucosa. After the passive application of 1 mg/ml RTX (in MES buffer, pH = 7) for 10 min, the delivery of antibody was poor; 0.47 ± 0.05 μg/cm^2 of RTX was deposited in the mucosa. RTX could not permeate across the mucosa.Application of 1.5 mA/cm2 current density for 10 min improved the amounts of RTX deposited in the mucosa over 5 times (2.2 ± 0.1 μg/cm^2). Amounts of RTX delivered and its extent of penetration in the subsequent layers of the mucosa increased linearly with the increase in the duration of current application. Biodistribution data of RTX confirmed that concentrations above the EC_{50} of RTX where achieved in less than 10 min in the lamina propria. Compared to passive transport where the delivery was superficial, iontophoresis was able to deliver RTX across the mucosa. After 2 h of iontophoretic transport 1.5 ± 0.6 μg/cm^2 RTX could permeate through the mucosa potentially reaching the regional target. The mechanism of electrotransport was found to be electroosmosis. It was expected since very high molecular weight antibodies cannot compete to carry the electric charge, they act like neutral molecules whose delivery is a function of the anionic nature of the mucosa. A correlation was found between the surface charge distribution of the antibody and its electrotransport. It was concluded that iontophoresis can successfully improve the delivery kinetics of RTX. In a practical time of less than 10 min, iontophoresis enabled the delivery of RTX to the local target and in 2 h at the regional target at therapeutically relevant concentrations.

The final part of the thesis deals with a new challenge: delivery of poorly water soluble drugs. The aims of **Chapter 4** were to develop aqueous solution/ hydrogel polymeric micelle formulations using D-α-

tocopheryl polyethylene glycol succinate di-block copolymer of triamcinolone acetonide (TA) and fluocinonide (FLU), and to investigate their ability to delivery of TA/FLU to the epithelium-lamina propria junction of the mucosa and compare it to marketed products. The aqueous solubility of TA and FLU was increased by 35-fold and 26- fold , respectively. In a 'head to head' comparison, the total delivery of TA after application of Kenacort® A Orabase® (0.1%) and micellar hydrogel (0.1%) for 60 min was 242.1 ± 68.5 and 5936.7 ± 1269.6 ng/cm^2, respectively. Total delivery of FLU after application of Novoter (0.05%) and micellar hydrogel (0.05%) for60 min of was 617.1 ± 126.5 and 2580.0 ± 285.5 ng/cm^2, respectively. The biodistribution study revealed that application of occluded TA/FLU micelle hydrogel for 30 min resulted in deposition of 117.0 ± 15.6 ng/cm^2 and 225.6 ± 36.7 ng/cm^2 for TA and FLU, respectively, in the target therapeutic area. The amounts of TA and FLU deposited after application of Kenacort® A Orabase® and Novoter were below the LOQ. Results indicate that TPGS copolymer micelles are highly efficient nanocarriers for topical mucosal delivery of TA and FLU and can improve the therapy of OLP.

INTRODUCTION

Topical administration of drugs into the oral cavity to treat locally occurring oral diseases is a logical alternative to the systemic route. In addition to shielding the drug from the highly acidic gastrointestinal environment, a topical administration will improve the local bioavailability of the drug leading to a better therapeutic response. Due to the accessibility of oral mucosa, a topical administration will also be convenient for the patients to apply and in case of an adverse event; drug formulation can be immediately removed from the body. However, effective topical drug delivery, which means delivering a therapeutic molecule at therapeutically relevant concentrations at the target site in a short time, is a challenge. Sometimes known as the gatekeeper, the buccal mucosa acts as a formidable barrier to all exogenous substances.

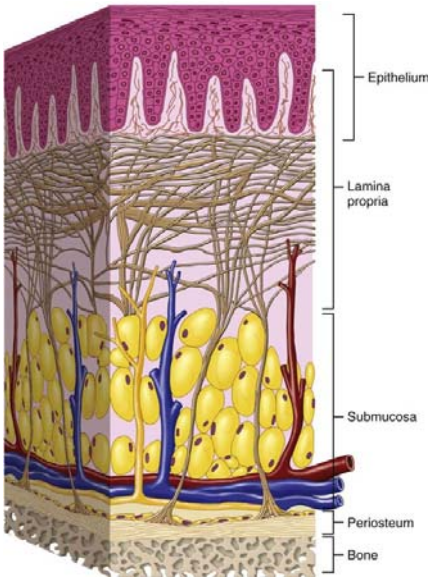

Figure 1. Schematic of the buccal mucosa. Adapted with permission from [1]

The buccal mucosa is composed of an outer most non-keratinized stratified squamous epithelium, below which lies the basement membrane followed by the lamina propria and at the bottom is the submucosa attached to the bone [1] (**Figure 1**). The junction between the epithelium and the lamina propria is more distinct than the lamina propria and the submucosa. The non-keratinized nature of the epithelium provides flexibility and elasticity that allows mastication and speaking with ease. The

primary function of the epithelium is to protect the organism from any foreign physical, chemical or microbial invasion [2]. The protective character of the buccal mucosa is moderated by the presence of lymphocytes and other immune competent cells within the epithelium-lamina propria junction, lamina propria and in the submucosa. The non-keratinized epithelium in the buccal mucosa is composed of 40 to 50 layers of tightly packed stratified squamous cells. It is divided in three layers: the topmost stratum distendum followed by stratum filamentosum and stratum basale. The buccal mucosa is a self-replenishing membrane – the bottom basal cell layer is mitotically active where epithelial cells are produced, which upon maturation migrate to the surface. As they migrate, the cells increase in size and flatten, with a cross-linked protein envelope while retaining their nuclei and other organelles. The turnover time for buccal epithelium is approximately 14 days [2, 3]. The barrier property of the buccal mucosa is attributed primarily to the epithelium. At the epithelial level, the upper one third contains membrane coating granules (MSG), that upon fusion with the plasma membrane secrete their content in the intercellular spaces, which maintains the epithelial cohesion [4]. Unlike skin or keratinized buccal epithelium, these secreted lipids are not arranged in lamellae [5]. This intercellular material is known to limit the permeation of molecules within the mucosa especially hydrophilic molecules [4, 6].

The lamina propria acts as a connective tissue to support the epithelium. It is highly vascularized and is composed of cells like – fibroblasts and mast cells, neural elements and support fibres which are held together in an amorphous ground structure [7]. The lamina propria can be divided in two parts: the topmost papillary layer and the reticular layer. The papillary layer is situated right under the epithelium and contains loosely organized thin collagen fibers. The papillary layer also contains nerve endings, which can extend to the epithelium. The reticular layers contains bundles of collagen fibers which are more organized than the papillary layer and are arranged parallel to the plane of the surface [8]. The reticular layer also constitutes major salivary glands (parotid, parietal and sublingual glands), minor salivary glands and sebaceous follicles.

The surface of the mucosa is constantly lubricated with saliva at a flow rate of 0.3-0.4 ml/min [9]. Saliva contains antimicrobial agents, enzymes and antibodies that play a significant role in the protection of the intraoral structures.

For all foreign substances including drug molecules, it is difficult to cross a healthy mucosal barrier. To topically treat a local buccal disease by an active pharmaceutical ingredient, there is a need to develop delivery strategies to overcome the biological barrier to ensure the therapeutic molecule can reach the target site at a relevant concentration to produce a therapeutic response.

1.1 **Part 1: Physical enhancement technique – *Iontophoresis***

In the last 20-30 years there has been an elevated interest in studying physical enhancement techniques like iontophoresis to improve the delivery kinetics of water-soluble drugs in and across the mucosa [10]. Iontophoresis is an active enhancement technique that leverages mild electrical potentials to deliver hydro soluble drugs into the mucosa (**Figure 2**). The technique has been used extensively to deliver drugs in and across skin, eye and the mucosa [11-14]. The amount of compound delivered in the biological membrane is proportional to the amount of charge passed, the applied current density, duration of current application and the area of the membrane in contact with the active electrode. The resulting iontophoretic flux is a sum of the two principle mechanisms: electromigration and electroosmosis; accompanied by a passive diffusion. Electromigration is the ordered movement of charged ions under the influence of an applied electrical field. The electromigratory flux is directly proportional to the current applied and related by Faraday's constant (F). The flux is inversely proportional to the thickness of the membrane [15]. This mechanism is responsible for majority of the electrotransport of ionic small molecules. **Chapter 1 and 2** will focus on to investigate the electrically assisted local delivery of a vasodilator buflomedil hydrochloride (BUF) and a corticosteroid dexamethasone disodium phosphate (Dex-P) in the mucosa for the treatment of oral submucous fibrosis.

Mucosa has a pI of 3.0, which means at a physiological pH 6.5-7.0 mucosa is cation permselective; mucosa favours the flow of cations, which try to neutralize the membrane [14].

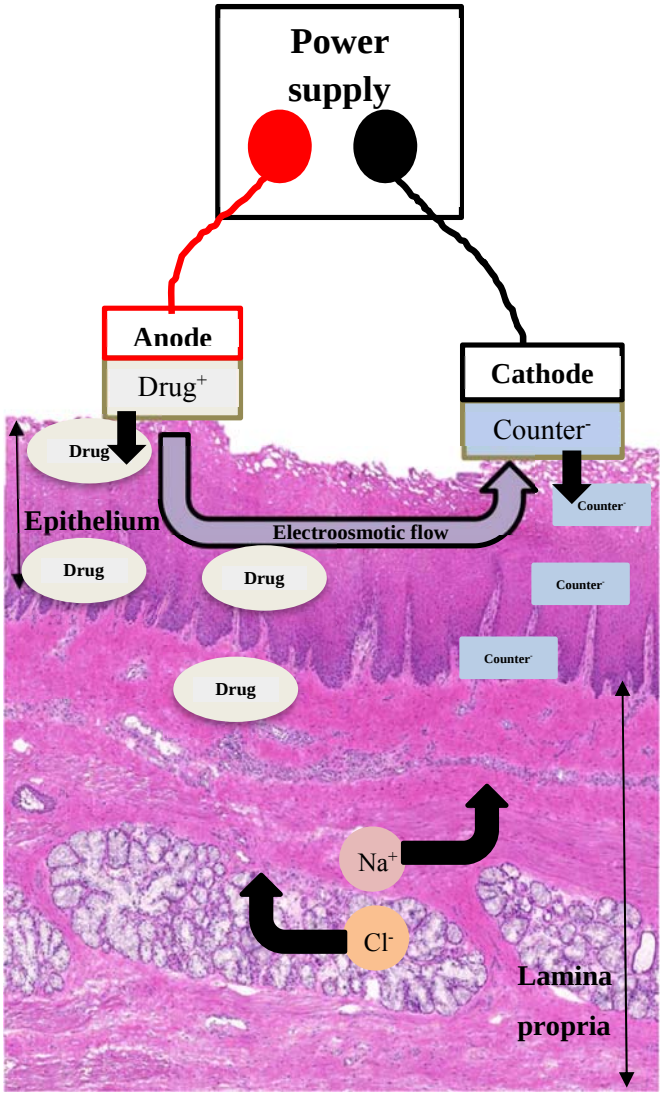

Figure 2: Schematic of an iontophoretic system

This phenomenon gives rise to a unidirectional convective flow of cations from the anode to the cathode [16]. Electroosmosis is a flow process induced by the electrical flow translating into a volume flow (e.g. µl $cm^{-2}h^{-1}$). It can also be defined as a solvent flow or solvent velocity (equivalent to the permeability coefficient of an ion) as the rate of movement of volume per unit time ($cm.h^{-1}$) [14, 15]. A unidirectional solvent flow means that the delivery of positively charged molecules as well as neutral molecule is

enhanced. This solvent flow can also enhance the delivery of high molecular weight molecules with low electrical mobility, which lags their delivery by electromigration [17]. **Chapter 3** elucidates an investigation into the electrically assisted delivery of an antibody (molecular weight: 150 kDa) in the mucosa after short term current application. The resulting delivery of the antibody in the mucosa was confirmed via quantitative biodistribution (amount of drug deposited as a function of position) in the mucosa.

The use of iontophoresis to enhance systemic and local drug delivery in the mucosa offers several advantages including bypass of hepatic first pass effect, avoidance of enzymatic degradation of the drug, controlling dosing, and ease of application and removal of the drug formulation. Once the drug molecule is able to penetrate the epithelium, it gains direct access to the systemic blood circulation via the vascularized lamina propria and the jugular vein [18]. Previously, iontophoresis has been investigated for the systemic delivery of lidocaine and prilocaine hydrochloride for local anaesthesia [19], ropinirole for Parkinson's disease [20], galantamine for Alzheimer's disease nicotine for tobacco use disorders [21] and naltrexone for opiate addiction [22]. Other molecules under investigation have been atenolol hydrochloride [23], ondansetron hydrochloride [24], sumatriptan succinate [14] including higher molecular weight molecules such as salmon calcitonin [25] and parvalbumin [26]. In an attempt to provide a controlled delivery system that provides sustained delivery of naltrexone, in a human study, Paderni et al employed an intraoral device IntelliDrug system containing a flow and fill level sensor able to communicate remotely to a software (**Figure 3**) [27]. Compared to oral administration of naltrexone, the buccal iontophoretic device delivered upto 31 times less drug

However, the delivery efficiency was over 17 times higher with the IntelliDrug device loaded with 0.5 mg of drug compared to the control group that was administered 50 mg tablet. This study concluded that current densities upto <2 mA/cm^2 are safe to use in human subjects [27].

Figure 3. Intraoral buccal iontophoresis device, Reproduced with permission from [27]

To date, this study remains the only investigation into iontophoresis on human subjects for transbuccal delivery of drugs. Studies enrolling human subjects to investigate the effect of iontophoresis on local delivery of drugs in the buccal mucosa are non-existent.

On the contrary, the use of iontophoresis for local delivery of therapeutics in dentin and enamel has been extensively explored. The technique is not new; in one of the earliest studies in 1966, Wagner *et al* examined electrotransport of sodium fluoride in rat teeth to provide a treatment option to reduce enamel acid solubility [28]. Research to date has focused primarily on transporting fluoride from solutions to control dental caries and dentin hypersensitivity [29-33]. Some researchers have also studied the electrotransport of anaesthetics for controlling pain prior to dental interventions in human subjects [34, 35].

1.2 Part 2: Chemical enhancement technique – *Polymeric micelles*

Drug delivery challenges for poorly water-soluble drugs are different. Unlike hydrophilic drugs, lipophilic drug molecules can partition in the buccal epithelium upon topical application with ease. However, to achieve a desirable therapeutic response, the drug must reach the epithelium in a relevant concentration. This can be challenging given that preparing topical formulations of poorly water-soluble drugs is difficult; especially if the formulation is to be used in a highly aqueous environment such as the mouth. One approach is to contain these lipophilic therapeutic molecules in carriers to conceal their unfavourable physicochemical properties that hinder their formulation preparation. An

ideal carrier will be able to encapsulate desired amount of the drug molecule, convey the drug onto the mucosa surface and allow the release of the drug locally in the mucosa. One such carrier is a polymeric micelle. Polymeric micelles are composed of self-assembling amphiphilic molecules that form a specific core-corona structure above their critical micelle concentration (**Figure 4**).

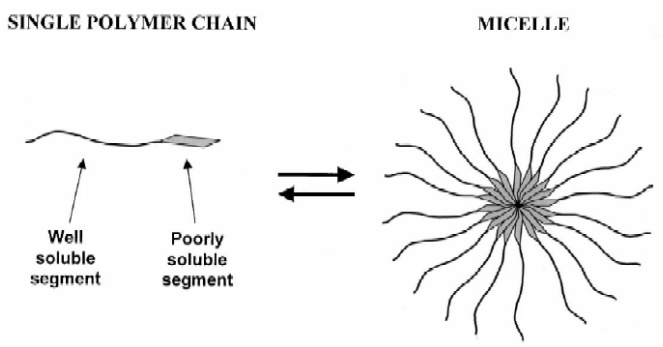

Figure 4. Schematic of the process of micelle formation. Reproduced with permission from [36]

The location of the encapsulated drug in the micelle depends on the lipophilicity of the drug. Lipophilic drugs can partition in the central core, whilst relatively less lipophilic drugs can remain partly in the core and in the shell, or completely in the shell [36]. The nature of the lipophilic part of the copolymer can affect the intermolecular interaction between the drug and the polymer, which has an impact on the extent of solubilisation of the drug in the micelle. Additionally, the size of the lipophilic moiety of the copolymer also influences the amount of drug that can be incorporated in the micelle [37].

These nanosized carriers have been under extensive investigation for their use in dermal and transdermal drug delivery [38-41]. The increasing interest in the nanocarriers for topical drug delivery is fuelled by their small size; ability to efficiently deliver therapeutic molecules, diagnostics and cosmetic material into the skin. Due to their small size, polymeric micelles have also enabled to preferentially deliver drugs to the hair follicle in skin providing treatment options for diseases originating from the pilosebaceous unit [41].

Polymeric micelle based formulations present a promising strategy to prepare aqueous formulations of poorly water-soluble drugs to treat diseases occurring locally in the buccal mucosa. In the highly

hydrated environment and 'slippery' surface in the mouth, lipophilic formulations will exhibit poor patient compliance. In addition to being tasteless and odourless, aqueous formulations such as a hydrogel, will allow improved adhesion by interacting with saliva. An aqueous formulation will also increase the thermodynamic activity of the delivery system, which can promote the rapid release of the drug from the formulation into the mucosa.

In the past, only a few studies have comprehensively examined the use of micellar carrier systems for buccal drug delivery. Lv *et al* formulated the poorly water-soluble drug, Cucurbitacin B, in a phospholipid bile salt mixed micelle formulation for the transbuccal delivery of the potent anti-cancer agent. To enforce mucoadhesion of the formulation, carboxymethyl chitosan was used as the bioadhesive polymer. 36 hours long *in vivo* study in rabbits revealed the longer formulation adhesion time, a greater and more extended delivery of the drug compared to the commercially marketed tablet [42]. Zhou *et al* reported the development of MPEG-PCL-g-PEI micelles containing amphotericin B for the local treatment of oral Candida albicans. Compared to amphotericin B alone, the micellar formulation showed enhanced antifungal activity against the fungal biofilm. It was hypothesized that the positively charged PEI moiety was able to interact with the negatively charged membrane of the fungus [43]. Suksiriworapong et al investigated the delivery of thiolated d-α-tocopheryl poly(ethylene glycol) 1000 succinate containing itraconazole micelles for the treatment of Candida albicans. An optimized micelle formulation was able to enhance the permeation of the drug through porcine buccal mucosa. Similar to the earlier study, micelles were able to improve the antifungal ability of the formulation [44].

Chapter 4 examines the development and the suitability of polymeric micelle based formulations of corticosteroids – triamcinolone acetonice (TA) and fluocinonide (FLU) using d-α-tocopheryl poly(ethylene glycol) 1000 succinate for the treatment of oral lichen planus. The objectives of the study were to provide a patient friendly and therapeutically relevant formulation of the drug. Micellar

hydrogel were formulated and the delivery of the drugs was compared to the commercial marketed formulations of the drugs at the target site after a short-term application.

References

1. Oral Mucosa. https://pocketdentistry.com/12-oral-mucosa/

2. Groeger S. and Meyle J. Oral Mucosal Epithelial Cells. *Front Immunol.* **2019** *10*: 208-208.

3. Qin R., Steel A. *et al.* Oral mucosa biology and salivary biomarkers. *Clinics in Dermatology.* **2017** *35(5)*: 477-483.

4. Hearnden V., Sankar V. *et al.* New developments and opportunities in oral mucosal drug delivery for local and systemic disease. *Adv. Drug Deliv. Rev.* **2012** *64(1)*: 16-28.

5. Squier C. A. Membrane coating granules in nonkeratinizing oral epithelium. *Journal of Ultrastructure Research.* **1977** *60(2)*: 212-220.

6. Hill M. W., Squier C. A. *et al.* A histological method for the visualization of the intercellular permeability barrier in mammalian stratified squamous epithelia. *The Histochemical journal.* **1982** *14(4)*: 641-8.

7. Bergmeier L., *Oral Mucosa in Health and Disease*. ed.; Springer International Publishing, 2018.

8. Dawson D. V., Drake D. R. *et al.* Organization, barrier function and antimicrobial lipids of the oral mucosa. *International journal of cosmetic science.* **2013** *35(3)*: 220-3.

9. Iorgulescu G. Saliva between normal and pathological. Important factors in determining systemic and oral health. *J Med Life.* **2009** *2(3)*: 303-307.

10. Wanasathop A. and Li S. K. Iontophoretic Drug Delivery in the Oral Cavity. *Pharmaceutics.* **2018** *10(3)*.

11. Singhal M., Merino V. *et al.* Controlled Iontophoretic Delivery in Vitro and in Vivo of ARN14140—A Multitarget Compound for Alzheimer's Disease. *Mol. Pharm.* **2019** *16(8)*: 3460-3468.

12. Kalaria D. R., Patel P. *et al.* Controlled iontophoretic transport of huperzine A across skin in vitro and in vivo: effect of delivery conditions and comparison of pharmacokinetic models. *Mol. Pharm.* **2013** *10(11)*: 4322-9.

13. Santer V., Chen Y. *et al.* Controlled non-invasive iontophoretic delivery of triamcinolone acetonide amino acid ester prodrugs into the posterior segment of the eye. *Eur. J. Pharm. Biopharm.* **2018** *132*: 157-167.

14. Telo I., Tratta E. *et al.* In-vitro characterization of buccal iontophoresis: the case of sumatriptan succinate. *Int. J. Pharm. (Amsterdam, Neth.).* **2016** *506(1-2)*: 420-8.

15. Kalia Y. N., Naik A. *et al.* Iontophoretic drug delivery. *Adv. Drug Deliv. Rev.* **2004** *56(5)*: 619-658.

16. Pikal M. J. The role of electroosmotic flow in transdermal iontophoresis. *Adv. Drug Deliv. Rev.* **1992** *9(2)*: 201-237.

17. Nicoli S., Ferrari G. *et al.* In vitro transscleral iontophoresis of high molecular weight neutral compounds. *Eur. J. Pharm. Sci.* **2009** *36(4-5)*: 486-92.

18. Smart J. D. Buccal drug delivery. *Expert Opin. Drug Deliv.* **2005** *2(3)*: 507-17.

19. Cubayachi C., Couto R. O. *et al.* Needle-free buccal anesthesia using iontophoresis and amino amide salts combined in a mucoadhesive formulation. *Colloids Surf. B Biointerfaces.* **2015** *136*: 1193-201.

20. De Caro V., Giandalia G. *et al.* New prospective in treatment of Parkinson's disease: studies on permeation of ropinirole through buccal mucosa. *Int. J. Pharm. (Amsterdam, Neth.).* **2012** *429(1-2)*: 78-83.

21. Wei R., Simon L. *et al.* Effects of iontophoresis and chemical enhancers on the transport of lidocaine and nicotine across the oral mucosa. *Pharm. Res.* **2012** *29(4)*: 961-71.

22. Campisi G., Giannola L. I. *et al.* Bioavailability in vivo of naltrexone following transbuccal administration by an electronically-controlled intraoral device: a trial on pigs. *J. Control. Release.* **2010** *145(3)*: 214-20.

23. Jacobsen J. Buccal iontophoretic delivery of atenolol.HCl employing a new in vitro three-chamber permeation cell. *J. Control. Release.* **2001** *70(1-2)*: 83-95.

24. Hu L., Damaj B. B. *et al.* Enhanced in vitro transbuccal drug delivery of ondansetron HCl. *Int. J. Pharm. (Amsterdam, Neth.).* **2011** *404(1-2)*: 66-74.

25. Oh D. H., Chun K. H. *et al.* Enhanced transbuccal salmon calcitonin (sCT) delivery: effect of chemical enhancers and electrical assistance on in vitro sCT buccal permeation. *Eur. J. Pharm. Biopharm.* **2011** *79(2)*: 357-63.

26. Patel M. P., Churchman S. T. *et al.* Electrically induced transport of macromolecules through oral buccal mucosa. *Dent Mater.* **2013** *29(6)*: 674-81.

27. Paderni C., Campisi G. *et al.* Controlled delivery of naltrexone by an intraoral device: in vivo study on human subjects. *Int. J. Pharm. (Amsterdam, Neth.).* **2013** *452(1-2)*: 128-34.

28. Wagner M. J. and Weil T. M. Reduction of enamel acid solubility with electrophoretic fluoride applications. *J. Dent. Res.* **1966** *45(5)*: 1563.

29. Kim H. E., Kwon H. K. *et al.* Application of fluoride iontophoresis to improve remineralization. *J Oral Rehabil.* **2009** *36(10)*: 770-5.

30. Kim H. E. and Kim B. I. Can the Application of Fluoride Iontophoresis Improve Remineralisation of Early Caries Lesions? *Oral health & preventive dentistry.* **2016** *14(2)*: 177-82.

31. Lee Y. E., Baek H. J. *et al.* Comparison of remineralization effect of three topical fluoride regimens on enamel initial carious lesions. *J Dent.* **2010** *38(2)*: 166-71.

32. Patil A. R., Varma S. *et al.* Comparative Evaluation of Efficacy of Iontophoresis with 0.33% Sodium Fluoride Gel and Diode Laser Alone on Occlusion of Dentinal Tubules. *Journal of clinical and diagnostic research : JCDR.* **2017** *11(8)*: Zc123-zc126.

33. Gupta M., Pandit I. K. *et al.* Comparative evaluation of 2% sodium fluoride iontophoresis and other cavity liners beneath silver amalgam restorations. *Journal of the Indian Society of Pedodontics and Preventive Dentistry.* **2010** *28(2)*: 68-72.

34. Smitayothin T. L., Vongsavan K. *et al.* The iontophoresis of lignocaine with epinephrine into carious dentine for pain control during cavity preparation in human molars. *Arch. Oral Biol.* **2015** *60(8)*: 1104-8.

35. Thongkukiatkun W., Vongsavan K. *et al.* Effects of the iontophoresis of lignocaine with epinephrine into exposed dentine on the sensitivity of the dentine in man. *Arch Oral Biol.* **2015** *60(8)*: 1098-103.

36. Torchilin V. P. Structure and design of polymeric surfactant-based drug delivery systems. *J. Control. Release.* **2001** *73(2)*: 137-172.

37. Lapteva M., Möller M. *et al.*, Polymeric Micelles in Dermal and Transdermal Delivery. In *Percutaneous Penetration Enhancers Chemical Methods in Penetration Enhancement: Nanocarriers*, ed.; Dragicevic, N.; Maibach, H. I., Springer Berlin Heidelberg, Berlin, Heidelberg, 2016.

38. Lapteva M., Mignot M. *et al.* Self-assembled mPEG-hexPLA polymeric nanocarriers for the targeted cutaneous delivery of imiquimod. *Eur. J. Pharm. Biopharm.* **2019**.

39. Lapteva M., Möller M. *et al.* Self-assembled polymeric nanocarriers for the targeted delivery of retinoic acid to the hair follicle. *Nanoscale.* **2015** *7(44)*: 18651-18662.

40. Lapteva M., Mondon K. *et al.* Polymeric Micelle Nanocarriers for the Cutaneous Delivery of Tacrolimus: A Targeted Approach for the Treatment of Psoriasis. *Mol. Pharm.* **2014** *11(9)*: 2989-3001.

41. Kandekar S. G., Del Rio-Sancho S. *et al.* Selective delivery of adapalene to the human hair follicle under finite dose conditions using polymeric micelle nanocarriers. *Nanoscale.* **2018** *10(3)*: 1099-1110.

42. Lv Q., Shen C. *et al.* Mucoadhesive buccal films containing phospholipid-bile salts-mixed micelles as an effective carrier for Cucurbitacin B delivery. *Drug delivery.* **2015** *22(3)*: 351-358.

43. Zhou L., Zhang P. *et al.* Preparation, characterization, and evaluation of amphotericin B-loaded MPEG-PCL-g-PEI micelles for local treatment of oral Candida albicans. *International journal of nanomedicine.* **2017** *12*: 4269-4283.

44. Suksiriworapong J., Mingkwan T. *et al.* Enhanced transmucosal delivery of itraconazole by thiolated d-a-tocopheryl poly(ethylene glycol) 1000 succinate micelles for the treatment of Candida albicans. *European journal of pharmaceutics and biopharmaceutics : official journal of Arbeitsgemeinschaft fur Pharmazeutische Verfahrenstechnik e.V.* **2017** *120*: 107-115.

CHAPTER I

Topical iontophoresis of buflomedil hydrochloride increases drug bioavailability in the mucosa: A targeted approach to treat oral submucous fibrosis

Vasundhara Tyagi, Sergio del-Rio Sancho, Maria Lapteva & Yogeshvar N. Kalia

School of Pharmaceutical Sciences,
University of Geneva & University of Lausanne,
Rue Michel-Servet 1,
1206 Geneva, Switzerland

Published in:
Int J Pharm. 2019 Oct 5;569:118610

Abstract

The aim was to investigate the effect of constant current iontophoresis on the delivery and biodistribution of buflomedil hydrochloride (BUF) in the buccal mucosa. Quantification was by UHPLC-MS/MS; in addition to total delivery, the amounts present in the epithelia and the lamina propria (the target tissue) were also determined. Two-compartment vertical diffusion cells were used to investigate the effect of current density (0.5, 1 and 2 mA/cm^2), application time (5, 10 and 20 min) and concentration (5, 10 and 20 mM) on iontophoretic delivery of BUF from aqueous solutions. In contrast to passive delivery, iontophoresis for 10 min at 1 mA/cm^2 resulted in statistically equivalent transport from a 20 mM solution and a 2% HEC hydrogel (with equivalent BUF loading; 20 µmol). BUF delivery from the hydrogel using diffusion cells and a new coplanar "side-by-side" set-up was statistically equivalent (304.2 ± 28.9 and 278.2 ± 40.3 µg/cm^2) – passive delivery was also similar. Iontophoresis (10 min at 1 mA/cm^2) using a thin film (20 µmol BUF) was superior to the passive control (323.3 ± 5.9 and 24.8 ± 5.9 µg/cm^2). Concentrations in the LP were ~700-fold >IC_{50} to block collagen production, potentially providing a new therapeutic strategy for oral submucous fibrosis.

Keywords: iontophoresis; topical delivery; buflomedil; fibrosis; buccal delivery

1. Introduction

Oral submucous fibrosis (OSF) is a potentially malignant chronic disease of the oral cavity that affects over 5 million people worldwide with the majority being in South-East Asia [1, 2]. It is mainly caused by areca nut (*Areca catechu*) chewing which results in an altered collagen production in the lamina propria (LP; connective tissue) of the oral mucosa. The changes in the LP progressively result in the loss of fibroelasticity, resulting in rigidity and stiffness in the oral cavity [3]. Although the molecular and cellular mechanisms underlying areca nut associated oral carcinogenicity have not been elucidated, the precancerous nature of the disease has been attributed to arecoline and its metabolites [4, 5]. It was reported that arecoline, the most common alkaloid present in areca nut, might contribute to oral carcinogenesis through inhibition of p53 and DNA repair [6]. In mild to moderate OSF, corticosteroids are indicated to reduce inflammation, fibrinolytic agents are used to promote fibrinolysis in the lesions and vasodilators are prescribed to increase blood flow in the ischemic tissue and thereby relieve trismus [7].

Buflomedil hydrochloride (BUF) is an adrenergic receptor antagonist that inhibits platelet aggregation and increases membrane elasticity in erythrocytes [8-10]. A 10 year clinical study showed that oral administration of BUF (450 mg thrice daily) with topical administration of triamcinolone acetonide and a biweekly submucosal injection of dexamethasone resulted in a significant improvement of symptoms [11]. Although BUF has good oral bioavailability (72%), it has a short half-life of ~3 h [12] and it is often associated with serious neurological and cardiovascular side effects – given their prevalence and the relatively narrow therapeutic index, its marketing authorization was suspended by the European Medicines Agency in 2012 [13, 14]. Topical delivery of BUF would enable its targeted administration to the affected tissue, and aim to increase its local bioavailability at the site, while reducing systemic exposure and hence the risk of side effects.

Nevertheless, local delivery to the oral mucosa has its own challenges since the non-keratinized stratified squamous epithelium of the buccal mucosa (**Figure 1a**) is a physiological barrier to exogenous substances and limits the permeation of drugs [15, 16]. The upper third of the epithelium, which is lipophilic in nature, constitutes the main permeability barrier [17], especially for hydrophilic molecules such as BUF. This barrier function is attributed to the presence of intercellular membrane coating granules [18, 19], which are most evident in the uppermost epithelium. Another "barrier" to effective local delivery to the mucosa is the need to have the shortest possible formulation application time. Any

disruption of routine activities or sensation of a foreign substance in the oral cavity will decrease patient compliance.

a)

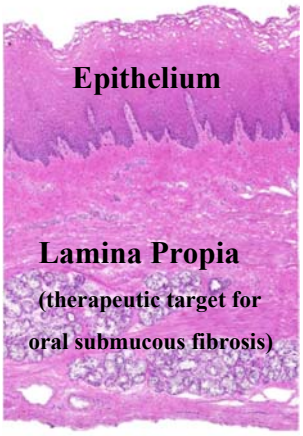

b)

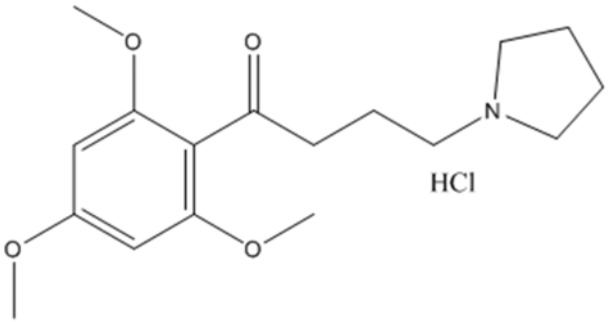

Figure 1. (a) Haematoxylin and eosin stained porcine esophageal mucosa cross section showing the epithelium and the connective tissue lamina propria (bar represents 200 μm), (b) chemical structure of buflomedil hydrochloride (BUF) – 343.8 Da, logD – 0.31 at pH 7.0.

Iontophoresis is a non-invasive technique that can improve drug delivery kinetics into and across biological membranes [20]. The iontophoretic flux is due to three possible electrotransport mechanisms: electromigration, electroosmosis and enhanced passive diffusion [21]. Their relative contributions depend on the physicochemical properties of the molecule, the formulation characteristics and the iontophoretic conditions. It has been extensively studied as a means to increase the delivery of low and high molecular weight therapeutic agents – in particular into and across the skin [20] and to the eye [22]. In recent years, buccal iontophoresis has also gained attention [23, 24] and recent work has investigated the buccal delivery of systemically-acting agents including atenolol, ropinirole, salmon calcitonin and

naltrexone including preclinical *in vivo* studies in rabbits and pigs [25-28]. However, we hypothesize that the hurdles for the development of locally-acting therapeutics would be lower. To-date, there have been several reports into the use of topical iontophoresis in dental practice [29-31]. The topical iontophoresis of local anesthetics (e.g. lidocaine and prilocaine) [32, 33] and the co-iontophoresis of 5-fluorouracil and leucovorin [23] have also been described.

BUF hydrochloride (**Figure 1b**; MW = 343.85 Da, log $D_{pH\ 7.0}$ = 0.31, pKa = 10.15) is a small molecule with good aqueous solubility (190 g/L) that is fully ionized at the physiological surface pH of buccal mucosa (~6.28) [34]. These physicochemical properties make it a good candidate for iontophoresis. Although BUF has previously been studied as a topical remedy for cutaneous wound healing [8, 35], its topical application to the buccal mucosa has not been investigated. The first objective of the current work was to investigate topical iontophoresis of BUF into the mucosa *in vitro* and to determine its biodistribution as a function of current density, drug concentration and duration of current application and to compare the results to those in the absence of current. We have previously employed this methodology to better understand the spatial distribution of drugs in the skin and in the cornea [36-40].

In vitro experiments typically employ two-compartment vertical Franz diffusion cells where the anodal and cathodal compartments are separated by the biological tissue. However, in clinical practice, buccal iontophoresis might require the electrodes to be placed adjacent ("side-by-side") to each other in the oral cavity of the patient. Therefore, in the second part of the project a new experimental set-up – "the coplanar set-up" – was developed to mimic these conditions (**Figure 2**) and was used to investigate delivery from a fast dissolving film formulation that might be more suited for use *in vivo*.

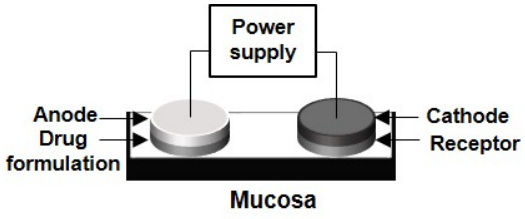

Figure 2. Schematic representation of the coplanar delivery set up showing the arrangement of the two electrodes over the drug formulation and the receptor formulation

2. Materials and methods

2.1 Materials

BUF, polyethylene glycol (PEG) (M.W~35000) and phosphate buffered saline were purchased from Sigma Aldrich (Buchs, Switzerland). NATROSOL 250 hydroxyethyl cellulose (HEC) was a generous gift from Hercules Inc. Klucel™ hydroxypropyl cellulose (HPC; MW 850,000 Da) was a kind gift from Ashland Inc (Schaffhausen, Switzerland). Acetonitrile (ACN) and methanol (MeOH) were of LC-MS grade and purchased from Fisher Scientific (Reinach, Switzerland). Formic acid of LC-MS grade was purchased from Brunschwig (Basel, Switzerland). All other chemicals were of at least analytical reagent grade. All aqueous solutions were prepared using Milli-Q water (resistivity > 18 MΩ.cm). Haematoxylin, eosin and Hoechst 33342 used for the histological evaluation of the mucosal tissue were bought from Thermo Fisher Scientific (Reinach, Switzerland).

2.2 Analytical method

Quantification of the mucosal biodistribution of BUF required the development of a highly sensitive UHPLC-MS/MS method using a Waters Acquity® UPLC®/Xevo® TQ-MS system; ESI positive mode and multiple reaction monitoring (MRM) were employed to ionize and analyze the ion of interest (308.287 → 237.139). Gradient separation was achieved using a Waters XBridge® BEH C18 (50 x 2.1 mm, 2.5 µm) reverse phase column maintained at 40°C (**Table S1 and S2**, **Supplementary Information**). The mobile phase consisted of 0.1% formic acid in acetonitrile and 0.1% formic acid. The flow rate and injection volume were 0.3 mL/min and 5 µL, respectively. The method was specific (**Figure S1**, **Supplementary Information)** and the limits of detection and quantification were 1 ng/mL and 5 ng/mL, respectively. BUF eluted at 1.6 min and the run time was 2 min. The method was validated and complete details about accuracy and precision are provided in **Table S3** (**Supplementary Information**).

2.3 Formulation preparation

2.3.1 Mucoadhesive hydrogel

Bioadhesive gels have been widely used as drug vehicles for buccal drug delivery systems [41]. HEC, a nonionic polymer, has been previously used to prepare mucoadhesive buccal formulations for iontophoresis [23]. It has the advantage for iontophoretic applications of being nonionic and so does not introduce competing charge carriers into the formulation. BUF was incorporated in a 2% HEC gel. Briefly, HEC was slowly added to 30 mL unbuffered aqueous solution (pH 5.9) containing 20 µmol of

BUF under constant stirring. The drug-polymer solution was stirred at room temperature for 4 h at 300 rpm. The polymer solution was left for swelling overnight.

2.3.2 Fast dissolving film

A Mathis LTE Labcoater (Werner Mathias AG; Zurich, Switzerland) was used to prepare the fast dissolving film. HPC (3.3%) was used as the polymer matrix while PEG (0.3 %) was employed as the plasticizer [42]. The polymer solution was coated onto a backing sheet (3M Scotchpak ™ 9733 backing polyester film laminate) at a coating speed of 0.2 mL/min and the surface temperature was set at 75°C. The coat thickness was set at 2 mm. After drying for 1 h the thickness of the film reduced to 300 ± 25 µm. 2 cm^2 disks were punched out of the film – each containing 20 µmol of BUF.

2.4 Preparation of mucosal tissue

In vitro studies were performed using fresh or frozen porcine esophageal mucosa as a surrogate for human buccal mucosa. The structural similarities between human buccal epithelium and porcine esophageal epithelium and similar lipid composition have been described previously [33, 43, 44]. The porcine esophagus was obtained from a local slaughterhouse (Abattoir de Loëx Sàrl; Bernex, Switzerland) a few hours after slaughter. It was longitudinally dissected and rinsed with isotonic saline. The mucosa was separated from the underlying muscular layer with a scalpel. The separated mucosa was cleaned with cold Krebs-Ringer bicarbonate buffer (KRB, pH 7.4). The full thickness mucosa was either used fresh or wrapped in Parafilm® and stored at -20 ºC for up to 3 months.

2.5 Transport studies

2.5.1 Franz diffusion cell set-up

Full thickness mucosal tissue was thawed and allowed to equilibrate for 30 min in PBS (pH 7.4). The tissue was then clamped in two-compartment vertical Franz diffusion cells (diffusion area 2 cm^2) with the epithelium facing the donor compartment. 1 mL of aqueous drug solution or 2% HEC gel – each containing 20 µmol BUF – was placed in the donor compartment, which was connected to the anodal compartment using a salt bridge (3% agarose in 0.15M NaCl). The receiver compartment was filled with 12 mL of PBS (pH 7.4) and contained the cathode. A constant current was applied using Ag/AgCl electrodes connected to a power supply (APH 1000 M, Kepco Inc; Flushing NY, USA). The first series of electrotransport experiments measured the effect of current density (i_d; 0.5, 1 and 2 mA/cm^2) on the mucosal deposition of BUF (10 mM at pH 5.5) after current application for 20 min. The second series investigated the effect of BUF concentration (5, 10 and 20 mM, pH 5.5-6.0) on mucosal delivery after iontophoresis for 20 min at 1 mA/cm^2 and the final series determined the impact of the duration of

current application (5, 10 and 20 min) on BUF transport (10 mM at pH 5.5) after iontophoresis at 1 mA/cm^2. All aqueous solutions were used unbuffered (pH 5.5-6.0). A "bridging" experiment was performed to compare passive and iontophoretic delivery of BUF from the aqueous solution and the hydrogel (1 mL of 20 mM BUF solution (20 µmol) and 1 mL of 2 % HEC gel also containing 20 µmol of BUF); iontophoresis for 10 min at 1 current density of mA/cm^2). Passive diffusion experiments were performed using the same set-up but in the absence of current and served as controls.

Upon completion of a delivery experiment, the mucosa was cleaned with running water and a 0.5 cm^2 piece in contact with the formulation was punched out. This was fixed in OCT embedding medium, and flattened using a glass slide. It was then snap-frozen in isopentane cooled by liquid nitrogen and sliced using a Microm HM 560 Cryostat (Thermo Scientific; Walldorf, Germany). The tissue was sliced in 40 µm thick lamellae from the mucosa surface to a depth of 320 µm corresponding to the epithelium layer. The biodistribution approach also enabled the quantification of BUF in the underlying lamina propria (LP) for each experimental condition and hence to identify the optimal parameters for delivery to this tissue (**Figure 1**). The individual lamellae and the remaining tissue (LP) were extracted overnight in 1.5 mL and 10 mL of MeOH:water (75:25 v/v), respectively. The extracts were centrifuged at 12,000 rpm for 15 min. They were then filtered using 0.22 µm PVDF filters (BGB Analytik SA) prior to analysis by UHPLC-MS/MS. The extraction method and filter selection were validated by spiking mucosa samples with known amounts of drug (complete details are provided in **Table S4** and **S5** in the **Supplementary Information**).

2.5.2 Coplanar electrode set-up

Full thickness mucosal tissue (approximately 8-9 cm in length) was placed on a surgical absorbent pad moistened with PBS to maintain tissue hydration. Anodal and cathodal compartments were placed side-by-side, 1.6 cm apart. 20 µmol of BUF was placed in the anodal compartment in the form of either 1 mL hydrogel or 2 cm^2 of fast dissolving film. A current density of 1 mA/cm^2 was applied for 10 min using a flat silver disk (area 2 cm^2) as the anode. The receptor compartment was 1 % HEC gel containing PBS buffer connected to the power supply via an AgCl electrode. The application area for the drug formulation and the receptor PBS gel was 2 cm^2. Passive diffusion experiments using the same set-up but in the absence of current served as controls.

2.6 Data analysis

Data are expressed as mean ± standard deviation. Statistical significance was evaluated by ANOVA or by Student's t-test (α =0.05).

3. Results and Discussions

3.1 Effect of iontophoretic parameters on iontophoretic transport of BUF from aqueous solution

3.1.1 Effect of current density

In the absence of current, the total amount of BUF deposited in the mucosa after application of a 10 mM solution (pH 5.5) for 20 min was 9.3 ± 3.2 µg/cm^2 ($Q_{passive}(T)$). The delivery efficiency (*DE*), i.e. the fraction of the amount applied that was deposited in the mucosa, was poor, only 0.6 % (**Table 1**). Iontophoresis of the same solution at 0.5 mA/cm^2 for 20 min increased the amount deposited to 46.8 ± 20 µg/cm^2. Increasing the current density (i_d) to 1.0 mA/cm^2 and 2.0 mA/cm^2 increased the total amounts deposited to 88.6 ± 9.5 and 252.2 ± 32.8 µg/ cm^2, respectively. For current densities 0.5 – 2 mA/cm^2, the delivery efficiencies were in the range of 3.0 – 16.4 %.

Mucosal deposition of BUF in the lamina propria (LP; 480 – 1500 µm) after passive application ($Q_{passive}(LP)$) for 20 min was 4.4 ± 2.4 µg/cm^2; this increased to 25.9 ± 15.5, 33.4 ± 9.2 and 111.1 ± 4.2 µg/ cm^2 after iontophoresis at current densities of 0.5, 1 and 2 mA/cm^2, respectively (**Table 1**). Although there was no statistically significant increase in BUF deposition on going from 0.5 to 1 mA/cm^2, there was a dramatic increase upon raising the current density to 2 mA/cm^2, with an enhancement ratio (*ER*) of 25.5 ± 13.8 (**Table 1**). The transport efficiencies (*TE*), i.e. the fraction of the charge that was carried by BUF, ranged from 2.5 to 3.3 % on passing from 0.5 to 2 mA/cm^2 (**Table 1**). The biodistribution data gave a more detailed look into the epithelial delivery of BUF. In the absence of current application, 2.3 ± 0.4 µg/ cm^2 was present in the upper 40 µm epithelium (**Figure 3a**), this corresponded to ~47 % of the total amount of BUF delivered, with only 130 ± 70 ng/cm^2 BUF reaching the basement epithelial layers.

Application of current densities from 0.5 mA/cm^2 to 2 mA/cm^2 for 20 min improved the delivery and distribution of BUF in the epithelium (**Figure 3a**). The amounts of BUF deposited in the superficial layers, up to a depth of 80 µm, after iontophoresis at 1 mA/cm^2 and 2 mA/cm^2 were comparable; however, the amounts deposited in subsequent layers were significantly different ($p < 0.05$). At 2 mA/cm^2 BUF was able to penetrate much deeper into the epithelia.

(a) Upper panel

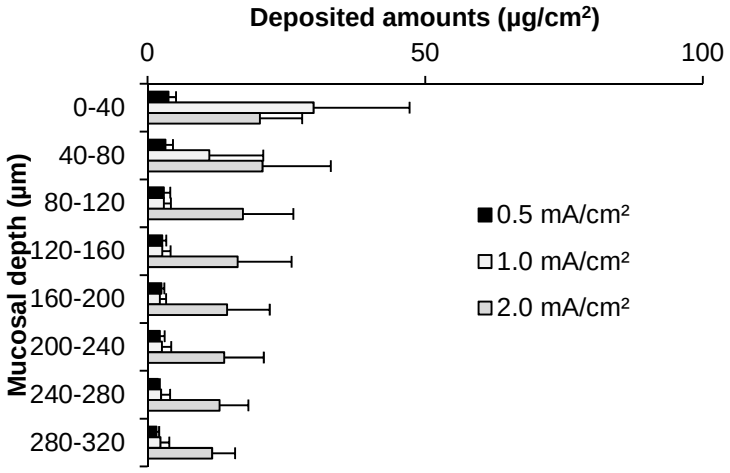

(a) Lower panel

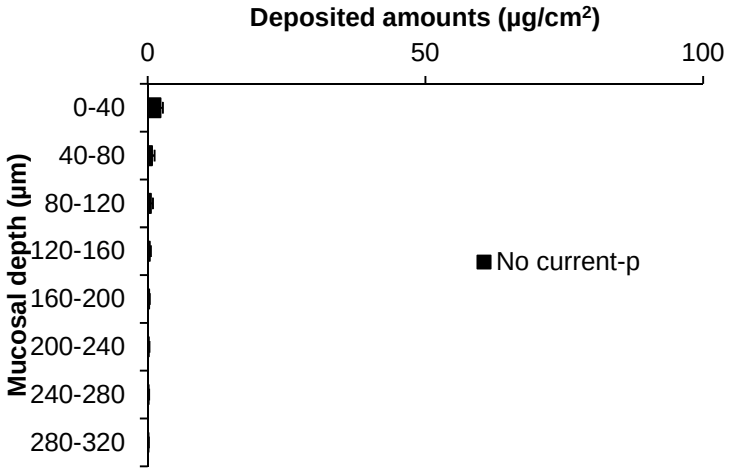

(b) Upper panel

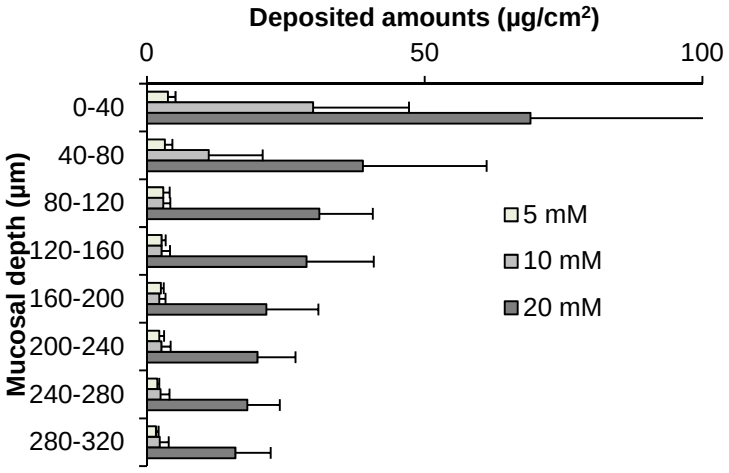

(b) Lower panel

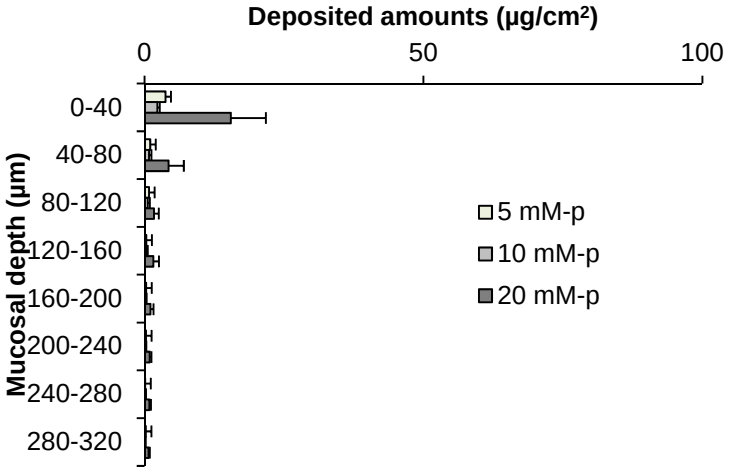

(c) Upper panel

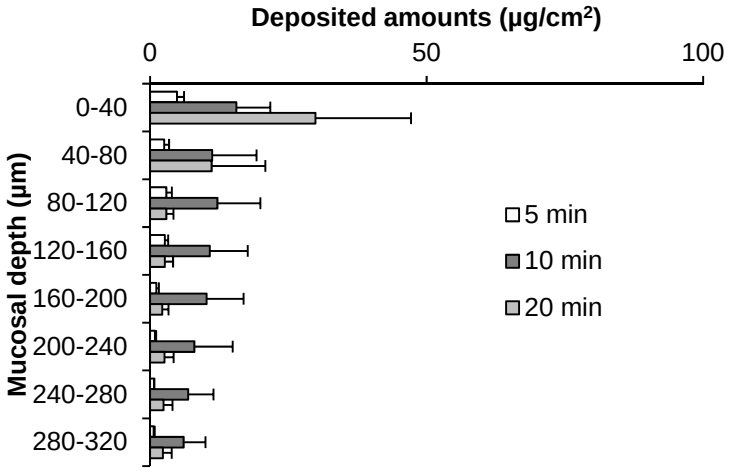

(c) Lower panel

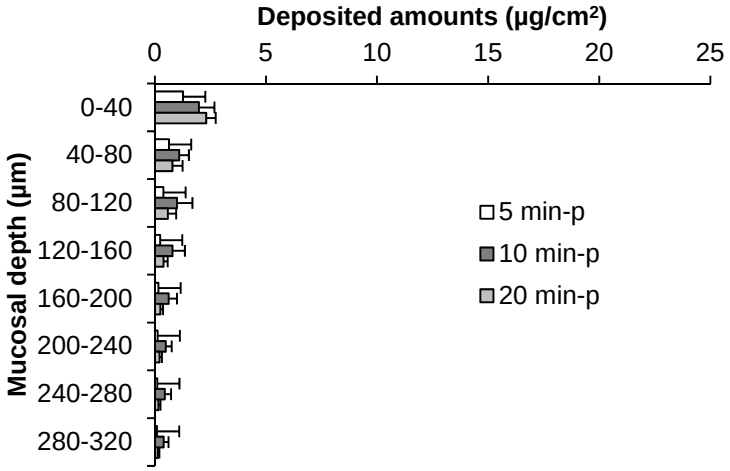

Figure 3. Influence of varying **(a)** current densities (i_d; 0.5 – 2.0 mA/cm^2) on iontophoretic delivery of BUF where concentration (10 mM BUF in water ; pH 5.5) and time (20 min) were constant, **(b)** BUF donor concentration (5 mM – 20 mM; pH 5.5 – 6.0) on iontophoretic delivery of BUF after 20 min at a current density of 1.0 mA/cm^2 and **(c)** application time on iontophoretic delivery of BUF (10 mM BUF in water; pH 5.5) at a current density of 1.0 mA/cm^2. Upper panels in each figure show the results following iontophoresis and the lower

panels are for passive controls performed for each condition using the same set-up but in the absence of current application.

3.1.2 Effect of concentration

There was no statistically significant difference in either the total delivery or the amount of BUF recovered from the epithelia on increasing the concentration from 5 to 10 mM under passive conditions ($Q_{passive(E)}$) (**Table 1**). However, a further increase in BUF concentration to 20 mM did produce a statistically significant increase in both quantities (**Table 1**). In contrast, there were statistically significant differences in the amounts of BUF present in the lamina propria at the three concentrations ($p < 0.05$) (**Table 1**). The amounts of BUF deposited in the epithelium by passive application of 5 or 10 mM were statistically equivalent ($p = 2$). On increasing the concentration to 20 mM, the amounts of BUF deposited in the epithelium increased >4-fold (**Table 1**). Due to a high concentration gradient present in this case, 15.4 ± 3.2 µg/ cm^2 of BUF was deposited in the first 40 µm of the epithelium (**Figure 3b**). However, the amount decreased steeply with only 0.7 ± 0.2 µg/ cm^2 deposited in the lower epithelium (280-320 µm) owing to poor partitioning of BUF in the mucosa. Iontophoresis for 20 min at 1.0 mA/cm^2 using 20 mM BUF solution deposited a total of 235.3 ± 62.3 µg/ cm^2 in the epithelia ($Q_{ionto(E)}$), of which 15.9 ± 6.3 µg/cm^2 was found as deep as 320 µm. The highest delivery to the LP (268.2 ± 20.7 µg/cm^2; $Q_{ionto(LP)}$) was also observed when the BUF concentration was 20 mM (**Table 1**). Under these conditions, transport efficiency was 13.1 %, higher than at any other condition tested.

3.1.3 Effect of duration of current application

As mentioned above, the duration of formulation application should be as short as possible. The total amounts deposited in the mucosa after passive application of a 10 mM BUF solution for 10 and 20 min were statistically equivalent although there was a trend indicating that more BUF reached the LP at the longer time-point (2.05 ± 0.6 and 4.4 ± 2.4 µg/cm^2). Total delivery after 5 min was significantly lower and BUF was quantified only in the epithelium (3.0 ± 0.7 µg/cm^2) – concentrations in the LP were <LOQ (**Table 1**). Iontophoresis at 1.0 mA/cm^2 for 5 min increased the total amount deposited in mucosa increased to 14.3 ± 1.5 µg/cm^2, of which 0.1 ± 0.01 µg/cm^2 reached the LP. Increasing the duration of current application to 10 and 20 min increased the amounts present in the LP to 12.3 ± 3.2 and 33.4 ± 9.2 µg/cm^2 respectively. The trend was similar for the amounts deposited in the epithelium after iontophoresis (**Figure 3c**).

STUDY	i_d (mA/cm²)	[BUF] (mM)	Time (min)	[a]$Q_{passive}$ (T) (µg/cm²)	[a]Q_{ionto} (T) (µg/cm²)	[b]$Q_{passive}$ (E) (µg/cm²)	[b]Q_{ionto} (E) (µg/cm²)	[c]$Q_{passive}$ (LP) (µg/cm²)	[c]Q_{ionto} (LP) (µg/cm²)	[d]ER Q_{ionto} (LP)/ $Q_{passive}$ (LP)	[e]DE (%)	[f]TE (%)
Effect of current density	-	10	20	9.3 ± 3.2	-	4.8 ± 2.5	-	4.4 ± 2.4	-	-	$0.6 \pm 7*10^{-4}$	-
	0.5	10	20	-	46.8 ± 20	-	20.8 ± 6.4	-	25.9 ± 15.5	5.8 ± 4.7	3.0 ± 1.3	2.5 ± 1.0
	1	10	20	-	88.6 ± 9.5	-	56.4 ± 14.4	-	33.4 ± 9.2	7.5 ± 4.6	5.7 ± 0.6	2.3 ± 0.2
	2	10	20	-	252.2 ± 32.8	-	122.1 ± 43.2	-	111.1 ± 4.2	25.5 ± 13.8	16.4 ± 0.02	3.35 ± 0.4
Effect of concentration	-	5	20	7.4 ± 1.8	-	6.8 ± 2.0	-	0.7 ± 0.03	-	-	0.9 ± 0.24	-
	-	10	20	9.3 ± 3.2	-	4.8 ± 2.5	-	4.4 ± 2.4	-	-	$0.6 \pm 7*10^{-4}$	-
	-	20	20	44.6 ± 11.1	-	26.6 ± 9.9	-	18.0 ± 5.1	-	-	1.3 ± 0.5	-
	1	5	20	-	69.05 ± 8.79	-	41.7 ± 10.5	-	27.3 ± 2.9	39 ± 4.4	9.0 ± 1.1	1.8 ± 0.2
	1	10	20	-	88.6 ± 9.5	-	56.4 ± 14.4	-	33.4 ± 9.2	7.5 ± 2.1	5.7 ± 0.6	2.3 ± 0.2
	1	20	20	-	503.5 ± 67.5	-	235.3 ± 62.3	-	268.2 ± 20.7	17.7 ± 1.5	16.4 ± 2.1	13.1 ± 1.7
Effect of duration	-	10	5	3.0 ± 0.7	-	3.0 ± 0.7	-	<LOQ	-	-	0.2 ± 0.04	-
	-	10	10	8.8 ± 2.9	-	6.8 ± 2.7	-	2.05 ± 0.63	-	-	0.5 ± 0.1	-
	-	10	20	9.3 ± 3.2	-	4.8 ± 2.5	-	4.4 ± 2.4	-	-	$0.6 \pm 7*10^{-4}$	-
	1	10	5	-	14.3 ± 1.5	-	14.2 ± 1.6	-	0.1 ± 0.01	20	0.9 ± 0.1	1.4 ± 0.1
	1	10	10	-	67.3 ± 20	-	64.3 ± 28.1	-	12.3 ± 3.2	6 ± 1.5	4.1 ± 1.8	3.4 ± 1.5
	1	10	20	-	88.6 ± 9.5	-	56.4 ± 14.4	-	33.4 ± 9.2	7.5 ± 2.0	5.7 ± 0.6	2.3 ± 0.2

Table 1. Iontophoretic and passive experimental parameters (current density (i_d), donor concentration [BUF] and time) and the resulting total deposition of BUF in the mucosa, and amounts present in the epithelium and the lamina propria.

[a] Q_X *(T)* : total deposition after passive ($Q_{passive}$) or iontophoretic (Q_{ionto}) administration

[b] Q_X *(E)* : deposition in epithelium after passive ($Q_{passive}(E)$) or iontophoretic ($Q_{ionto}(E)$) administration

[c] Q_X *(LP)* : deposition in lamina propria after passive ($Q_{passive}(LP)$) or iontophoretic ($Q_{ionto}(LP)$) administration

[d] *ER* : enhancement ratio: the ratio between the amounts of BUF deposited in the LP in presence and absence of current

[e] *DE* : Delivery efficiency – ratio of the amount of BUF deposited to the amounts of BUF applied in the donor compartment

[f] *TE* : Transport efficiency – ratio of the fraction of charge carried by BUF to the total charge passed during iontophoresis.

3.2 Comparison of BUF delivery from aqueous solution and hydrogel

Based on the above results, the following "optimal" conditions were selected for the next phase: iontophoresis for 10 min at a moderate current density of 1.0 mA/cm^2 using a BUF concentration of 20 mM. These parameters also avoided the need for salt bridges since sufficient Cl^- ion was available for Ag/AgCl anodal electrochemistry from the BUF hydrochloride salt. These conditions were used to compare passive and iontophoretic delivery of BUF deposition from aqueous solution and the 2% HEC gel (pH ~5.9).

After passive delivery from the aqueous solution and hydrogel (both containing 20 µmol BUF) for 10 min, the total amounts of BUF deposited in the mucosa were significantly greater from the solution than the hydrogel (15.5 ± 4.6 and 4.2 ± 0.4 µg/cm^2, respectively) ($p = 0.0017$). This was attributed to the poor passive diffusion of BUF inside the three-dimensional polymeric network of the hydrogel. Iontophoresis increased the amounts of BUF deposited in the mucosal tissue – the application of the electric field meant that movement of the BUF ion was now governed by its electric mobility and no longer by the diffusion coefficient alone. The total amounts deposited were statistically equivalent ($p = 0.27$) and constituted a 15-fold increase in delivery from the solution and a >50-fold increase for the gel (333.8 ± 120.6 and 315.2 ± 24.2 µg/cm^2 for solution and gel, respectively). This suggested that the presence of the electric field could overcome the diffusional resistance of the hydrogel network. Passive delivery of BUF from solution and gel to the mucosal epithelium was also significantly different after 10 min (13.7 ± 4.6 and 3.5 ± 0.4 µg/cm^2, respectively); in contrast, the amounts of BUF deposited in the mucosal epithelium after iontophoresis were again statistically equivalent (201.9 ± 99.5 and 198.4 ± 19.3 µg/cm^2, respectively) (**Figure 4**).

The trend was similar for the quantity of BUF reaching the target area LP. Upon passive application of the solution and gel for 10 min, the amounts reaching the LP were 1.8 ± 0.5 and 0.6 ± 0.1 µg/cm^2, respectively; these increased to 103.3 ± 14.4 and 116.8 ± 14.5 µg/cm^2 ($p = 0.1779$), respectively, after iontophoresis at 1 mA/cm^2 for the same duration.

(a)

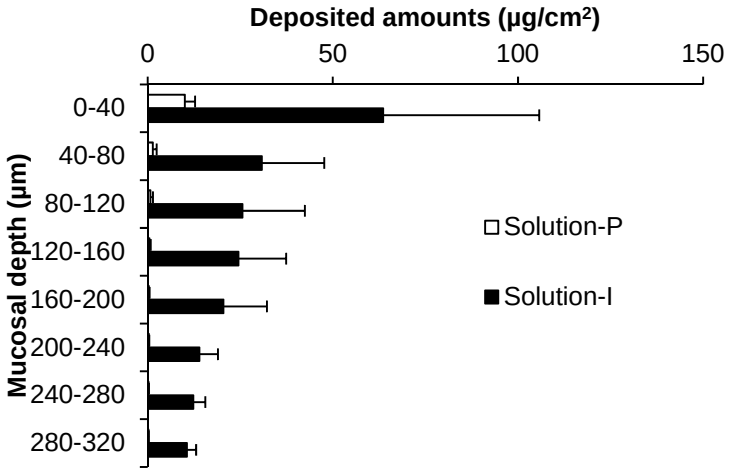

(b)

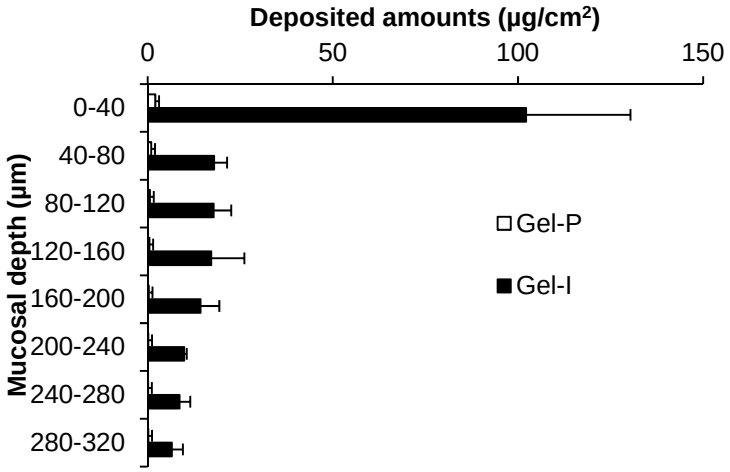

Figure 4. Comparison of amounts of BUF deposited in successive layers of mucosal epithelium by passive and iontophoretic transport from **(a)** an aqueous solution **(b)** a hydrogel formulation. Suffix – P means passive (10 min) and – I means iontophoresis (10 min at a current density of 1 mA/cm^2).

3.3 Passive and iontophoretic delivery using the coplanar set-up

The final part of the project focused on the development of a new experimental set-up for short duration iontophoresis that would better approximate clinical use. For buccal mucosa, the counter electrode can

be placed on either the epithelial side or outside the oral cavity on the cheek. A mathematical simulation using the COMSOL Multiphysics software to compare the effect of electrode placement on drug delivery suggested that placing the counter electrode on cheek skin outside the oral cavity was more efficient for transbuccal drug delivery [45-47] and a three-compartment vertical diffusion cell, where both electrodes were on the epithelial side of the mucosa and which better mimicked *in vivo* conditions was used to investigate the buccal iontophoretic delivery of atenolol [28]. The coplanar iontophoretic system proposed in the present study enabled "same-side" current application since both electrode compartments were placed on the epithelial surface – there was no receiver compartment since the experiments were of short duration and the tissue was hydrated using a surgical absorbent pad moistened with PBS (**Figure 2**).

A bridging study was performed to compare passive and iontophoretic delivery of BUF from the hydrogel (containing 20 µmol of BUF) using conventional two-compartment vertical Franz cells and the coplanar set-up to confirm that changing the electrode configuration did not influence the iontophoretic delivery of BUF to the mucosa (**Figure 5**). After application of the hydrogel for 10 min, passive delivery from the Franz cell and the coplanar set-up was 4.2 ± 0.4 and 4.1 ± 1.8 µg/cm^2 ($p = 0.9065$), the corresponding amounts after iontophoresis at 1 mA/cm^2, were 304.2 ± 28.9 and 278.2 ± 40.3 µg/cm^2, respectively – they were also statistically equivalent ($p = 0.1164$). The amounts of BUF deposited in the different layers of the epithelium after passive or iontophoretic application using the vertical diffusion cells or coplanar set-up were also statistically equivalent (**Figure 5a** and **5b**). This confirmed that the electrode configuration did not affect iontophoretic transport of BUF.

The set-up was then used to explore iontophoretic delivery of BUF from a fast disintegrating oral film. These dosage forms have gained increasing attention for their ease of application, discreetness and ability to control dosing. They dissolve in a few minutes upon hydration, increase the local bioavailability at the diseased sites in the mucosa and improve therapeutic response. An example of a film used for intra-oral disease management is Oramoist®, which is indicated for xerostamia [48]; the Rivelin® patch containing clobetasol is in Phase II clinical trial. Rapid transmucosal delivery of systemically-acting drugs is also possible: Onsolis® and Breakyl® contain fentanyl and are approved for management of acute cancer pain [49].

(a)

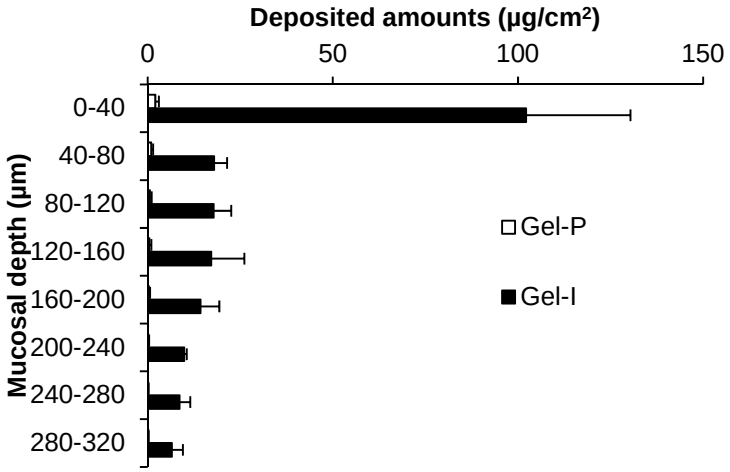

(b)

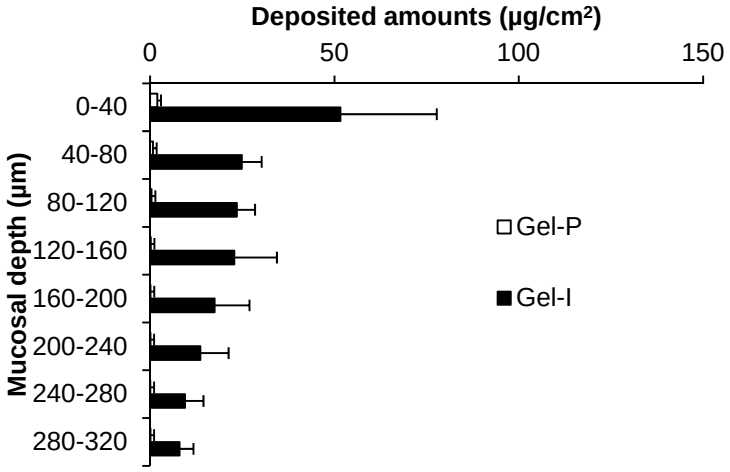

Figure 5. Amounts of BUF deposited in successive layers of the mucosal epithelium by passive (10 min) and iontophoretic (10 min at 1 current density of mA/cm^2) transport when using **(a)** two compartmental Franz diffusion cells and **(b)** the coplanar set-up.

The fast dissolving film developed in this study contained the same molar amount of BUF (20 µmol) as the gel discussed above; it was moistened by the addition of 70 µL of water before being placing on the mucosa. A circular silver anode covered the film entirely and delivery studies were performed at the optimized parameters mentioned above. There was a statistically significant difference in the total passive delivery from the two formulations (4.1 ± 1.8 and 24.8 ± 5.9 µg/cm^2 for the gel and film respectively; $p < 0.0001$) despite the same amount of BUF being applied to the mucosal surface from the two formulations. This was attributed to the lower water content and therefore higher concentration of BUF at the surface of the film facing the mucosa. Iontophoresis for 10 min at 1 mA/cm^2 enabled 13-fold more BUF to be delivered to the epithelium as compared to passive administration ($p < 0.0001$) (**Figure 6a**). The total iontophoretic delivery of BUF from the hydrogel and the film was statistically equivalent ($p > 0.05$); thus, the difference in BUF concentration did not influence the amounts delivered by iontophoresis.

(a)

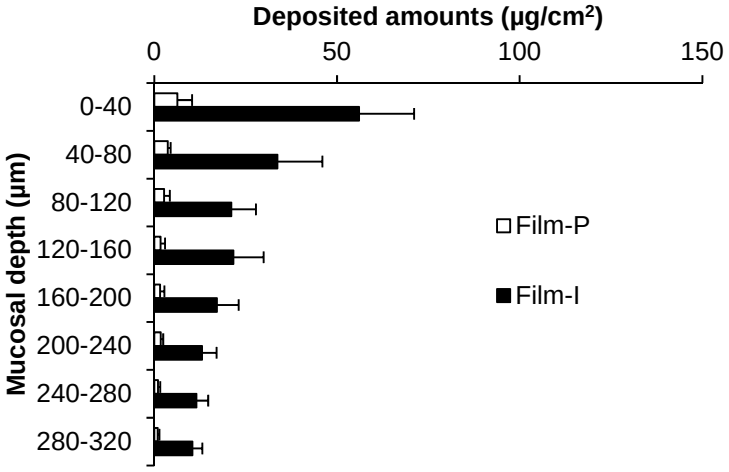

(b)

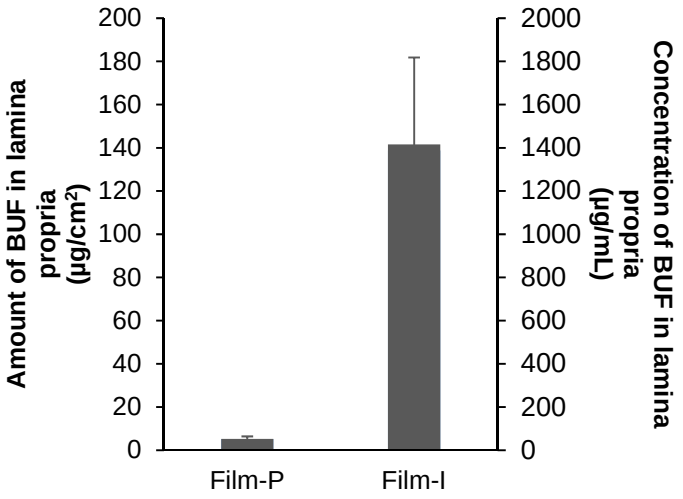

Figure 6. (a) Passive and iontophoretic delivery of BUF to the mucosal epithelium from the film **(b)** Amounts and corresponding concentrations of BUF deposited by passive and iontophoretic transport in LP by the film. Suffix –P means passive (10 min) and –I means iontophoresis (10 min at 1 current density of mA/cm^2).

It has been previously suggested that in a system where there are no competing ions present in the donor compartment, the flux of the drug becomes independent of the donor concentration and is governed by the ratio between the drug diffusivity and the counter-ion present in the receptor compartment [50-53]) and this has also been observed experimentally [50-54]. This could explain why iontophoretic delivery from the hydrogel and the hydrated film is statistically equivalent. Having said that, it is reasonable to assume that there is a threshold concentration for each molecule above which the independence of the flux from donor concentration is observed [52, 54]. This is consistent with the observation that iontophoretic delivery of BUF from the 5, 10, 20 mM solutions was statistically different (section 3.1). The results are in agreement with those seen with huperzine A where a 4-fold increase flux was seen upon increasing the drug concentration from 1 to 4 mM [52]. In the experiments conducted using aqueous BUF solutions at 5, 10 and 20 mM, the ratio of BUF with the counter ion (Cl^-) is in the range of 0.03-0.14 suggesting that the BUF concentration at 5 and 10 mM was still below the "threshold concentration" required so that the drug:counter-ion ratio is sufficient for flux independence to be observed [52]. More investigation is required to determine how this threshold concentration differs for individual cations.

It has been reported that a BUF concentration of 1.8 µg/mL produces a significant vasodilation [55]. The amount of BUF deposited in the LP by iontophoresis from the BUF mucoadhesive film and the corresponding estimated concentrations (**Figure 6b**) suggest that iontophoresis resulted in BUF concentrations in the LP – the therapeutic target area – that were >700-fold higher than the concentration reported to inhibit collagen production. This demonstrates that further optimization of iontophoretic conditions and a reduction to an even shorter current application period is possible – this would obviously facilitate treatment and compliance.

4. Conclusions

Advances in drug delivery technologies and the advent of efficient drug delivery strategies mean that pharmacokinetic limitations of existing dosage forms can be overcome. Here, short duration constant current buccal iontophoresis was successfully used to deliver potentially supra-therapeutic amounts of BUF to the mucosa. Electrotransport of BUF could be modulated using iontophoretic parameters and this could prove to be a useful tool to attenuate BUF delivery as a function of disease severity. Biodistribution studies provided precise information about the amounts of BUF delivered to the different tissues and showed that it was possible to reach the LP, which is the therapeutic target for treatment of OSF. A novel experimental set-up was also developed and tested in order to mimic *in vivo* conditions more closely. Nevertheless, it is worth noting that xerostomia and the diseased state of epithelium associated with OSF were not taken into account in this *in vitro* study and this could influence iontophoretic transport. However, it is considered that these would have a greater impact on passive delivery rather than iontophoretic transport but further preclinical studies are required.

5. Supplementary information

5.1 Validation of UHPLC-MS/MS method for quantification of BUF

BUF was detected using UHPLC-MS/MS. A gradient chromatographic elution method was developed; details are provided **in Table S1**.

Table S1. **Gradient chromatographic elution method**

Time (min)	Flow rate (mL/min)	Mobile phase A (%)	Mobile phase B (%)
0.00	0.30	10.0	90.0

0.75	0.30	10.0	90.0
1.00	0.30	50.0	50.0
1.80	0.30	20.0	80.0
2.00	0.30	90.0	10.0

The mass spectrometer settings are provided in **Table S2**.

Table S2. **MS/MS parameters for the detection of BUF**

Parameters	Value
Nature of parent ion	$[M+H]^+$
Parent ion (m/z)	308.287
Daughter ion (m/z)	237.139
MS mode collision energy (V)	2.0
MS/MS mode collision energy (V)	20.0
Cone voltage (V)	21.0
Capillary voltage (kV)	3.30
Source temperature (°C)	150
Desolvation temperature (°C)	350
Desolvation gas flow (L h−1)	650
Cone gas flow (L h−1)	50

LM resolution 1	2.90
HM resolution 1	14.8
Ion energy 1 (V)	0.40
LM resolution 2	2.90
HM resolution 2	14.8
Ion energy 2 (V)	0.70

5.1.1 *Specificity*

The developed method was considered specific for BUF quantification using the MRM transition observed for 308.287 → 237.139. BUF was eluted at 1.68 min. The chromatogram is presented in **Figure S1**.

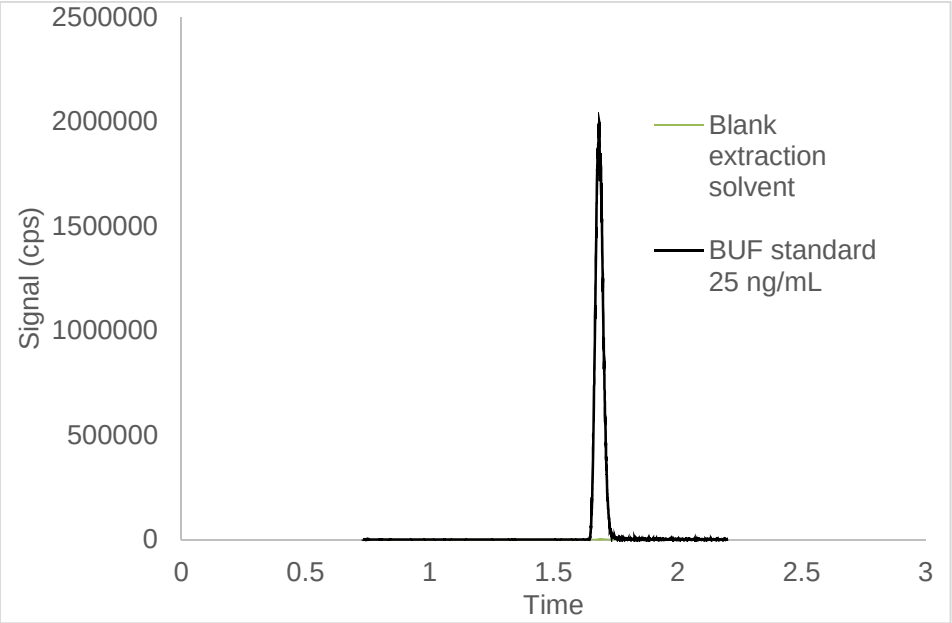

Figure S1 showing (i) blank extraction solvent (ii) BUF standard in mucosa extract

5.1.2 *Limit of detection and limit of quantification*

The limit of detection (LOD) and limit of quantification (LOQ) were 1.0 ng/mL and 5.0 ng/mL, respectively.

5.1.3 *Linearity*

The standards were prepared in the mucosa extract, which was prepared by soaking 2 cm^2 mucosa in 10mL of the extraction solvent MeOH:water (3:1) mixture or MeOH:PBS (1:1) . The method was found to be linear in the concentration range of 5-500 ng/mL. (R^2 = 0.99)

5.1.4 *Accuracy and precision*

Intra- and inter-day accuracy and precision were determined using 10, 50 and 500 ng/mL standards. **Table S3** shows the accuracy and precision values for BUF quantification method.

Table S3: Intra- and inter- day accuracy and precision values for BUF quantification

	Intra day			**Inter day 1**		
$[BUF]_{theo}$ (ng/mL)	$[BUF]_{mean}$ (ng/mL)	RSD (%)	Recovery (%)	$[BUF]_{mean}$ (ng/mL)	RSD (%)	Recovery (%)
5	5.4 ± 0.0	2.6	109.0	5.7 ± 0.4	2.4	109.0
50	50.1 ± 1.1	1.6	100.6	51.5 ± 1.7	2.8	103.0
500	504.1 ± 7.8	0.8	100.8	519.6 ± 24.9	0.2	100.6

5.2 Selection of BUF extraction solvent and filter type

Extraction solvent: In order to find the most suitable solvent for extracting BUF from mucosal tissue, 1.1 cm^2 mucosa tissue (n=3) was spiked with 1000 ng/cm^2 of BUF in methanol. After evaporation of the solvent, the tissue was cut into small pieces and soaked in 10 mL of either i) 75/25 methanol/water (v/v) or ii) 50/50 methanol/water (v/v) or iii) methanol. The extracts were analysed after centrifugation

by UPLC-MS/MS. The recovery percentages presented in **Table S4** were calculated by dividing the recovered amounts by the applied amounts.

Table S4: Selection of BUF extraction solvent from mucosal tissue

Solvent	Recovery (%)
75:25 methanol:water	90.1 ± 1.2
50:50 methanol:water	68.1 ± 1.6
methanol	65 ± 0.6

For all delivery experiments, 75/25 methanol/water (v/v) was used as the extraction solvent.

Filter selection: 0.22 µm pore size (i) nylon, (ii) polyvinylidene fluoride (PVDF) and (iii) polytetrafluoroethylene (PTFE) filters were tested to select the filter that allowed the maximum recovery of BUF. 100 ng/mL BUF in 75/25 (v/v) methanol/water containing mucosal extract was passed through the three filters (n=3). The filtered solution was injected in the UHPLC-MS/MS and the recovery percentage was calculated (**Table S5**)

Table S5: Selection of filter

Filter type	Recovery (%)
Nylon	59.4 ± 7.8
PVDF	83.6 ± 2.6
PTFE	37.5 ± 13.5

PVDF filer offered the maximum recovery of BUF and so was used to prepare all mucosal extracts before analysing in UPLC-MS/MS.

5.3 Biodistribution sample preparation

Upon completion of each delivery experiment experiment, the mucosa was cleaned with running water and a 0.5 cm^2 piece in contact with the formulation was punched out. This was fixed in OCT embedding medium, and flattened using a glass slide. It was instantly snap-frozen in isopentane cooled by liquid nitrogen. The tissue was sliced using Microm HM 560 Cryostat (Thermo Scientific; Walldorf, Germany) in 40 μm thick individual lamellae from the mucosa surface to a depth of 320 μm corresponding to the epithelium layer. The individual lamellae and the remaining tissue were extracted overnight in 1.5 mL and 10 mL of methanol:water (75:25 v/v), respectively. The extracts were centrifuged at 12,000 rpm for 15 minutes. They were then filtered using 0.22 μm PVDF filters (BGB Analytik SA) prior to analysis by UHPLC-MS/MS.

6. Acknowledgment

We would like to thank the University of Geneva for the financial support. VT is grateful to the Swiss Federal Commission of Scholarships for Foreign Students for the award of a PhD studentship. YNK and SdR would like to thank the Swiss Commission for Technology and Innovation for financial support (CTI 13933.2). The authors also thank the CMU Bioimaging platform and, in particular, Olivier Brun for his help with the wide-field slide scanner microscope for the histological slides.

7. References

1. Pindborg J. J., Murti P. R. *et al.* Oral submucous fibrosis as a precancerous condition. *Scand. J. Dent. Res.* **1984** *92(3)*: 224-9.

2. Aziz S. R. Coming to America: Betel Nut and Oral Submucous Fibrosis. *J. Am. Dent. Assoc.* **2010** *141(4)*: 423-428.

3. Papke R. L., Horenstein N. A. *et al.* Nicotinic Activity of Arecoline, the Psychoactive Element of "Betel Nuts", Suggests a Basis for Habitual Use and Anti-Inflammatory Activity. *PloS one.* **2015** *10(10)*: e0140907.

4. Sharan R. N., Mehrotra R. *et al.* Association of Betel Nut with Carcinogenesis: Revisit with a Clinical Perspective. *PloS one.* **2012** *7(8)*: e42759.

5. Lin K.-H., Lin C.-Y. *et al.* Arecoline N-Oxide: Its Mutagenicity and Possible Role as Ultimate Carcinogen in Areca Oral Carcinogenesis. *J. Argic. Food Chem.* **2011** *59(7)*: 3420-3428.

6. Tsai Y. S., Lee K. W. *et al.* Arecoline, a major alkaloid of areca nut, inhibits p53, represses DNA repair, and triggers DNA damage response in human epithelial cells. *Toxicology.* **2008** *249(2-3)*: 230-7.

7. James L., Shetty A. *et al.* Management of Oral Submucous Fibrosis with Injection of Hyaluronidase and Dexamethasone in Grade III Oral Submucous Fibrosis: A Retrospective Study. *J. Int. Oral Health.* **2015** *7(8)*: 82-85.

8. Dubourg A. and Scamuffa R. F. An Experimental Overview of a New Vasoactive Drug: Buflomedil HCl. *Angiology.* **1981** *32(10)*: 663-675.

9. Clissold S. P., Lynch S. *et al.* Buflomedil. A review of its pharmacodynamic and pharmacokinetic properties, and therapeutic efficacy in peripheral and cerebral vascular diseases. *Drugs.* **1987** *33(5)*: 430-60.

10. Aronson J. K., Buflomedil. In *Meyler's Side Effects of Drugs (Sixteenth Edition)*, ed.; Aronson, J. K., Elsevier, Oxford, 2016.

11. Lai D. R., Chen H. R. *et al.* Clinical evaluation of different treatment methods for oral submucous fibrosis. A 10-year experience with 150 cases. *J. Oral Pathol. Med.* **1995** *24(9)*: 402-6.

12. Gundert-Remy U., Weber E. *et al.* The clinical pharmacokinetics of buflomedil in normal subjects after intravenous and oral administration. *Eur. J. Clin. Pharm.* **1981** *20(6)*: 459-63.

13. Bourguignon L., Ducher M. *et al.* The value of population pharmacokinetics and simulation for postmarketing safety evaluation of dosing guidelines for drugs with a narrow therapeutic index: buflomedil as a case study. *Fundam. Clin. Pharmacol.* **2012** *26(2)*: 279-85.

14. Neri C., Barbareschi M. *et al.* Suicide by buflomedil HCl: a case report. *J. Clin. Forensic Med.* **2004** *11(1)*: 15-6.

15. Squier C. A. The permeability of oral mucosa. *Crit Rev Oral Biol Med.* **1991** *2(1)*: 13-32.

16. Sankar V., Hearnden V. *et al.* Local drug delivery for oral mucosal diseases: challenges and opportunities. *Oral Dis.* **2011** *17 Suppl 1*: 73-84.

17. Law S., Wertz P. W. *et al.* Regional variation in content, composition and organization of porcine epithelial barrier lipids revealed by thin-layer chromatography and transmission electron microscopy. *Arch. Oral Biol.* **1995** *40(12)*: 1085-1091.

18. Squier C. A. and Kremer M. J. Biology of oral mucosa and esophagus. *J. Natl. Cancer Inst. Monogr.* **2001** *(29)*: 7-15.

19. Matoltsy A. G. and Parakkal P. F. MEMBRANE-COATING GRANULES OF KERATINIZING EPITHELIA. *J. Cell Bio.* **1965** *24(2)*: 297-307.

20. Kalia Y. N., Naik A. *et al.* Iontophoretic drug delivery. *Adv. Drug Deliv. Rev.* **2004** *56(5)*: 619-658.

21. Gratieri T. and Kalia Y. N. Mathematical models to describe iontophoretic transport in vitro and in vivo and the effect of current application on the skin barrier. *Adv. Drug Deliv. Rev.* **2013** *65(2)*: 315-329.

22. Gratieri T., Santer V. *et al.* Basic principles and current status of transcorneal and transscleral iontophoresis. *Expert Opin. Drug Deliv.* **2017** *14(9)*: 1091-1102.

23. Gratieri T. and Kalia Y. N. Targeted local simultaneous iontophoresis of chemotherapeutics for topical therapy of head and neck cancers. *Int. J. Pharm. (Amsterdam, Neth.).* **2014** *460(1-2)*: 24-7.

24. Wanasathop A. and Li S. K. Iontophoretic Drug Delivery in the Oral Cavity. *Pharmaceutics.* **2018** *10(3)*.

25. Oh D. H., Kim M. J. *et al.* Strategic approaches for enhancement of in vivo transbuccal peptide drug delivery in rabbits using iontophoresis and chemical enhancers. *Pharm. Res.* **2015** *32(3)*: 929-40.

26. Campisi G., Giannola L. I. *et al.* Bioavailability in vivo of naltrexone following transbuccal administration by an electronically-controlled intraoral device: a trial on pigs. *J. Control. Release.* **2010** *145(3)*: 214-20.

27. De Caro V., Giandalia G. *et al.* New prospective in treatment of Parkinson's disease: studies on permeation of ropinirole through buccal mucosa. *Int. J. Pharm. (Amsterdam, Neth.).* **2012** *429(1-2)*: 78-83.

28. Jacobsen J. Buccal iontophoretic delivery of atenolol.HCl employing a new in vitro three-chamber permeation cell. *J. Control. Release.* **2001** *70(1-2)*: 83-95.

29. Thongkukiatkun W., Vongsavan K. *et al.* Effects of the iontophoresis of lignocaine with epinephrine into exposed dentine on the sensitivity of the dentine in man. *Arch. Oral Biol.* **2015** *60(8)*: 1098-103.

30. Gangarosa L. P., Sr. Current strategies for dentist-applied treatment in the management of hypersensitive dentine. *Arch. Oral Biol.* **1994** *39 Suppl*: 101s-106s.

31. Wilson J. M., Fry B. W. *et al.* Fluoride levels in dentin after iontophoresis of 2% NaF. *J. Dent. Res.* **1984** *63(6)*: 897-900.

32. Cubayachi C., Couto R. O. *et al.* Needle-free buccal anesthesia using iontophoresis and amino amide salts combined in a mucoadhesive formulation. *Colloids Surf. B Biointerfaces.* **2015** *136*: 1193-201.

33. Telo I., Tratta E. *et al.* In-vitro characterization of buccal iontophoresis: the case of sumatriptan succinate. *Int. J. Pharm. (Amsterdam, Neth.).* **2016** *506(1-2)*: 420-8.

34. Aframian D. J., Davidowitz T. *et al.* The distribution of oral mucosal pH values in healthy saliva secretors. *Oral Dis.* **2006** *12(4)*: 420-3.

35. Roesken F., Uhl E. *et al.* Acceleration of wound healing by topical drug delivery via liposomes. *Langenbecks Arch. Surg.* **2000** *385(1)*: 42-9.

36. Chen Y., Zahui T. *et al.* Cutaneous biodistribution of ionizable, biolabile aciclovir prodrugs after short duration topical iontophoresis: Targeted intraepidermal drug delivery. *Eur. J. Pharm. Biopharm.* **2016** *99*: 94-102.

37. Kandekar S. G., Singhal M. *et al.* Polymeric micelle nanocarriers for targeted epidermal delivery of the hedgehog pathway inhibitor vismodegib: formulation development and cutaneous biodistribution in human skin. *Expert Opin. Drug Deliv.* **2019** *16(6)*: 667-674.

38. Lapteva M., Mondon K. *et al.* Polymeric Micelle Nanocarriers for the Cutaneous Delivery of Tacrolimus: A Targeted Approach for the Treatment of Psoriasis. *Mol. Pharm.* **2014** *11(9)*: 2989-3001.

39. Lapteva M., Mignot M. *et al.* Self-assembled mPEG-hexPLA polymeric nanocarriers for the targeted cutaneous delivery of imiquimod. *Eur. J. Pharm. Biopharm.* **2019**.

40. Santer V., Del Rio Sancho S. *et al.* Targeted intracorneal delivery-Biodistribution of triamcinolone acetonide following topical iontophoresis of cationic amino acid ester prodrugs. *Int. J. Pharm. (Amsterdam, Neth.).* **2017** *525(1)*: 43-53.

41. Smart J. D. Drug delivery using buccal-adhesive systems. *Adv. Drug Deliv. Rev.* **1993** *11(3)*: 253-270.

42. Rajput G., Majmudar F. *et al.* Formulation and evaluation of mucoadhesive glipizide films. *Acta Pharm.* **2011** *61(2)*: 203-16.

43. Diaz Del Consuelo I., Pizzolato G. P. *et al.* Evaluation of pig esophageal mucosa as a permeability barrier model for buccal tissue. *J. Pharm. Sci. (Philadelphia, PA, U. S.).* **2005** *94(12)*: 2777-88.

44. Diaz Del Consuelo I., Falson F. *et al.* Transport of fentanyl through pig buccal and esophageal epithelia in vitro: influence of concentration and vehicle pH. *Pharm. Res.* **2005** *22(9)*: 1525-9.

45. Moscicka-Studzinska A. and Ciach T. Mathematical modelling of buccal iontophoretic drug delivery system. *Chem. Eng. Sci.* **2012** *80*: 182-187.

46. Naghipoor J., Jafary N. *et al.* Mathematical and computational modeling of drug release from an ocular iontophoretic drug delivery device. *Int. J. Heat Mass Tranf.* **2018** *123*: 1035-1049.

47. Scholz O. A., Wolff A. *et al.* Drug delivery from the oral cavity: focus on a novel mechatronic delivery device. *Drug Discov. Today.* **2008** *13(5)*: 247-253.

48. Kerr A. R., Corby P. M. *et al.* Use of a mucoadhesive disk for relief of dry mouth: a randomized, double-masked, controlled crossover study. *J. Am. Dent. Assoc.* **2010** *141(10)*: 1250-6.

49. Garnock-Jones K. P. Fentanyl Buccal Soluble Film: A Review in Breakthrough Cancer Pain. *Clin. Drug. Investig.* **2016** *36(5)*: 413-9.

50. Marro D., Kalia Y. N. *et al.* Contributions of electromigration and electroosmosis to iontophoretic drug delivery. *Pharm Res.* **2001** *18(12)*: 1701-8.

51. Padmanabhan R. V., Phipps J. B. *et al.* In vitro and in vivo evaluation of transdermal iontophoretic delivery of hydromorphone. *J. Control. Release.* **1990** *11(1)*: 123-135.

52. Kalaria D. R., Patel P. *et al.* Controlled iontophoretic transport of huperzine A across skin in vitro and in vivo: effect of delivery conditions and comparison of pharmacokinetic models. *Mol. Pharm.* **2013** *10(11)*: 4322-9.

53. Kasting G. B. and Keister J. C. Application of electrodiffusion theory for a homogeneous membrane to iontophoretic transport through skin. *J. Control. Release.* **1989** *8(3)*: 195-210.

54. Singh P., Boniello S. *et al.* Transdermal iontophoretic delivery of methylphenidate HCl in vitro. *Int. J. Pharm. (Amsterdam, Neth.).* **1999** *178(1)*: 121-8.

55. Vanhoutte P. M., Aarhus L. L. *et al.* Effects of buflomedil on the responsiveness of canine vascular smooth muscle. *J. Pharmacol. Exp. Ther.* **1983** *227(3)*: 613-20.

CHAPTER II

Controlled simultaneous iontophoresis of buflomedil hydrochloride and dexamethasone sodium phosphate to the mucosa for oral submucous fibrosis

Vasundhara Tyagi, César E. Serna-Jiménez, Yogeshvar N. Kalia

School of Pharmaceutical Sciences,
University of Geneva & University of Lausanne,
Rue Michel-Servet 1,
1206 Geneva, Switzerland

Manuscript in preparation

Abstract

The aim was to investigate simultaneous co-iontophoretic delivery of buflomedil hydrochloride (BUF) and dexamethasone phosphate (DEX-P) to the oral mucosa. A novel concentric set-up enabling simultaneous delivery of the two oppositely charged drugs was designed in house. Drug deposition in the different regions of the mucosa was quantified using UHPLC-MS/MS and UHPLC-UV methods. A constant current of 3.0 mA (0.6 mA/cm^2 for BUF and 1.95 mA/cm^2 for Dex-P) was applied to porcine esophageal mucosa for 5, 10 and 20 minutes. Iontophoresis for only 5 min increased total delivery of (i) BUF from 29.8 ± 5.1 nmol/cm^2 to 194.3 ± 23.8 nmol/cm^2 (ii) and DEX-P from 29.4 ± 1.2 nmol/cm^2 to 193.3 ± 19.8 nmol/cm^2 as compared to the passive controls. The biodistribution data offered provided into the extent of lateral migration by quantifying the amounts of drugs delivered to the tissue between the electrode compartments. In the absence of current, Dex-P was unable to migrate laterally to any neighbouring area and was found only under its application area. 5 minutes of current application increased the delivery of DEX-P > 5-fold under its application area and >8-fold in the adjacent area. Similarly, the delivery of BUF was enhanced ~ 6.8-fold under the area where it was applied and ~ 12.8-fold in the area where Dex-P was applied. Overall iontophoresis enabled the delivery of the two drugs at therapeutically relevant concentration in a rapid application time of 5 min. Moreover, iontophoresis provided a possibility to regioselectively deliver therapeutic agents and control their delivery kinetics. Short duration iontophoretic delivery of multiple therapeutic agents simultaneously to the mucosa may increase their bioavailability in the area and present a patient friendly treatment option for oral submucous fibrosis.

Keywords: iontophoresis; topical delivery; buflomedil; dexamethasone disodium phosphate; fibrosis; buccal delivery

1. Introduction

Oral submucous fibrosis (OSF) is a chronic disease characterized by inflammation, blanching and reduced mouth opening due to excessive collagen production [1, 2]. Patients suffering from early stage OSF have shown improvement after multi-target therapy involving oral administration of buflomedil (BUF), a vasodilator, in conjunction with a corticosteroid – topical triamcinolone acetonide (TA) or intralesional injection of dexamethasone (DEX) [3]. However, (i) oral administration of BUF can produce vascular and cardiac adverse effects and this led to the withdrawal of its marketing authorization by the European Medicines Agency [4], (ii) TA has been reported to be ineffective at a concentration of 0.1% for inflammation management [5], and (iii) intralesional injection of DEX alone or in conjunction with hyaluronidase, can cause patient discomfort [6, 7].

We have previously demonstrated the feasibility of using short duration iontophoresis [8, 9], to improve drug delivery to the buccal mucosa [10, 11]. The physicochemical properties of BUF make it an excellent candidate for iontophoresis and the amounts delivered to the mucosa in 10 min corresponded to supratherapeutic concentrations [11]. The objective of the present study was to extend the earlier work and to investigate the simultaneous co-iontophoresis of BUF and dexamethasone disodium phosphate (DEX-P), the water-soluble precursor of DEX, from the anodal and cathodal compartments, respectively (**Table 1**). The transdermal and ocular iontophoretic delivery of DEX-P have been extensively studied – including clinical trials in vivo [12-17] – there are no reports into its electrically-assisted delivery to the buccal mucosa.

Table 1. Physicochemical properties of the ions

	BUF	**Dex-P**
Molecular weight	307.3 g/mol	472.4 g/mol
logD	$0.07_{pH\ 6.0}$	$-4.49_{pH\ 7.0}$
pKa	10.15 ± 0.2	1.67 ± 0.1
logP	3.1 ± 0.4	-0.2 ± 0.5

There are few reports on the co-iontophoretic delivery of multiple therapeutic agents. We have previously investigated the co-iontophoretic delivery *in vitro* and *in vivo* of (i) pramipexole and

rasagiline – two cationic drugs – by anodal iontophoresis [18] and (ii) granisetron and metoclopramide and DEX-P – the first two by anodal iontophoresis and anionic DEX-P by cathodal iontophoresis [19]. These co-iontophoretic studies involved the transdermal delivery of drugs that acted systemically in the CNS and were performed with vertical diffusion cells. The simultaneous co-iontophoretic delivery of oppositely charged drugs treating a localized lesion required us to develop and to optimize a different electrode configuration – the "concentric set-up" (**Figure 1a**). The central circular electrode compartment was separated from the outer annular electrode compartment, by a ring of insulating material and the electrodes were customized to fit the respective compartments (**Figure 1b**). The set-up allowed the simultaneous administration of oppositely charged drugs to the same region in the mucosa and given the different surface areas in contact with the tissue in the two electrode compartments, it was possible to apply different current densities for anodal and cathodal iontophoresis.

a)

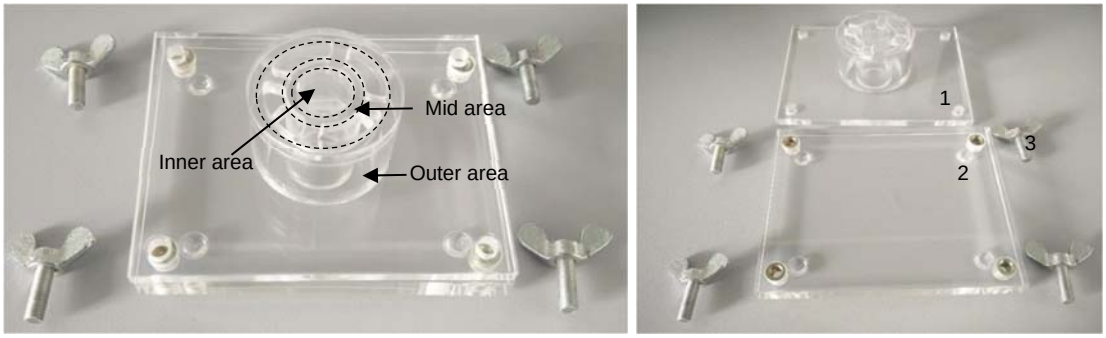

b)

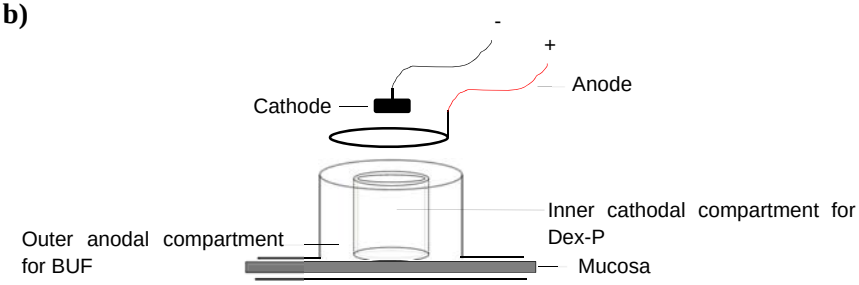

c)

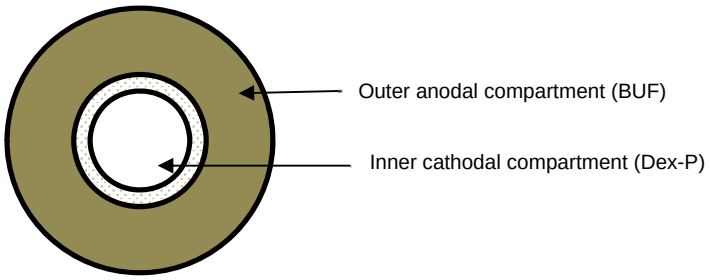

Figure 1 a) Different components of the concentric experimental set up 1. top tray 2. bottom tray 3. wing screws **b)** Schematic of experimental paradigm **c)** Mucosa application area after an experiment

Elucidation of the spatial distribution of drug delivery to the mucosa was achieved by quantifying the amounts of each drug present beneath the respective electrode compartments and from the tissue below the insulator separating the two compartments. Thus, it was possible to investigate the effect of iontophoretic parameters on the lateral electrotransport of drugs into and through the buccal mucosa from one electrode compartment towards the other.

The specific aims of the study were (i) to examine the stability of prodrug DEX-P in the presence of mucosal tissue, (ii) to investigate the simultaneous co-iontophoretic delivery of the two oppositely charged drugs and to determine the drug distribution in the mucosa following anodal iontophoresis of BUF and cathodal iontophoresis of DEX-P), (iii) to study the influence of experimental parameters – duration of current application and current density – on delivery and distribution, and (iv) to determine whether the amounts of BUF and DEX-P deposited in the mucosa after short duration co-iontophoresis were therapeutically relevant.

2. Materials and methods

2.1 Materials

DEX-P, DEX, BUF and phosphate buffered saline were purchased from Sigma Aldrich (Buchs, Switzerland). NATROSOL™ 250 hydroxyethylcellulose (HEC) was a generous gift from Hercules Inc.). LC-MS grade acetonitrile (ACN) and methanol (MeOH) were purchased from Fisher Scientific (Reinach, Switzerland). LC-MS grade formic acid was purchased from Chemie Brunschwig (Basel, Switzerland). All aqueous solutions were prepared using Milli-Q water (resistivity > 18 MΩ.cm.

2.2 Analytical method

DEX-P and DEX were quantified using a Waters Acquity® UPLC® H-Class system (Baden-Dättwil, Switzerland) coupled with a UV Detector (Waters; Baden-Dättwil, Switzerland). Gradient separation was accomplished using a Waters XBridge® BEH C18 (100 x 2.1 mm, 2.5 µm; (Baden-Dättwil, Switzerland)) column maintained at 45°C. The mobile phase consisted of 5 mM ammonium acetate (pH 6.8) and acetonitrile (ACN). The flow rate was 0.3 mL/ min and the injection volume was 5 µL. The run time was 4 min and DEX-P and DEX eluted at 1.6 min and 3.6 min, respectively. The limits of detection (LOD) for DEX and DEX-P were 0.1 µg/mL and 0.25 µg/mL, respectively, and the corresponding limits of quantification (LOQ) were 0.5 µg/mL and 1.0 µg/mL. BUF was quantified using a Waters Acquity® UPLC® core system coupled to a Xevo® TQ-MS system (Baden-Dättwil, Switzerland) in ESI^+ mode and with multiple reaction monitoring (MRM). BUF was separated by a gradient method using Waters XBridge® BEH C18 (50 x 2.1 mm, 2.5 µm) reverse phase column maintained at 40°C. The mobile phase comprised 0.1 % formic acid and 0.1% formic acid in acetonitrile and the flow rate was 0.3 mL/min. Injection volume was 5 µL and the run time was 2 min and BUF eluted at 1.6 min. The LOD and LOQ were 1 ng/mL and 5 ng/mL, respectively. Complete details including the validation of the methods according to ICH guidelines are presented in the **Supplementary Information.**

2.3 Formulation development

Non-ionic HEC was used to prepare hydrogels of DEX-P and BUF (i) to avoid competition from charge carriers present in an ionic polymer and (ii) because the mucoadhesive properties of HEC are not affected by electrolytes present in the formulation [20]. Under constant stirring, (i) 3.5% w/v HEC was added to an unbuffered aqueous solution of 40 mM DEX-P (10 mL, pH 7.2) and (ii) 2% w/v HEC was added to an unbuffered aqueous solutions of 20 mM BUF (10 mL, pH 5.9), respectively. The polymeric solutions were stirred at 200 rpm for 4 h until they became clear. They were left overnight for swelling of the polymeric chains.

2.4 Preparation of mucosal tissue

The studies described below were performed using porcine oesophageal mucosa as a surrogate for human buccal mucosa [21, 22]. Porcine oesophagus was collected from a local abattoir (Abbatoir de Loëx Sàrl, Bernex, Switzerland) within 2 h of slaughter. Once in the laboratory, the oesophagus was rinsed with isotonic saline and cut longitudinally to reveal the mucosa. The mucosa was carefully isolated from the underlying muscle using a scalpel. After isolation, the mucosa was cleaned with cold Krebs-

Ringer bicarbonate buffer (KRB, pH 7.4). The mucosa was wrapped in Parafilm® and stored at -20°C for a maximum period of 3 months. Prior to an experiment, the mucosa was thawed and equilibrated in KRB for 30 min.

2.5 In vitro studies with porcine oesophageal mucosa

2.5.1 Stability of DEX-P in contact with the mucosal tissue

Briefly, 2 cm^2 of fresh mucosa was cut into small pieces and placed in a glass vial containing 10 mL of of DEX-P solution (100 µg/mL in PBS (pH 7.4)). The vials were constantly stirred at room temperature. Controls to assess solution stability of DEX-P were performed in PBS alone. Aliquots were collected every 10 min for 2 h and were analysed using UHPLC-UV. All analyses were performed in triplicate. Similarly, the stability of DEX-P was also studied in the extraction solvent for 24 h and is presented in the **Supplementary Information.**

2.5.2 Concentric delivery setup and transport studies

The concentric set-up (**Figure 1a**) used for all delivery experiments (Elega SA; Vernier, Switzerland) consisted of two poly(methyl methacrylate) trays that were held together using four winged screws. The upper tray contained the two formulation-containing "donor/electrode" compartments; the circular central compartment was separated from the outer ring by a concentric insulating section. The exact dimensions of the set-up are provided in the **Supplementary Information**. The lower tray acted as the base on which the mucosal tissue was placed. A surgical absorbent pad moistened with PBS pH 7.4 was placed under the mucosa to ensure tissue hydration during the experiment. The mucosa was fixed between the two trays by fastening the screws. The areas of the circular central compartment and the outer ring compartment were 1.5 cm^2 and 4.8 cm^2, respectively and this difference was reflected in the current densities applied in the two compartments. At physiological pH, the mucosa is negatively charged, and anodal iontophoresis of cations (e.g. BUF) is favoured over cathodal iontophoresis of anions (e.g. DEX-P), since cation electrotransport is due to both electromigration and electroosmosis [8, 19, 23]. Therefore, the DEX-P HEC gel was applied to the inner circular compartment while the BUF HEC gel was applied in the outer ring – ensuring that a higher current density would be used to deliver DEX-P. For the anodal compartment (outer ring containing the BUF gel), a customized flat silver ring was used to ensure the current was applied uniformly to the surface (**Figure 1b**). For the iontophoresis experiments, a constant current was applied using Ag/AgCl electrodes connected to a power supply (APH 1000 M, Kepco Inc; Flushing NY, USA). DEX-P in the circular central compartment was connected to the cathodal compartment via a salt bridge to avoid any competition from Cl- generated

at the cathode. Salt bridges were not required for BUF as use of its the hydrochloride salt enabled sufficient Cl^- ions to be present to ensure Ag/AgCl electrochemistry at the anode.

Electrotransport experiments were performed to investigate (i) the duration of current application and (ii) the current density, on iontophoretic delivery of BUF and DEX-P (**Table 2)**.

Table 2. Experimental conditions

Condition	**Current density (mA/cm^2)**		**Number of moles applied (µmoles)**		**Application time (minutes)**
	BUF	Dex-P	BUF	Dex-P	
I_{20}	0.61	1.95	20	40	20
I_{10}	0.61	1.95			10
I_5	0.61	1.95			5
$I_{0.2/0/61}$	0.2	0.65			10
P_{20}	-	-			20
P_{10}	-	-			10
P_5	-	-			5

2.5.2.1 Effect of duration of current application

An iontophoretic current of 3 mA corresponding to current densities of 1.95 mA/cm^2 and 0.6 mA/cm^2 in the cathodal (central) compartment containing the DEX-P HEC gel (1 mL of 40 mM DEX-P, pH 7.1) and the anodal (ring) compartment containing the BUF HEC gel (4 mL of 20 mM BUF, pH 5.9), was applied for – 5, 10 and 20 min (I_5, I_{10} and I_{20}). Control experiments were performed using the same set-up without the application of current (P_5, P_{10} and P_{20}).

2.5.2.2 Effect of current density

The second series of experiments measured the effect of current density on the iontophoretic delivery of DEX-P (and DEX) and BUF after application of the gel formulations described above for 10 min. Two current conditions were tested: (i) 3 mA current, i.e. 1.95 mA/cm^2 for DEX-P ($I_{1.95}$) and 0.6 mA/cm^2 for BUF ($I_{0.6}$) and (ii) 1 mA current – 0.65 mA/cm^2 for DEX-P ($I_{0.65}$) and 0.2 mA/cm^2 for BUF

($I_{0.2}$). Passive experiments performed using the same set-up but in the absence of current application served as controls (P).

After the completion of the experiment, the formulations were carefully removed from the mucosal surface and the set-up dismantled. The mucosa samples were cleaned with water and PBS. The three areas of the mucosal tissue – the area under the DEX-P formulation (circular central area), the BUF formulation (outer ring) and the ring of tissue under the insulator ring between the two applications areas, were punched out (**Figure 1c**). They were cut into small pieces and extracted separately in 5 mL of 75:25 (MeOH:water) for 12 h.

2.6 Data analysis

Data are expressed as mean ± standard deviation. Statistical significance was evaluated by ANOVA or by Student's t-test (α =0.05).

3. Results and Discussions

3.1 Stability of DEX-P in solution and in the presence of mucosa

The stability of DEX-P in solution in the absence/presence of mucosa was monitored over 120 min (**Figure 2**). In the absence of mucosa, the concentration of DEX-P in PBS solution after 120 min was 99.8 ± 0.6 % of the initial value (indeed, after 24 h it was 96.9 ± 0.2 % of the initial value) indicating that it was essentially unaltered in solution over this time period. Conversion of DEX-P to DEX increased in the presence of mucosa; in this case, the concentration of DEX-P in solution after 120 min was 89.0 ± 0.4 % of the initial value. The mucosal tissue clearly had an influence over the hydrolysis of the phosphoester linkage. The esterase/phosphatase activity of the mucosa is well established [24, 25]. It should noted that the hydrolysis of ester prodrugs *in vitro* is reported to be slower than *in vivo* [19, 26]. It is expected that the biotransformation of DEX-P to DEX could be more rapid in the mouth due to the enzymatic activity of saliva and once the prodrug reaches the subepithelial capillaries that contain the circulating esterases [27].

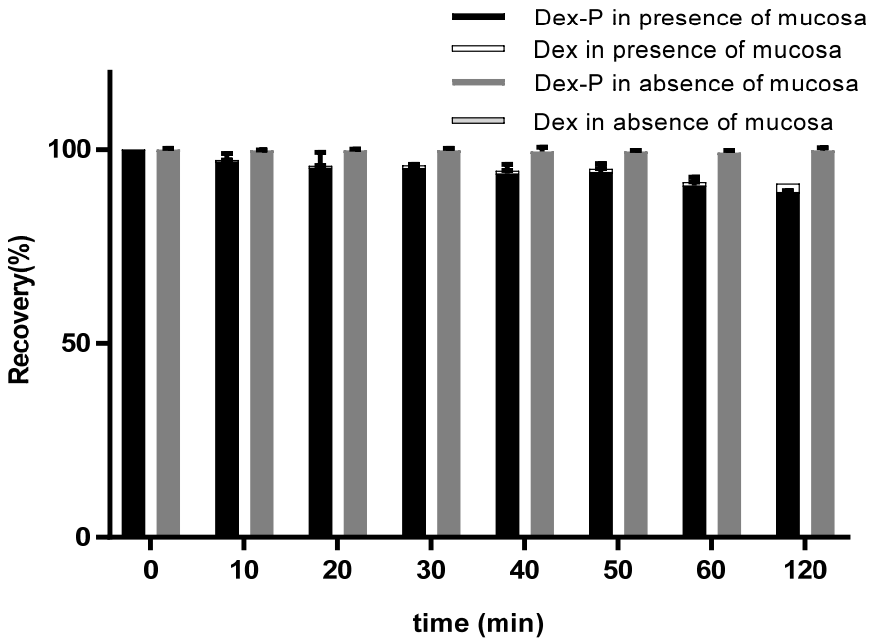

Figure 2. Effect of presence of mucosal tissue on the bioconversion of DEX-P to DEX

Nevertheless, given that the iontophoretic transport experiments had durations of 5-20 min, the solution stability was more than sufficient to proceed (at 20 min, the concentration of DEX-P in solution was 95.3 ± 3.9 %). The presence of the phosphate group is essential to the iontophoretic transport of the drug, since its cleavage leads to the loss of the two ionisable groups (pKa of 2.0 and 6.0) that are key to the electromigration of DEX-P. As we have shown previously, the kinetics of prodrug hydrolysis condition the depth of prodrug/drug (in this case, DEX-P/DEX) penetration into the tissue [28].

3.2 Transport studies using the concentric set-up

3.2.1 Effect of duration of current application

In these experiments, the aim was to determine the amount of drug delivered to the buccal mucosa as a function of decreasing current application times, given that the shorter the duration the better the adherence and ease of use *in vivo*. The deposition of BUF in the different areas of the mucosa, moving from the tissue directly under the application site (outer area), under the insulating ring (mid area) and the central circular compartment (inner area) following different durations of current application (and the corresponding passive controls) are shown in **Figure 3a**.

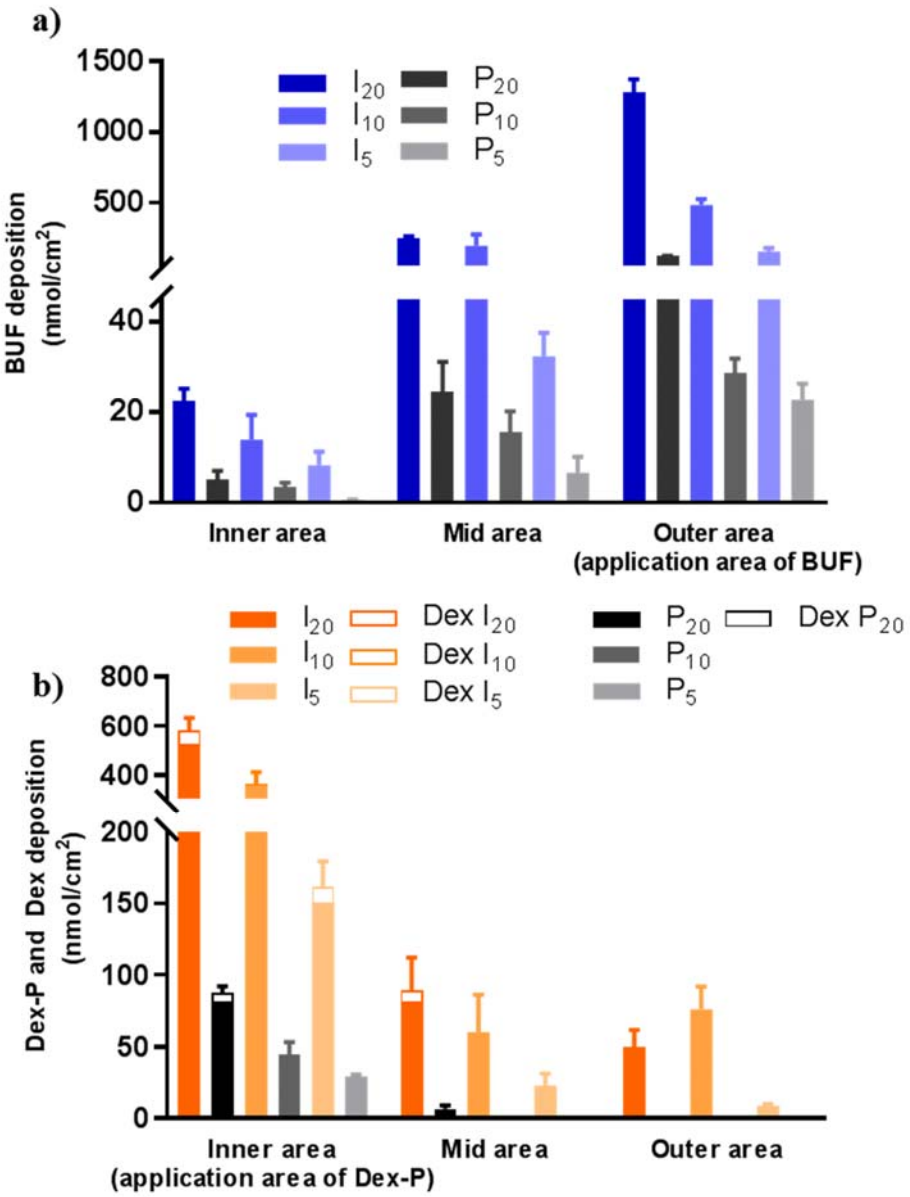

Figure 3. a) Effect of application time BUF: fixed current density, I_{20}, I_{10}, I_5 and passive controls P_{20}, P_{10}, P_5, b) Effect of application time DEX-P and DEX (empty box): fixed current density, I_{20}, I_{10}, I_5 and passive controls P_{20}, P_{10}, P_5

After 20 min of passive application of HEC gel containing 20 µmol BUF (pH 5.9), total BUF deposition under its own application area (outer ring) was 120.1 ± 2.4 nmol/cm^2 (**Figure 3a;** (P_{20})); the amounts under the neighbouring mid area (under the insulator) and the inner circular area were 24.6 ± 6.5 and 5.0 ± 2.0 nmol/cm^2, respectively. Thus, BUF was partitioning into the mucosa from the gel and then

diffusing from the ring below the application area and along a concentration gradient towards the central circular space. When the formulation application time was reduced to 10 and 5 min, P_{10} and P_5, respectively, the total deposited amounts decreased to 49.1 ± 5.8 and 29.8 ± 5.1 nmol/cm^2. The amounts of BUF found under the application area, i.e. the outer area after 10 and 5 min were statistically similar ($p > 0.05$) but there was more BUF under the mid and inner areas after 10 min (P_{10}) than after 5 min (P_5) – e.g. for in the inner circular area, the amounts were 3.4 ± 0.9 and 0.64 ± 0.05 nmol/cm^2, respectively.

Application of a 3.0 mA current corresponding to current densities of 0.61 mA/cm^2 for anodal iontophoresis of BUF and 1.95 mA/cm^2 for cathodal iontophoresis of DEX-P, respectively, for 20 min (I_{20}) increased BUF deposition in the outer ring more than 10-fold to 1279.8 ± 92.2 nmol/cm^2. The amounts of BUF migrating to the mid and inner areas were also increased as compared to simple passive diffusion: 244.7 ± 14.7 and 22.4 ± 2.8 nmol/cm^2 were found in the mid and inner area, respectively, after iontophoresis for 20 min, corresponding to ~20 % of total BUF deposition. Decreasing the duration of current application to 10 and 5 min still resulted in total BUF deposition in the mucosal tissue that was 14- and 6.6-fold higher than the passive controls. After current application for 5 min BUF transport to the inner area was 12-fold greater than the passive control (8.21 ± 3.0 versus0.64 ± 0.05 nmol/cm^2).

After 20 min of passive transport (P_{20}), 81.2 ± 4.1 nmol/cm^2 of DEX-P (and 6.1 ± 2.3 nmol/cm^2 of DEX) were found under the circular, inner application area and DEX-P had also diffused to the neighbouring mid area under the insulator, (6.8 ± 2.25 nmol/cm^2) . However, the amounts of DEX-P found in the distal outer circular ring were <LOQ. On decreasing the application time to 10 and 5 min (P_{10} and P_5), amounts of DEX-P found under the application area were 44.6 ± 8.8 and 29.2 ± 1.2 nmol/cm^2 ($p < 0.05$), respectively, but no DEX-P was found in the mid or outer areas (**Figure 3b**).

Application of the 3 mA current for 20 minutes (I_{20}), which corresponded to a current density of 1.95 mA/cm^2 in the inner area, resulted in a 6-fold increase in the amount of DEX-P below the application site, while 14-fold and 50-fold increases were seen in the amounts migrating to the mid and outer areas, respectively (**Figure 3b**). Furthermore, in contrast to the passive controls (P_{10} and P_5), deposition of DEX-P under the application area after iontophoresis for 10 and 5 min (I_{10} and I_5) were significantly different ($p < 0.05$) (**Figure 3b**). It was also noted that DEX-P was detected in the mid- and outer areas for each condition, I_{20}, I_{10} and I_5 – which was not the case for the corresponding passive controls, except for the mid area with P_{20}.

3.2.2 Effect of applied current density

For the second series of experiments, the applied current was decreased from 3 mA to 1 mA, corresponding to current densities of 0.2 mA/cm^2 for BUF and 0.65 mA/cm^2 for DEX-P, respectively, and applied for 10 min. The decrease in current density resulted in a ~7-fold decrease in BUF deposition under the application area (**Figure 4a**). The extent of BUF transport towards the inner compartment also decreased. BUF deposition under the outer, mid and inner areas after iontophoresis at 0.2 mA/cm^2 for 10 min was 69.1 ± 21.7, 27.9 ± 11.5 and 5.0 ± 0.9 nmol/cm^2, which was significantly less than that seen after iontophoresis at 0.61 mA/cm^2 (481.15 ± 43.3, 191.9 ± 81.3 and 13.8 ± 5.4 nmol/cm^2, respectively).

Decreasing the current density from 1.95 mA/cm^2 to 0.65 mA/cm^2 resulted in a 3.8-fold decrease in the total deposition of DEX-P in the mucosa, 499.8 ± 55.8 and 129.08 ± 18.1 nmol/cm^2, respectively (**Figure 4b**). The decrease in current density also had an effect on the radial migration of DEX-P: although iontophoresis at 1.95 mA/cm^2 enabled 75.7 ± 16.1 nmol/cm^2 of DEX-P to be delivered to the outer ring (anodal compartment), no DEX-P was detected there after iontophoresis at 0.65 mA/cm^2: DEX-P was only observed under the inner and mid areas.

The amounts and spatial distribution of BUF and DEX-P in the three areas of the mucosa following the different experimental conditions tested are given in **Table 3**. The results clearly demonstrate the lateral movement of the drug ions from the respective compartments containing the formulations towards the counter electrode – confirming the hypothesis that the concentric set-up can be used to deliver oppositely charged drugs simultaneously to the same region of tissue. Buccal bioavailability of both drugs was significantly improved upon current application as compared to simple passive diffusion. (**Table 3**).

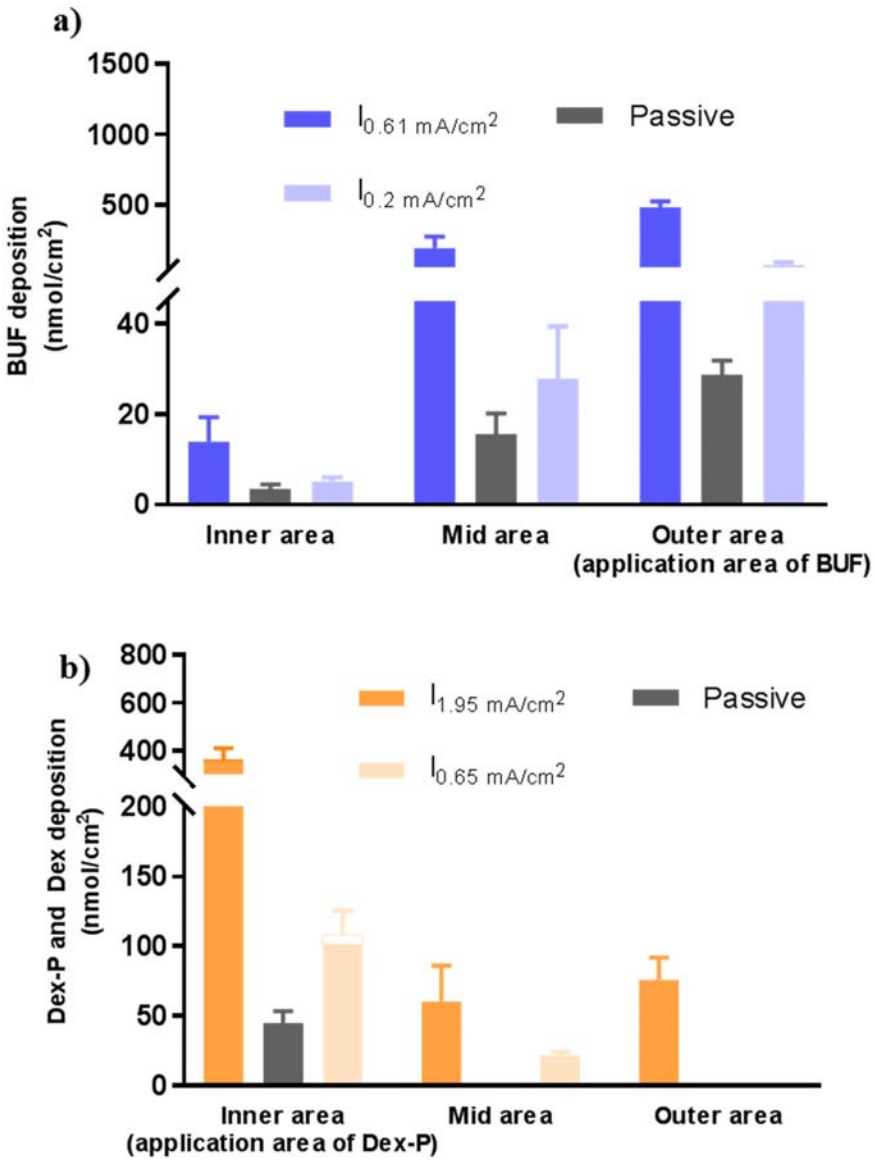

Figure 4. a) Effect of current density BUF: $I_{0.6}$, $I_{0.2}$ mA/cm^2 and passive control b) Effect of current density DEX-P: $I_{1.95}$, $I_{0.65}$ mA/cm^2 and passive control

Table 3. Amount of BUF and Dex-P deposited in the different regions of the mucosa (nmoles/cm^2)

	Cathode (application area of Dex-P)		Mid area		Anode (application area of BUF)	
	Q_{Dex-P}^{C-A}	Q_{BUF}^{A-C}	Q_{Dex-P}^{C-A}	Q_{BUF}^{A-C}	Q_{Dex-P}^{C-A}	Q_{BUF}^{A-C}
I_{20}	524.6 ± 51.8	22.4 ± 2.8	80.8 ± 22.5	244.7 ± 14.7	50.1 ± 11.8	1279.8 ± 92.2
P_{20}	81.2 ± 4.1	5.0 ± 2.0	6.8 ± 2.2	24.6 ± 6.5	<LOQ	120.1 ± 2.4
I_{10}	356.0 ± 46.7	13.8 ± 5.4	60.3 ± 25.8	191.9 ± 81.3	75.7 ± 16.1	481.1 ± 43.3
P_{10}	44.6 ± 8.8	3.4 ± 0.9	<LOQ	15.6 ± 4.6	<LOQ	28.6 ± 3.2
I_5	150.7 ± 17.9	8.2 ± 3.0	23.1 ± 8.2	32.3 ± 5.2	8.9 ± 1.0	153.7 ± 23.0
P_5	29.2 ± 1.2	0.6 ± 0.0	<LOQ	6.6 ± 3.4	<LOQ	22.6 ± 3.8
$I_{0.2/0.65}$	101.5 ± 17.7	5.0 ± 0.9	21.4 ± 2.7	27.9 ± 11.5	<LOQ	69.1 ± 21.7

Q_{Dex-P}^{C-A} is the number of moles of Dex-P deposited in the area, Q_{BUF}^{A-C} is the number of moles of BUF deposited in the area

Delivery efficiency is the ratio between the amounts delivered per cm^2 to the amount of drug applied per cm^2. When 3 mA current was applied to the mucosa for 5 min (I_5), the molar amount of DEX-P applied in the donor compartment was double as compared to BUF; however, the delivery efficiency (%) for BUF was over 7 times more than DEX-P (5.7% versus 0.8%). The transport efficiency (%) which defines the ratio of the fraction of charge carried by an ion to the total charge passed, of BUF was significantly higher than DEX-P (11.3 ± 2.6 versus 2.8 ± 0.3). We already showed in previous studies that BUF is an exceptional candidate for iontophoresis displaying good transport efficiencies of up to 13% with short duration iontophoresis. DEX-P has been extensively studied for transdermal and ocular iontophoresis and has displayed significant enhancement compared to passive transport [13, 29, 30]. The isoelectronic point of mucosa is reported as 3 therefore at physiological pH, the mucosa behaves as a negatively charged that is permselective for cations [31]. To maintain the electroneutrality, a preferential solvent flow, electroosmosis, occurs from the anodal to the cathodal compartment. Hence, a cation such as BUF is transported by electromigration and electroosmosis while the delivery of an anion could be hindered by this solvent flow, which might explain the superior delivery efficiency of

BUF over Dex-P [32]. Transport studies with a neutral marker to investigate the contribution of electromigration and electroosmosis are required to confirm the hypothesis.

It is clear that shorter durations of current application would increase ease of use and favour patient adherence. Therefore, it was decided to investigate the therapeutic relevance of the amounts of BUF and DEX-P delivered after iontophoresis at 3 mA for 5 min and to see how these amounts compared to the concentrations required to elicit pharmacological effects (**Figure 5**). It has been reported that DEX significantly inhibited leukocyte infiltration at a concentration 0.6 nmol/mL [33] and that BUF significantly inhibited collagen-induced aggregation at a concentration of 6 nmol/mL [34]. Iontophoresis for 5 min at a current density of 1.95 mA/cm^2 enabled delivery of DEX-P to all regions, including the tissue under the outer ring at a concentrations superior to those inhibiting leukocyte infiltration (e.g. for the outer ring, 99 –fold >IC_{50}).; in contrast, no DEX-P was detected in this area after passive application. The concentration achieved under its own application area was 1790-fold > IC_{50}.

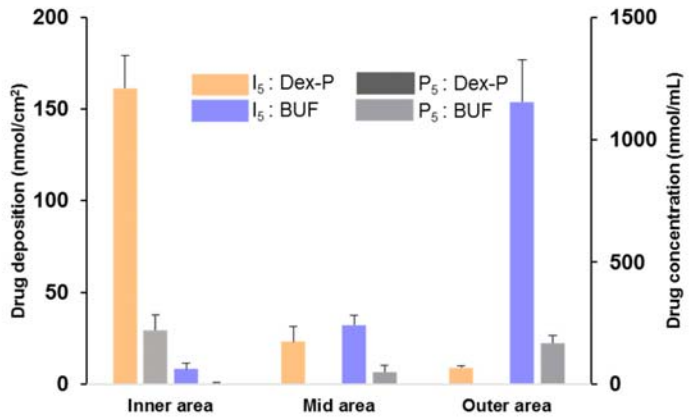

Figure 5. Drug deposition and concentrations in the mucosa after 5 min of passive and iontophoretic transport

In the absence of current, superior lipophilicity of BUF (logD value at pH ~ 6.5 : 0.31 versus – 4.49) facilitated its entry into the mucosa from where it could diffuse to the inner area but therapeutic concentrations could not be reached. Iontophoresis at 0.61 mA/cm^2 for 5 min, resulted in a 13-fold increase in BUF delivery to the inner area, which meant that the concentration was 5-fold > than than the IC_{50} (6 nmol/mL). Under its own application site, iontophoresis resulted in concentrations that were ~170-fold > the IC_{50}. In summary, iontophoresis was able to deliver both the drugs in the entire mucosal tissue at therapeutically relevant concentrations in only 5 minutes.

4. Conclusions

The concentric set up demonstrated its utility for topical delivery studies involving co-iontophoresis of drugs with opposite polarity to the same target area. The configuration, with both drugs being placed on the epithelial side of the membrane, better mimicked the conditions in vivo. Results confirm that constant current iontophoresis can be used to achieve pharmacologically relevant concentrations of DEX-P and BUF in the mucosa in 5 minutes.

Iontophoresis afforded higher transport and superior delivery efficiencies compared to a simple passive transport. Nevertheless, it is worth mentioning that the delivery studies described here do not take into account saliva flushing, mucin barrier and the vascularization of mucosa. Hence, these promising results will need to be confirmed in preclinical studies in vivo.

5. Supplementary information

Details of analytical method development and validation of BUF are mentioned in **Chapter I**

5.1 Quantification of Dex-P and Dex using UHPLC-TUV detector

Table S4 shows the details of the gradient chromatographic elution method for simultaneous quantification of Dex-P and Dex

Table S4: Gradient chromatographic elution method of Dex-P and Dex

Time (min)	Flow rate (mL/min)	Mobile phase A (%)	Mobile phase B (%)
0.00	0.30	75.0	25.0
1.20	0.30	75.0	25.0
1.30	0.30	50.0	50.0
2.30	0.30	50.0	50.0
2.35	0.30	75.0	25.0

5.1.1 Specificity

The method was specific for Dex-P and the metabolite Dex at 240nm. Dex-P and Dex were eluted at 1.68 min and 3.67 min respectively. Figure S2 shows the chromatograms of Dex-P, Dex standard solutions in the mucosa matrix and blank extraction solvent MeOH:water (75:25). Mucosa matrix preparation is mentioned in section 1.1.

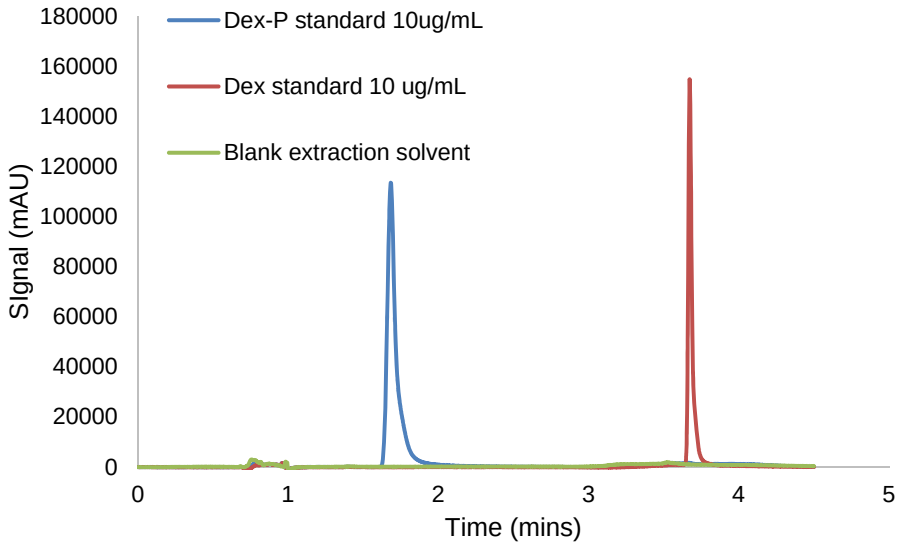

Figure S1. Chromatogram from UHPLC-UV for the simultaneous quantification of Dex-P and Dex

5.1.2 Limit of detection and limit of quantification

The LOD and LOQ of Dex-P were 0.25 and 1 µg/mL respectively. For Dex they were 0.1 and 0.5 µg/mL respectively.

5.1.3 Linearity

The method was linear for Dex-P from the concentration range of 1-100 µg/mL ($R^2 = 0.99$). For Dex the concentration range was 0.5-50 ($R^2 = 1$).

5.1.4 Accuracy and precision

Table S5 and S6 show the accuracy and precision values for Dex and DexP quantification method respectively.

Table S5: Intra- and inter- day accuracy and precision values for Dex quantification

	Intra day			**Inter day 1**		
$[Dex]_{theo}$ (µg/mL)	$[Dex]_{mean}$ (µg/mL)	RSD (%)	Recovery (%)	$[Dex]_{mean}$ (µg/mL)	RSD (%)	Recovery (%)
0.5	0.46 ± 0.0	1.3	93.3	0.47 ± 0.0	2.8	93.4
5	4.9 ± 0.0	1.6	98.7	5.0 ± 0.0	0.5	100.0
50	50.2 ± 0.2	0.5	100.4	50.1 ± 0.7	1.5	100.2

Table S6: Intra- and inter- day accuracy and precision values for Dex-P quantification

	Intra day			**Inter day 1**		
$[Dex\text{-}P]_{theo}$ (µg/mL)	$[Dex\text{-}P]_{mean}$ (µg/mL)	RSD (%)	Recovery (%)	$[Dex\text{-}P]_{mean}$ (µg/mL)	RSD (%)	Recovery (%)
1	1.0 ± 0.0	1.0	101.9	1.0 ± 0.0	0.8	103.4
5	5.0 ± 0.1	0.05	101.0	5.5 ± 0.05	1.0	110.0
50	51.8 ± 0.4	0.9	103.7	51.7 ± 0.2	0.5	103.4

5.2 Stability of Dex-P in the extraction solvent

The metabolic stability of DEX-P in the presence of mucosal tissue stability was studied by placing DEX-P solution prepared in the extraction solvent (used for the experiments) in contact with fresh mucosa. Briefly, 2 cm^2 mucosa cut into small pieces was placed in a glass vial containing 10mL of 100µg/mL of Dex-P in 75:25 (MeOH:water). The vials were constantly stirred. Mucosa was absent from the vials that served as control. Aliquots were collected after 0, 1, 2, 4, 8, 18 and 24 hours and were analysed using UPLC-UV. All analysis were performed in triplicate. **Figure S3** shows the extent of metabolism of Dex-P to Dex in presence and absence of mucosa. Similar to the stability study performed in PBS, mucosa had a significant effect on the hydrolysis of Dex-P to Dex.

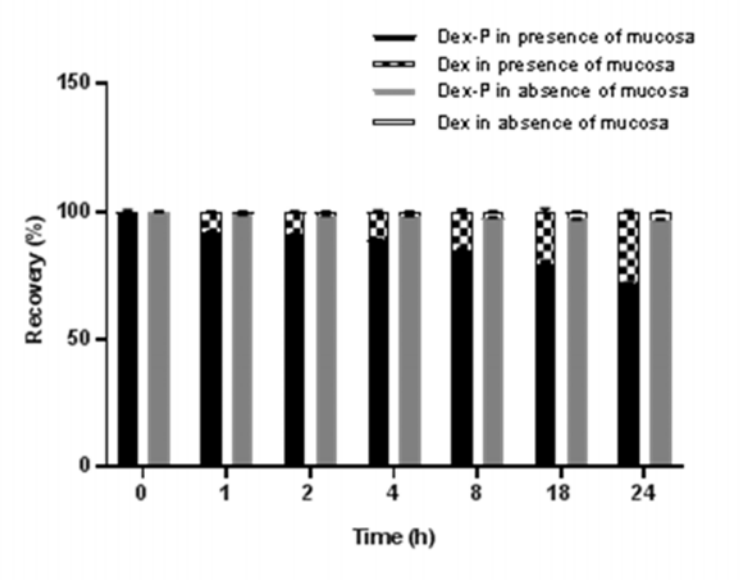

Figure S3. Effect of mucosal tissue on the metabolism of Dex-P

5.3 Concentric set-up

The set-up was designed in house and constructed by Elega SA (Le Lignon, Switzerland). The set-up was made of polymethly(methacrylate). The base of the set-up on which the mucosa piece was placed was 10 x 8 cm. The top part of the set-up, which sandwiched the mucosa had the concentric donor compartment was also 10 x 8 cm. The height of the cylinder from the base of the tray was 2 cm. Thickness of both the trays was 1 cm. Figure S4 shows a schematic of the top tray and the bottom of the top tray which had the donor area. Photographs of the concentric set-up are displayed in Figure S5.

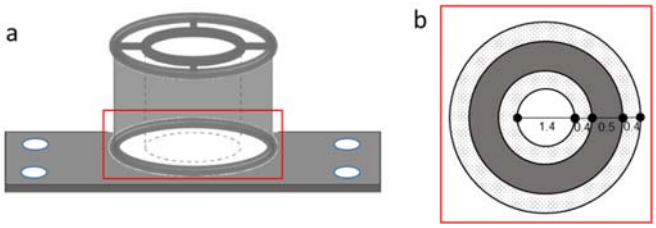

Figure S4. a) Schematic of the top tray with the two donor compartments b) Dimensions of the floor of the cylinder.

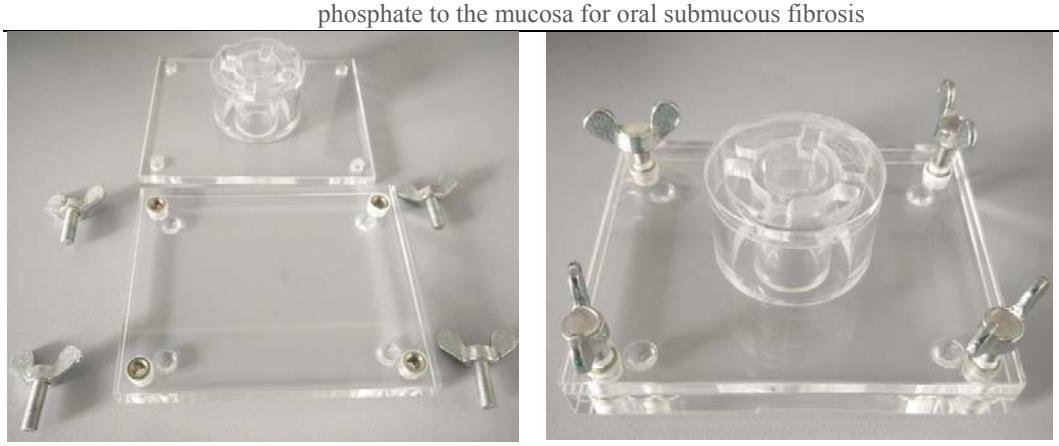

Figure S5. Photographs of a) individual components of the concentric set-up b) working model of the set-up.

6. Acknowledgment

We would like to thank University of Geneva for financial support. VT is grateful to the Swiss Federal Commission for Scholarships for Foreign Students for the award of a PhD fellowship. YNK would like to thank the University of Geneva, the Fondation Ernst and Lucie Schmidheiny and the Société Académique de Genève for providing financial support to enable the acquisition of the Waters Xevo® TQ-MS detector.

7. References

1. Wollina U., Verma S. B. *et al.* Oral submucous fibrosis: an update. *Clinical, cosmetic and investigational dermatology.* **2015** *8*: 193-204.

2. Rajalalitha P. and Vali S. Molecular pathogenesis of oral submucous fibrosis--a collagen metabolic disorder. *Journal of oral pathology & medicine : official publication of the International Association of Oral Pathologists and the American Academy of Oral Pathology.* **2005** *34(6)*: 321-8.

3. Lai D. R., Chen H. R. *et al.* Clinical evaluation of different treatment methods for oral submucous fibrosis. A 10-year experience with 150 cases. *J. Oral Pathol. Med.* **1995** *24(9)*: 402-6.

4. Bucolo C., Longo L. *et al.* Safety profile assessment of buflomedil: an overview of adverse reactions between 1975 and 2011. *Pharmacoepidemiology and drug safety.* **2012** *21(11)*: 1190-6.

5. Breza T., Taylor R. *et al.* Noninflammatory destruction of actinic keratoses by fluorouracil. *Archives of dermatology.* **1976** *112(9)*: 1256-8.

6. Kakar P. K., Puri R. K. *et al.* Oral Submucous Fibrosis—treatment with hyalase. *The Journal of Laryngology & Otology.* **1985** *99(1)*: 57-60.

7. James L., Shetty A. *et al.* Management of Oral Submucous Fibrosis with Injection of Hyaluronidase and Dexamethasone in Grade III Oral Submucous Fibrosis: A Retrospective Study. *Journal of international oral health.* **2015** *7(8)*: 82-5.

8. Kalia Y. N., Naik A. *et al.* Iontophoretic drug delivery. *Adv. Drug Deliv. Rev.* **2004** *56(5)*: 619-658.

9. Moscicka-Studzinska A. and Ciach T. Mathematical modelling of buccal iontophoretic drug delivery system. *Chem. Eng. Sci.* **2012** *80(Supplement C)*: 182-187.

10. Gratieri T. and Kalia Y. N. Targeted local simultaneous iontophoresis of chemotherapeutics for topical therapy of head and neck cancers. *Int. J. Pharm. (Amsterdam, Neth.).* **2014** *460(1-2)*: 24-7.

11. Tyagi V., Sancho S. d.-R. *et al.* Topical iontophoresis of buflomedil hydrochloride increases drug bioavailability in the mucosa: A targeted approach to treat oral submucous fibrosis. *Int. J. Pharm. (Amsterdam, Neth.).* **2019** *569*: 118610.

12. Patane M. A., Cohen A. *et al.* Ocular iontophoresis of EGP-437 (dexamethasone phosphate) in dry eye patients: results of a randomized clinical trial. *Clin Ophthalmol.* **2011** *5*: 633-643.

13. Cázares-Delgadillo J., Balaguer-Fernández C. *et al.* Transdermal iontophoresis of dexamethasone sodium phosphate in vitro and in vivo: Effect of experimental parameters and skin type on drug stability and transport kinetics. *Eur. J. Pharm. Biopharm.* **2010** *75(2)*: 173-178.

14. Sylvestre J. P., Díaz-Marín C. *et al.* Iontophoresis of dexamethasone phosphate: competition with chloride ions. *J. Control. Release.* **2008** *131(1)*: 41-46.

15. Gurney A. B. and Wascher D. C. Absorption of dexamethasone sodium phosphate in human connective tissue using iontophoresis. *The American journal of sports medicine.* **2008** *36(4)*: 753-9.

16. Patane M. A., Schubert W. *et al.* Evaluation of ocular and general safety following repeated dosing of dexamethasone phosphate delivered by transscleral iontophoresis in rabbits. *journal of ocular pharmacology and therapeutics.* **2013** *29(8)*: 760-9.

17. Cazares-Delgadillo J., Ganem-Rondero A. *et al.* Controlled transdermal iontophoresis for poly-pharmacotherapy: Simultaneous delivery of granisetron, metoclopramide and dexamethasone sodium phosphate in vitro and in vivo. *European journal of pharmaceutical sciences : official journal of the European Federation for Pharmaceutical Sciences.* **2016** *85*: 31-8.

18. Kalaria D. R., Singhal M. *et al.* Simultaneous controlled iontophoretic delivery of pramipexole and rasagiline in vitro and in vivo: Transdermal polypharmacy to treat Parkinson's Disease. *Eur. J. Pharm. Biopharm.* **2018**.

19. Cázares-Delgadillo J., Ganem-Rondero A. *et al.* Controlled transdermal iontophoresis for poly-pharmacotherapy: Simultaneous delivery of granisetron, metoclopramide and dexamethasone sodium phosphate in vitro and in vivo. *Eur. J. Pharm. Sci.* **2016** *85*: 31-38.

20. Grabovac V., Guggi D. *et al.* Comparison of the mucoadhesive properties of various polymers. *Adv. Drug Deliv. Rev.* **2005** *57(11)*: 1713-23.

21. Diaz Del Consuelo I., Pizzolato G. P. *et al.* Evaluation of pig esophageal mucosa as a permeability barrier model for buccal tissue. *J. Pharm. Sci. (Philadelphia, PA, U. S.).* **2005** *94(12)*: 2777-88.

22. Diaz-Del Consuelo I., Jacques Y. *et al.* Comparison of the lipid composition of porcine buccal and esophageal permeability barriers. *Arch. Oral Biol.* **2005** *50(12)*: 981-7.

23. Pikal M. J. The role of electroosmotic flow in transdermal iontophoresis. *Adv. Drug Deliv. Rev.* **2001** *46(1-3)*: 281-305.

24. Hansen L. B., Christrup L. L. *et al.* Enhanced delivery of ketobemidone through porcine buccal mucosa in vitro via more lipophilic ester prodrugs. *Int. J. Pharm. (Amsterdam, Neth.).* **1992** *88(1)*: 237-242.

25. Yamahara H. and Lee V. H. L. Drug metabolism in the oral cavity. *Adv. Drug Deliv. Rev.* **1993** *12(1)*: 25-39.

26. Derendorf H., Rohdewald P. *et al.* HPLC determination of glucocorticoid alcohols, their phosphates and hydrocortisone in aqueous solutions and biological fluids. *Journal of pharmaceutical and biomedical analysis.* **1986** *4(2)*: 197-206.

27. Hansen L. B., Christrup L. L. *et al.* Saliva-catalyzed hydrolysis of a ketobemidone ester prodrug: Factors influencing human salivary esterase activity. *Int. J. Pharm. (Amsterdam, Neth.).* **1992** *88(1)*: 221-227.

28. Santer V., Del Rio Sancho S. *et al.* Targeted intracorneal delivery-Biodistribution of triamcinolone acetonide following topical iontophoresis of cationic amino acid ester prodrugs. *International journal of pharmaceutics.* **2017** *525(1)*: 43-53.

29. Paturi J., Kim H. D. *et al.* Transdermal and intradermal iontophoretic delivery of dexamethasone sodium phosphate: quantification of the drug localized in skin. *Journal of drug targeting.* **2010** *18(2)*: 134-40.

30. O'Neil E. C., Huang J. *et al.* Iontophoretic delivery of dexamethasone phosphate for non-infectious, non-necrotising anterior scleritis, dose-finding clinical trial. *The British journal of ophthalmology.* **2018** *102(8)*: 1011-1013.

31. Telo I., Tratta E. *et al.* In-vitro characterization of buccal iontophoresis: the case of sumatriptan succinate. *Int J Pharm.* **2016** *506(1-2)*: 420-8.

32. Pindborg J. J., Murti P. R. *et al.* Oral submucous fibrosis as a precancerous condition. *Scandinavian journal of dental research.* **1984** *92(3)*: 224-9.

33. Tsurufuji S., Kurihara A. *et al.* Mechanisms of anti-inflammatory action of dexamethasone: blockade by hydrocortisone mesylate and actinomycin D of the inhibitory effect of dexamethasone on leukocyte infiltration in inflammatory sites. *J. Pharmacol. Exp. Ther.* **1984** *229(1)*: 237-243.

34. Vanhoutte P. M., Aarhus L. L. *et al.* Effects of buflomedil on the responsiveness of canine vascular smooth muscle. *J. Pharmacol. Exp. Ther.* **1983** *227(3)*: 613-20.

CHAPTER III

Intramucosal delivery of rituximab by topical iontophoresis: for a targeted management of moderate oral pemphigus vulgaris

Vasundhara Tyagi, Maria Lapteva, Yogeshvar N. Kalia

School of Pharmaceutical Sciences,
University of Geneva & University of Lausanne,
Rue Michel-Servet 1,
1206 Geneva, Switzerland

Manuscript in preparation

Abstract

The objective was to investigate whether iontophoresis could be used for the topical delivery of rituximab (RTX; molecular weight, 145 kDa) to the lamina propria, which together with the submandibular lymph nodes, constitutes the therapeutic target for the treatment of oral pemphigus vulgaris. Experiments were performed to investigate (i) the effect of pH and hence to identify the electrotransport mechanism, (ii) any potential interaction between RTX and fixed anionic sites in skin by determining its impact on the iontophoretic transport of acetaminophen, and (iii) the duration of current application on RTX delivery. In addition to quantification, by ELISA, of total RTX deposition and permeation, the experiments into the effect of time were accompanied by determination of the spatial biodistribution of RTX in the mucosa – i.e. as a function of depth – to identify the amounts present in the epithelium and the lamina propria. Mucosal deposition of RTX was independent of pH, but permeation at pH 7 was significantly greater despite the lower net cationic charge on RTX – suggesting an important role for electroosmosis. The absence of any effect on acetaminophen flux at pH 7, suggested that cationic RTX did not bind to fixed anionic sites in the mucosa at this pH. After the passive application of RTX (1 mg/ml in MES buffer, pH 7) for 10 min, mucosal deposition was 0.47 ± 0.05 μg/cm^2 of RTX and permeation was < LOQ. Iontophoresis at 1.5 mA/cm^2 for 10 min increased mucosal deposition of RTX to 2.2 ± 0.1 μg/cm^2. Total RTX deposition and the extent of penetration into the mucosa, as revealed by the biodistribution data, increased linearly with the duration of current application. The biodistribution resulted confirmed that RTX concentrations in the lamina propria were > EC_{50} after iontophoresis for 10 min. These preliminary results suggest that topical iontophoresis might be used for the targeted local delivery of antibody therapeutics to the oral cavity.

Keywords: buccal drug delivery, antibody, rituximab, iontophoresis, pemphigus vulgaris

1. Introduction

Pemphigus vulgaris (PV) is the most common form of this life threatening autoimmune disease, characterized by loss of epidermal and epithelial cell adhesion resulting in bullous lesions on skin and mucosal tissue, mainly in the mouth [1]. The blisters are caused by pathogenic auto-antibodies against desmosomal proteins, e.g. desmoglein 1 or 3 [2]. Treatment options include oral administration of high dose corticosteroids together with steroid-sparing immunosuppressants [2] – both pharmacotherapies result in numerous side effects [3-6]. Another approach consists of depleting auto-reactive $CD20^+$ B-lymphocytes by using an anti-CD20 monoclonal antibody such as rituximab (RTX) [7], which binds specifically to CD20-expressing B cells and instigates cellular cytotoxicity, complement dependent cytotoxicity and apoptosis.[8] It acts in the germinal centre of the lymph nodes draining the diseased area and in the bloodstream [1]; $CD20^+$ B-lymphocytes were also shown to infiltrate the diseased tissue [9-11]. RTX is administered intravenously and is often associated with mild to severe infusion reactions and more importantly immunosuppression leading to opportunistic infections [12, 13]. Remission is observed upon depletion of $CD20^+$ B-lymphocytes but relapse can occur after RTX treatment due to the incomplete depletion of B $CD20^+$ memory cells in solid lymphoid organs such as lymph nodes [14, 15].

It is clear that for PV affecting both skin and mucosa, a systemic treatment is necessary; however, for moderate cases – the International Pemphigus Study Group has proposed a disease severity classification of moderate, significant and extensive forms [16]) – the accessibility of mucosal blisters, opens the door to topical treatment. Indeed, the application of a topical corticosteroid produced remission in more than half of a small patient population with mild PV [17]. There are only a few reports into the delivery of macromolecules to the oral cavity [18].

The aim of this study was to investigate the feasibility of using topical iontophoresis for the non-invasive local delivery of RTX to the mucosa. The principal iontophoretic transport mechanisms are electromigration (EM) and electroosmosis (EO) with a potentially minor contribution from enhanced passive diffusion (**Equation 1**) [19, 20].

$$J_T = J_{EM} + J_{EO} + J_P \qquad \text{Equation 1}$$

Based on the work done on transdermal iontophoresis, it was hypothesized that EM would be the dominant electrotransport mechanism for low molecular weight species, but that as molecular weight increased, i.e. MW ~ 1000 Da, electroosmosis would take over as the principal driving force [21].

However, it has been shown that small cationic proteins of much higher molecular weight, e.g. cytochrome c (12.4 kDa), ribonuclease A (13.6 kDa), and human fibroblast growth factor (17.4 kDa) were all delivered by iontophoresis with EM as the dominant electrotransport mechanism [22-24]. More strikingly, it was also possible to use cathodal iontophoresis to deliver an anionic protein, ribonuclease T1 (11.1 kDa) at physiological pH, thereby going against the direction of the electroosmotic solvent flow.[25] Therefore, for these proteins, the electric mobility was sufficient to ensure that electromigration was more important than EO and that the cut-off where electroosmosis became the dominant electrotransport mechanism must be at higher molecular weight. The anatomy and composition of the mucosa means that higher current densities can be used than is possible with skin, which has a much higher electrical resistance [18]; it was reported in a preclinical *in vivo* study in pigs that iontophoresis at 2 mA/cm^2 for 10 min did not reveal any histological changes. In the present study, the main objectives were to evaluate the feasibility of using iontophoresis to deliver RTX to the mucosa and to evaluate the role of EM and EO by quantifying transport as a function of formulation pH, which would affect the degree of ionisation of RTX and the permselectivity of the mucosa. Then, under the optimal electrotransport conditions, the duration of current application was progressively reduced to determine whether relatively short periods of iontophoresis would be sufficient to achieve therapeutically relevant concentrations of RTX in the mucosa. Biodistribution experiments were performed to quantify the amounts of RTX present in the epithelia and the lamina propria since RTX needs to enter the lymphatic vessels present in the lamina propria [26],which drain the disease site, so that it can be transported to the submandibular lymph nodes [27, 28] in order to bind to $CD20^+$ B lymphocytes. Additionally, infiltrated $CD20^+$ B cells can also be targeted inside the mucosal tissue itself, near the basement membrane where the acantholysis is most prominent [11, 29].

2. Materials and methods

2.1 Materials

RTX (MabThera® 10 mg/mL, Roche Pharma SA) was purchased from a local pharmacy. 2-(N-morpholino)ethanesulfonic acid (MES) and Tween 20 were purchased from AppliChem Axon Lab AG (Baden-Dattwil, Switzerland). HCl, NaCl, AgCl, phosphate buffered saline, Fab specific Anti-human IgG, HRP-linked Fc specific Anti-Human IgG and 3,3',5,5'-tetramethylbenzidine (TMB) liquid substrate and bovine serum albumin (BSA) were purchased from Sigma Aldrich Chemie (Steinheim, Germany). All other chemicals and solvents were of analytical grade. Ultrapure water (Millipore Milli-Q Gard 1 Purification Pack resistivity > 18 MΩ.cm; Zug, Switzerland) was used to prepare all solutions.

2.2 Quantitative analysis of RTX by enzyme linked immunosorbent assay (ELISA)

A sandwich ELISA was developed to quantify RTX. Each well of a high surface binding 96-well plate (Costar® EIA/RIA, Corning, NY, USA) was coated with 100 µL of 10 µg/ml goat anti-mouse IgG for 1 h and incubated at 37 ºC. After washing once with PBST (PBS containing 0.1% Tween 20, pH 7.4), the plate was blocked with 250µL of 3% BSA for 1 h and incubated at 37ºC again. After 1 h, the plate was washed 3 times with PBST and 100 µL of samples containing RTX and calibration standards of RTX were loaded. The samples were incubated for 2 h at room temperature. After washing 3 times, 100 µL of HRP detection antibody (anti-human IgG, Fc specific-peroxidase antibody (1:4000)) was added to each well. After incubating for 1 h at RT, the plate was washed with PBST. Finally, 100 µL of TMB was added and the plate was incubated in the dark for ~10 min. The reaction was terminated by addition of 100 µL of 1N HCl. The absorbance was read at 450 nm with a microtiter plate reader (Biotek Instruments, VT, USA). Quantification of RTX in mucosal extracts after delivery experiment using ELISA indicated that these domains were not influenced by current application. Gel electrophoresis studies confirmed that RTX did not fragment in presence of current (details are provided in the **Supplementary Information**).

2.3 Preparation of mucosal tissue

All delivery studies were performed using fresh or frozen porcine esophageal mucosa which has been shown to be a good surrogate for human buccal mucosa.[30, 31] The porcine esophagus was obtained from a local slaughterhouse (Abattoir de Loëx Sàrl, Bernex, Switzerland). Once in the laboratory, the esophagus was longitudinally dissected and separated from the underlying submuscular layer with a scalpel. The separated mucosa was cleaned with cold Krebs-Ringer bicarbonate buffer (KRB, pH 7.4). The full thickness mucosa was either used fresh or wrapped in Paraffin® and stored at -20ºC.

2.4. Transport studies

2.4.1 Experimental set up

Full thickness porcine esophageal mucosa was clamped in vertical Franz diffusion cells (area = 2.0 cm2) and the receiver compartment was filled with 10 ml of PBST (pH 7.4). The commercial formulation of RTX was diluted in 25mM MES buffer to achieve a concentration of 1 mg/ml. 1ml of diluted RTX was placed in the donor compartment and was connected to the anode (Ag) via salt bridge assembly (3% agarose in 0.1 M NaCl). The cathode (AgCl) was placed in the sampling arm of the receptor compartment. A constant current was applied by a power generator (APH 1000 M, Kepco Inc; Flushing NY, USA) for 120, 60, 30 and 10 min. Passive diffusion experiments using the same setup but in the absence of current served as controls. At the end of the experiment, a 1 ml aliquot was withdrawn from the receiver compartment. The application area of the mucosa was cleaned with PBST. After the completion of the experiment, 1 ml aliquot was collected from the receiver compartment and 0.5 cm2 of the mucosal area in contact with the RTX formulation was punched out, cut into smaller pieces and extracted in 10 ml of PBST overnight. Control experiments were performed using the same set-up but in the absence of current application. Unless stated otherwise, all experiments were performed with six replicates.

2.4.2 Effect of pH on iontophoretic transport of RTX

The influence of donor pH on the iontophoretic delivery of RTX was studied by measuring iontophoretic delivery of RTX from MES buffer solutions at pH 4.0, 5.5 and 7.0.upon application of a current density of 1.5 mA/cm^2 for 120 min.

2.4.3 Effect of RTX on iontophoretic transport of acetaminophen

Potential interaction of RTX with the fixed negative charges in the mucosa was investigated by co-iontophoresis (1.5 mA/cm^2 for 6 h) of RTX (1 mg/ml) with acetaminophen (ACM; 15 mM in MES buffer, pH 7). Aliquots were collected hourly from the receiver compartment.

2.4.4 Time dependent delivery of RTX to the mucosa

RTX (1 mg/mL; MES buffer pH 7) was iontophoresed at 1.5 mA/cm^2 for 10, 30, 60 and 120 min. For the preliminary experiment (120 min), the entire mucosal area in contact with the RTX solution was punched out and extracted in 10 ml of PBST overnight. For the experiments at 10, 30 and 60 min, the intramucosal biodistribution profile of RTX in the mucosa as function of depth was determined following iontophoretic and passive application. The diffusion cells were dismantled, RTX solution was carefully removed and the mucosal tissue was cleaned with PBST. The mucosal tissue in contact

with the formulation was punched out and fixed in an embedding medium. It was snap frozen in isopentane cooled by liquid N_2 and finely sectioned into lamellae with a thickness of 40 µm using a Microm HM 560 Cryostat (Thermo Scientific; Walldorf, Germany). The lamellae were individually extracted in 1 ml of PBST for 12 h. The mixture was centrifuged at 10,000 rpm for 15 min and the supernatant was analysed using ELISA after appropriate dilution.

2.6 Data analysis

All data are expressed as mean ± standard deviation. Statistical significance was evaluated by analysis of Student's t-test. Groups were compared using analysis of variance (ANOVA). Student Newman Keuls test was used when necessary as *post-hoc* procedure. The level of significance was fixed at (α =0.05) for all tests.

3. Results and Discussions

3.1 Effect of pH on the iontophoretic transport of RTX and importance of electromigration and electroosmosis

The isoelectric point of RTX is calculated to be 9.1 [32]. Which means at physiological pH of 6.5 – 7 the dominant resulting charge on the antibody is positive. Ranging the pH of the solution from 4, 5.5 to 7 would increase the cationic charge of RTX from ~ 121.3, 49.6 to 24.3 respectively. This consequently *could* affect its transport number.

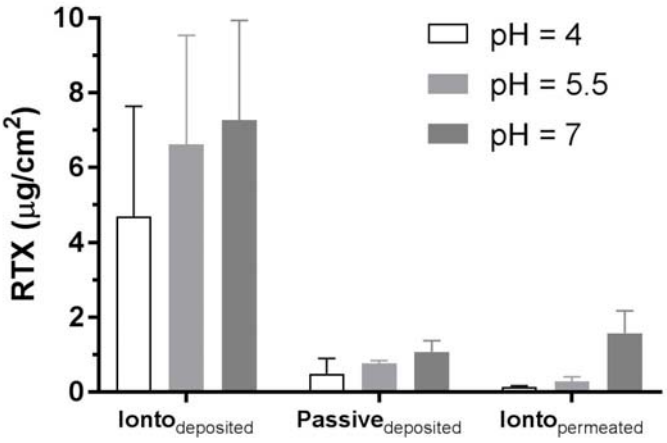

Figure 1. Effect of pH on RTX (1 mg/ml in MES buffer) mucosal deposition and permeation after passive and iontophoretic application (1.5 mA/cm^2) for 120 min. (Mean ± SD; n = 3).

There was no statistically significant difference between the total amounts of RTX deposited after passive application for 120 min of a 1 mg/ml RTX solution in MES buffer at pH 4, 5.5 and 7 , 1.0 ± 0.3, 0.7 ± 0.1 and 0.6 ± 0.4 µg/cm^2, respectively (p-value = 0.2). The amounts increased after iontophoresis (at 1.5 mA/cm^2) to 4.6 ± 2.9, 6.6 ± 2.9 and 7.2 ± 2.6 µg/cm^2 at pH 4, 5.5 and 7, respectively. Which means ~ 4.6 folds more at pH 4 compared to passive and ~ 9.4 and ~ 11 folds for pH 5.5 and pH 7 respectively. Similar to passive delivery, there was no statistically significant difference between the amounts of RTX deposited after iontophoresis at each pH (p = 0.45).

Cumulative permeation of RTX after iontophoresis at pH 4 and 5.5 was 0.1 ± 0.04 and 0.28 ± 0.1 µg/cm^2, respectively, and significantly increased to 1.57 ± 0.6 µg/cm^2 at pH 7 ($p < 0.05$). It was previously reported that the transscleral iontophoretic delivery of uncharged high molecular weight dextran and bevacizumab was dominated by electroosmosis EO [33, 34]. Given that the isoelectric point of mucosa is reported as 3, increasing the pH of the donor solution which bathes the mucosal surface from 4 to 7 increases the degree of ionisation of the negatively charged groups, thereby increasing solvent flow and the iontophoretic delivery of RTX, despite a reduction in net charge from ~ 121.3 to 24.3.

It has previously been demonstrated that certain cationic peptides and proteins are able to bind to fixed negative charges in skin and thereby neutralize permselectivity and decrease EO solvent flow. The standard method to investigate this is to co-iontophorese an uncharged molecule – in this case, ACM – whose electrotransport relies on EO alone and to whether there is any EO inhibition in the presence of the protein. **Figure 2** shows the iontophoretic and passive cumulative iontophoretic permeation of ACM in the presence and absence of RTX for 6 h. The amounts permeated after 6 h were 24.7 ± 5.1 and 27.9 ± 4.1 µg/cm^{2}h corresponding to an ACM flux in the presence and absence of RTX of, respectively. The EO flow was 10.7 ± 2.1 and 12.1 ± 1.78 µl/cm^{2}h in the presence and absence of RTX respectively and were statistically equivalent (p = 0.2). Thus, any interaction between RTX and the mucosa did not involve the negative charges present or was sufficiently weak so as not to affect EO flow. The passive control experiments showed that after 6 h cumulative ACM permeation was 25.6 ± 9.8 and 12.8 ± 4.9 µg/cm^2 in the presence and absence of RTX.

These values are slightly higher than the electroosmotic flow of isolated porcine oesophageal mucosal epithelium reported by Telo et al (~ 7 µl/cm^{2}h at 1.5 mA/cm^2) .[35] It was possible that the greater EO flow seen with full thickness oesophageal mucosa was due to the thickness of the membrane – 1500-1800 µm as opposed to 340-490 µm for isolated oesophageal epithelium. Thicker tissue might result in

a greater number of fixed negative charges, which would induce a greater electroosmotic flow upon application of an electric field.

a)

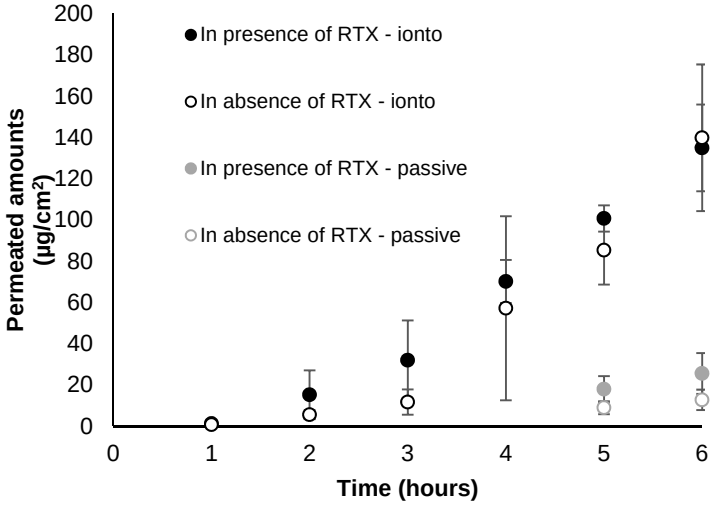

b)

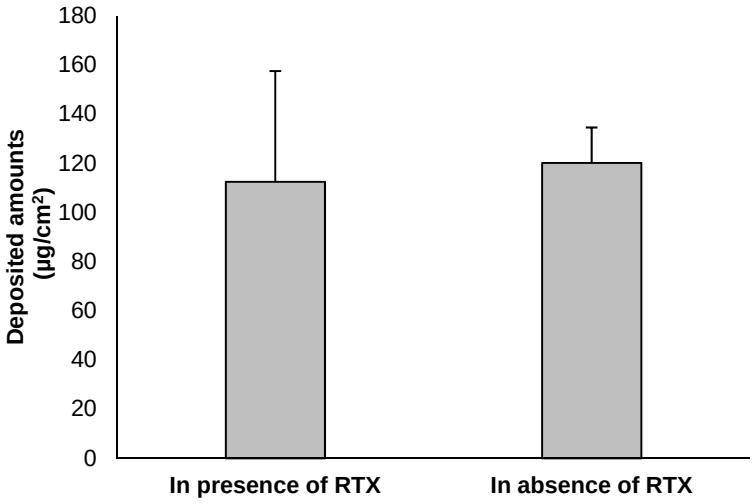

Figure 2 a) Iontophoretic and passive permeation of ACM (15 mM)when applied in the presence and absence of RTX (1 mg/mL), b) Deposition of ACM in the mucosa applied in the presence and absence of RTX after 6 hours

3.2 Effect of duration of current application

It was decided to perform subsequent experiments at pH 7 to benefit from a higher electroosmotic flow. Iontophoresis at 1.5 mA/cm^2 for 120 min resulted in RTX deposition of 7.2 ± 2.6 µg/cm^2, this was significantly greater than the corresponding passive control (1.07 ± 0.3µg/cm^2). After iontophoresis for 120 min, RTX was detected in the receiver compartment – cumulative permeation was 1.5 ± 0.6 µg/cm^2. The deposition value (~ 48 µg/mL upon conversion) and permeation value (~ 7 µg/mL upon conversion) were more than the reported RTX EC_{50} to induce depletion of human B cells, which is 1 µg/ml [36].

Since iontophoretic administration of RTX for 120 min was sufficient to enable delivery of potentially therapeutic amounts of RTX into the mucosa, it was decided to shorten the duration of current application to 60, 30 and 10 min and to determine spatial biodistribution of RTX as a function of depth. PV is characterised by acantholysis at the epithelium-lamina junction[1]. The acantholysis occurs due to the steric hindrance by the autoantibodies that are produced by competent plasma cells in the lymphatic blood vessels present in the lamina propria.[37, 38] A similar situation can be seen in skin, were CD20+ cells are present in PV lesions perivascularly.[39] Given the similarity of the blisters in cutaneous and mucous blisters, the local target site for of RTX is the lamina propria where immune infiltration begins.[40, 41] Biodistribution data provide a direct insight into the delivery of RTX at the target site. Iontophoresis at 1.5 mA/cm^2 for 60, 30 and 10 min resulted in RTX deposition of 3.0 ± 0.3, 2.2 ± 0.3 and 2.2 ± 0.1 µg/cm^2 – this was again significantly greater than the corresponding passive controls (0.96 ± 0.17, 0.92 ± 0.16 and 0.47 ± 0.05 µg/cm^2) (**Figure 3**).

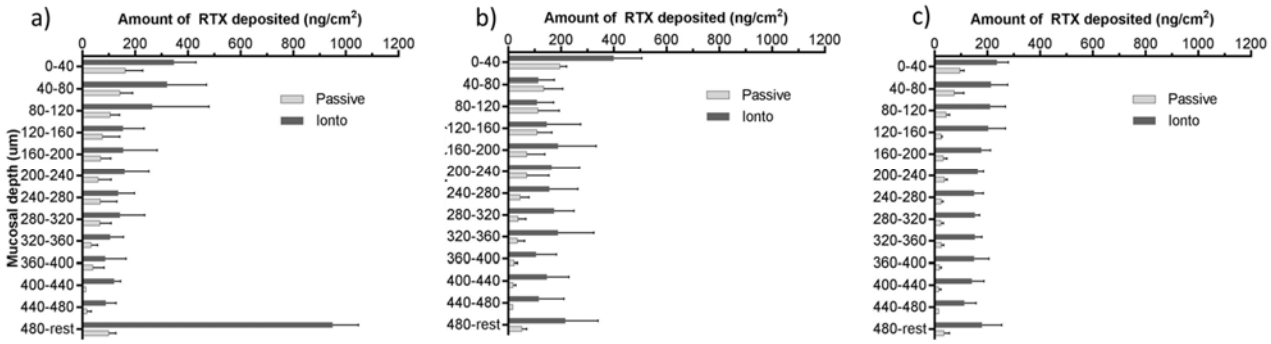

Figure 3. Mucosal deposition of RTX as a function of position in full thickness porcine esophageal mucosa: epithelia and lamina propria, after passive and iontophoretic (1.5 mA/cm^2) administration for (a) 60 min, (b) 30 min and (c) 10 min. (Mean ± SD; n=5)

In the absence of current application, RTX was mainly present in the upper 150-200 microns of the epithelium. For example, after 10 min less than 40 ng/cm^2 reached the deeper layers beyond .

The enhancement ratio (the ratio between the amounts of RTX deposited in the mucosa in the presence and absence of current) is shown in **Table 1.**

Table 1. Enhancement ratio in the successive layers of the mucosa

	Enhancement ratios		
Thickness (µm)			
	60 min	**30 min**	**10 min**
0-40	2.1	2.0	2.5
40-80	2.2	0.8	2.9
80-120	2.5	1.0	4.8
120-160	2.0	1.3	7.9
160-200	2.2	2.7	5.4
200-240	2.6	2.4	4.3
240-280	2.0	3.4	5.8

In the top 40 microns of the epithelium, the enhancement ratio was at least 2 folds which increased to over 5 folds in the subsequent layers until 480 microns. The most striking influence of the duration of current application was on the delivery of RTX to the lamina propria (480 – 1500 µm). In those layers, the enhancement ratio was in the range of 4 - 9 folds in 10 - 60 min of iontophoresis. It was clear that iontophoresis was able to deliver RTX in more amounts and deeper in the tissue compared to passive control.

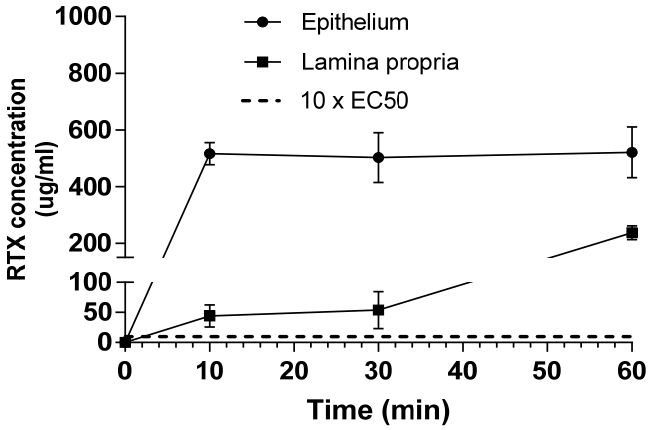

Figure 4. Delivery kinetics of RTX accumulation inside the different musical layers after 10, 30 and 60 min of iontophoresis at 1.5 mA/cm^2 current density.

The RTX concentration in the epithelium was effectively constant between 10 and 60 min. However, the RTX concentration achieved in the lamina propria did increase as a function of the duration of current application. EC_{50} of RTX required to induce depletion of human B cells in the vascularized connective tissue is 1 µg/ml (marked with a dashed line in Figure 5) [36]. The concentration in the lamina propria after 10 min was 44.4 ± 18.7 µg/ml and was this already 44-fold higher; this suggests that shorter duration of current application could be envisaged. For patients with moderate PV having mucosal manifestation with localized blisters (PDAI activity value ≥ 15 and ABSIS value ≥ 17), a short duration targeted treatment for a controlled delivery of RTX to the lamina propria and potentially to the draining lymph nodes could improve the quality of life.

4. Conclusions

The results mentioned in the study clearly demonstrate that in vitro topical iontophoresis of RTX for only 10 min using safe current density of 1.5 mA/cm^2 was able to deliver therapeutic concentrations of RTX in the lamina propria. It should be noted that the ruptured state of mucosa during the disease was

not taken into account in these studies and will need to be addressed in animal models. The non-invasive topical delivery of RTX into the oral mucosa may pave the way for local therapies enabling the direct neutralization of the cause of the disease at the epithelial junction.

5. Supplementary information

5.1 SDS PAGE

Sodium dodecyl sulfate- polyacrylamide gel electrophoresis (SDS PAGE) was performed to study the stability of the antibody in presence of current. A 12% SDS PAGE gels were poured, run and stained with Coomassie Blue. Briefly, Rituxan® commercial formulation containing 10 mg/ml Rituximab (RTX) was diluted to 1 mg/ml in MES buffer and treated with 1.5 mA/cm^2 current density for 3 h. Protein marker, untreated RTX samples and current treated samples were diluted with SDS. RTX reduced with dithiothreitol (DTT) served as control. All samples were loaded on to gels. Electrophoresis was carried out at a constant voltage of 120 V with 1 × Tris-glycine-SDS running buffer for 50 min. SDS PAGE confirmed the structural intergrity of RTX even after the application of current (**Figure 1**)

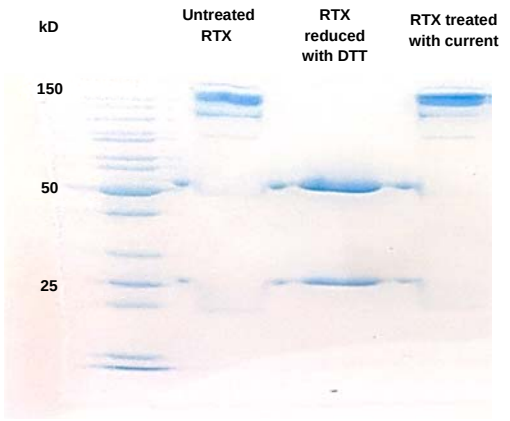

Figure 1 Structural integrity of RTX in absence and presence of current

5.2 Validation of sandwich ELISA

Intra- and inter-day accuracy and precision was determined using a range 1000 – 5 ng/mL standards. Table 1 shows the intraday accuracy and precision values for BUF quantification method.

Table 1. Intra day accuracy and precision of RTX

$[RTX]_{theoretical}$ (ng/mL)	$[RTX]_{mean}$ (ng/mL)	Precision (%)	Accuracy (%)
1000	867.0 ± 15.8	0.17	86.70
500	495.6 ± 91.5	2.03	99.14
300	333.0 ± 9.2	0.34	111.03
100	104.0 ± 9.1	1.53	104.06
20	21.8 ± 0.5	0.70	109.39
15	14.3 ± 0.5	1.17	95.75
10	11.0 ± 0.09	0.32	110.84
5	5.5 ± 0.5	0.74	110.12

6. Acknowledgment

We would like to thank University of Geneva for financial support. VT is grateful to the Swiss Federal Commission for Scholarships for Foreign Students for the award of a PhD fellowship.

7. References

1. Kasperkiewicz M., Ellebrecht C. T. *et al.* Pemphigus. *Nature reviews. Disease primers.* **2017** *3*: 17026-17026.

2. Pollmann R., Schmidt T. *et al.* Pemphigus: a Comprehensive Review on Pathogenesis, Clinical Presentation and Novel Therapeutic Approaches. *Clinical reviews in allergy & immunology.* **2018** *54(1)*: 1-25.

3. Gregoriou S., Efthymiou O. *et al.* Management of pemphigus vulgaris: challenges and solutions. *Clinical, cosmetic and investigational dermatology.* **2015** *8*: 521-7.

4. Dietze J., Hohenstein B. *et al.* Successful and well-tolerated bi-weekly immunoadsorption regimen in pemphigus vulgaris. *Atheroscler Suppl.* **2017** *30*: 271-277.

5. Enk A. H., Hadaschik E. N. *et al.* European Guidelines (S1) on the use of high-dose intravenous immunoglobulin in dermatology. *Journal of the European Academy of Dermatology and Venereology.* **2016** *30(10)*: 1657-1669.

6. Baum S., Scope A. *et al.* The role of IVIg treatment in severe pemphigus vulgaris. *Journal of the European Academy of Dermatology and Venereology.* **2006** *20(5)*: 548-552.

7. Joly P., Maho-Vaillant M. *et al.* First-line rituximab combined with short-term prednisone versus prednisone alone for the treatment of pemphigus (Ritux 3): a prospective, multicentre, parallel-group, open-label randomised trial. *Lancet (London, England).* **2017** *389(10083)*: 2031-2040.

8. Smith M. R. Rituximab (monoclonal anti-CD20 antibody): mechanisms of action and resistance. *Oncogene.* **2003** *22(47)*: 7359-68.

9. Egbuniwe I. U., Karagiannis S. N. *et al.* Revisiting the role of B cells in skin immune surveillance. *Trends in Immunology.* **2015** *36(2)*: 102-111.

10. Nagel A., Hertl M. *et al.* B-Cell-Directed Therapy for Inflammatory Skin Diseases. *Journal of Investigative Dermatology.* **2009** *129(2)*: 289-301.

11. Hussein M. R., Ali F. M. *et al.* Immunohistological analysis of immune cells in blistering skin lesions. *J Clin Pathol.* **2007** *60(1)*: 62-71.

12. Levin A. S., Otani I. M. *et al.* Reactions to Rituximab in an Outpatient Infusion Center: A 5-Year Review. *The journal of allergy and clinical immunology. In practice.* **2017** *5(1)*: 107-113.e1.

13. Drug information. *https://www.accessdata.fda.gov/drugsatfda_docs/label/2010/103705s5311lbl.pdf.*

14. Ellebrecht C. T. and Payne A. S. Setting the target for pemphigus vulgaris therapy. *JCI insight.* **2017** *2(5)*: e92021.

15. Leandro M. J., Cambridge G. *et al.* Reconstitution of peripheral blood B cells after depletion with rituximab in patients with rheumatoid arthritis. *Arthritis and rheumatism.* **2006** *54(2)*: 613-20.

16. Boulard C., Duvert Lehembre S. *et al.* Calculation of cut-off values based on the Autoimmune Bullous Skin Disorder Intensity Score (ABSIS) and Pemphigus Disease Area Index (PDAI) pemphigus scoring systems for defining moderate, significant and extensive types of pemphigus. *British Journal of Dermatology.* **2016** *175(1)*: 142-149.

17. Dumas V., Roujeau J. C. *et al.* The treatment of mild pemphigus vulgaris and pemphigus foliaceus with a topical corticosteroid. *The British journal of dermatology.* **1999** *140(6)*: 1127-9.

18. Wanasathop A. and Li S. K. Iontophoretic Drug Delivery in the Oral Cavity. *Pharmaceutics.* **2018** *10(3)*.

19. Kalia Y. N., Naik A. *et al.* Iontophoretic drug delivery. *Adv. Drug Deliv. Rev.* **2004** *56(5)*: 619-658.

20. Gratieri T. and Kalia Y. N. Mathematical models to describe iontophoretic transport in vitro and in vivo and the effect of current application on the skin barrier. *Adv. Drug Deliv. Rev.* **2013** *65(2)*: 315-329.

21. Guy R. H., Kalia Y. N. *et al.* Iontophoresis: electrorepulsion and electroosmosis. *J. Control. Release.* **2000** *64(1)*: 129-132.

22. Cazares-Delgadillo J., Naik A. *et al.* Transdermal delivery of cytochrome C--A 12.4 kDa protein--across intact skin by constant-current iontophoresis. *Pharm. Res.* **2007** *24(7)*: 1360-8.

23. Dubey S. and Kalia Y. N. Non-invasive iontophoretic delivery of enzymatically active ribonuclease A (13.6 kDa) across intact porcine and human skins. *J. Control. Release.* **2010** *145(3)*: 203-9.

24. Dubey S., Perozzo R. *et al.* Noninvasive transdermal iontophoretic delivery of biologically active human basic fibroblast growth factor. *Mol. Pharm.* **2011** *8(4)*: 1322-31.

25. Dubey S. and Kalia Y. N. Electrically-assisted delivery of an anionic protein across intact skin: cathodal iontophoresis of biologically active ribonuclease T1. *J. Control. Release.* **2011** *152(3)*: 356-62.

26. Marchetti C. and Poggi P. Lymphatic vessels in the oral cavity: different structures for the same function. *Microscopy research and technique.* **2002** *56(1)*: 42-9.

27. Vorwerk H. and Hess C. F. Guidelines for delineation of lymphatic clinical target volumes for high conformal radiotherapy: head and neck region. *Radiat Oncol.* **2011** *6*: 97.

28. Werner J. A. [The lymph vessel system of the mouth cavity and pharynx]. *Laryngo- rhino- otologie.* **1995** *74(10)*: 622-8.

29. Scully C. and Challacombe S. J. Pemphigus Vulgaris: Update on Etiopathogenesis, Oral Manifestations, and Management. *Critical Reviews in Oral Biology & Medicine.* **2002** *13(5)*: 397-408.

30. Diaz Del Consuelo I., Pizzolato G. P. *et al.* Evaluation of pig esophageal mucosa as a permeability barrier model for buccal tissue. *J. Pharm. Sci. (Philadelphia, PA, U. S.).* **2005** *94(12)*: 2777-88.

31. Diaz-Del Consuelo I., Jacques Y. *et al.* Comparison of the lipid composition of porcine buccal and esophageal permeability barriers. *Arch. Oral Biol.* **2005** *50(12)*: 981-7.

32. Goyon A., Excoffier M. *et al.* Determination of isoelectric points and relative charge variants of 23 therapeutic monoclonal antibodies. *Journal of chromatography. B, Analytical technologies in the biomedical and life sciences.* **2017** *1065-1066*: 119-128.

33. Nicoli S., Ferrari G. *et al.* In vitro transscleral iontophoresis of high molecular weight neutral compounds. *Eur. J. Pharm. Sci.* **2009** *36(4-5)*: 486-92.

34. Pescina S., Ferrari G. *et al.* In-vitro permeation of bevacizumab through human sclera: effect of iontophoresis application. *The Journal of pharmacy and pharmacology.* **2010** *62(9)*: 1189-94.

35. Telo I., Tratta E. *et al.* In-vitro characterization of buccal iontophoresis: the case of sumatriptan succinate. *Int J Pharm.* **2016** *506(1-2)*: 420-8.

36. Vugmeyster Y., Howell K. *et al.* Effect of anti-CD20 monoclonal antibody, Rituxan, on cynomolgus monkey and human B cells in a whole blood matrix. *Cytometry. Part A : the journal of the International Society for Analytical Cytology.* **2003** *52(2)*: 101-9.

37. Sciubba J. J. Autoimmune Aspects of Pemphigus Vulgaris and Mucosal Pemphigoid. *Advances in dental research.* **1996** *10(1)*: 52-56.

38. Marchetti C. and Poggi P. Lymphatic vessels in the oral cavity: different structures for the same function. *Microscopy research and technique.* **2002** *56(1)*: 42-9.

39. Hussein M. R., Ali F. M. *et al.* Immunohistological analysis of immune cells in blistering skin lesions. *Journal of clinical pathology.* **2007** *60(1)*: 62-71.

40. van Loon L. A., Krieg S. R. *et al.* Quantification and distribution of lymphocyte subsets and Langerhans cells in normal human oral mucosa and skin. *Journal of oral pathology & medicine : official publication of the International Association of Oral Pathologists and the American Academy of Oral Pathology.* **1989** *18(4)*: 197-201.

41. Wu R.-Q., Zhang D.-F. *et al.* The mucosal immune system in the oral cavity—an orchestra of T cell diversity. *International Journal Of Oral Science.* **2014** *6*: 125.

CHAPTER IV

Polymeric micelle based corticosteroid therapy for oral lichen planus

Vasundhara Tyagi[1], Valerie Suter[2], Somnath Kandekar[1], Maria Lapteva[1], Yogeshvar N. Kalia[1]

[1]School of Pharmaceutical Sciences,
University of Geneva & University of Lausanne,
Rue Michel-Servet 1,
1206 Geneva, Switzerland

[2]Clinic for oral surgery and stomatology
Freiburgstrasse 7,
CH-3010 Berne, Switzerland

Manuscript in preparation

Abstract

The lack of approved products to treat oral lichen planus (OLP) compels off-label use of medications that are often inefficient and uncomfortable for patients. The aims of this study were to develop aqueous solution/hydrogel polymeric micelle formulations using D-α- tocopheryl polyethylene glycol succinate (TPGS) di-block copolymer of (i) triamcinolone acetonide (TA) and (ii) fluocinonide (FLU), and to investigate their ability to delivery of TA or FLU to the epithelium-lamina propria junction of the mucosa. Incorporation of TA and FLU in TPGS increased their aqueous solubility by 35-fold (from 43 µg/mL to 1.5 mg/mL) and 26- fold (from 29 µg/mL to 0.75 mg/mL), respectively (d_n<15 nm). Optimized micelles solutions were stable for at least 2 months. Application of micelle solutions of TA and FLU to full thickness porcine esophageal mucosa for 60 min resulted in deposition of 644.6 ± 125.9 and 61.4 ± 12.7 ng/cm^2 respectively. In a 'head to head' comparison, the total delivery of TA after application of Kenacort® A Orabase® (0.1%) and micellar hydrogel (0.1%) for 60 min was 242.1 ± 68.5 and 5936.7 ± 1269.6 ng/cm^2, respectively. Total delivery of FLU after application of Novoter (0.05%) and micellar hydrogel (0.05%) for 60 min was 617.1 ± 126.5 and 2580.0 ± 285.5 ng/cm^2, respectively. Application of TA/FLU micelle hydrogel with occlusion for 30 min resulted in deposition in the epithelial-lamina propria junction of 117.0 ± 15.6 ng/cm^2 and 225.6 ± 36.7 ng/cm^2, for TA and FLU, respectively. The amounts of TA and FLU deposited in the epithelial-lamina propria junction region after application of Kenacort® A Orabase® and Novoter were below the LOQ. Results indicate that TPGS copolymer micelles are highly efficient nanocarriers for topical mucosal delivery of TA and FLU and might be able to improve therapy of OLP.

Keywords: oral lichen planus, Triamcinolone acetonide, Fluocinonide, Mucosal delivery, Polymeric micelles, biodistribution, occlusion

1. Introduction

Oral lichen planus (OLP) is an immune-mediated inflammatory disease of the oral cavity that affects up to 5% of the population worldwide [1]. The etiology of OLP is still under investigation but most studies suggest the involvement of dysregulated T-cells as a response to either exogenous triggers or to autologous antigens [1]. Based on the clinical forms of the lesions observed in patients, OLP is classified in three categories – reticular, erythematous and erosive [2]. Reticular lesions are most common and are characterized by white striations and hyperkeratotic papules. Erythematous lesions usually present as mucosal atrophy and erosive lesions are ulcerative and bullous [2].

Topical corticosteroids form the mainstay for the management of all clinical forms of OLP, [3] and exert biological effects through several mechanisms including cell receptor binding, inhibition of neutrophil and monocyte chemotaxis and eicosanoid production [4-6]. Topical application of corticosteroids is the preferred route of administration given the safety profile and cost effectiveness [7]. Triamcinolone acetonide (TA) is a well-studied synthetic glucocorticoid that has been effective in treating oral lesions topically [8, 9]. More potent fluorinated glucocorticoids, such as fluocinonide (FLU), have demonstrated advantages in treating oral lesions especially in patients suffering from chronic lesions who did not respond well to other therapies [10, 11].

Although the pharmacological and clinical effects of these drugs are proven, there is a lack of approved formulations designed and optimized for the management of OLP. An ideal topical formulation containing TA or FLU would deliver he drug to the target site (the epithelial-lamina propria (LP) junction where the T cell-containing lymphocytic infiltrates are present) in a short time to ensure patient compliance [12, 13]. Since there is a risk of accidental swallowing, the formulation must be safe and preferably without taste.

TA has been administered via an intralesional injection (0.5 ml of 40 mg/ml) or as a mouthwash or a paste [14, 15]. For patients already suffering from lesions, injections are invasive and understandably painful. Alcohol based mouthwashes have been reported to increase the risk of oral cancer and presumably more so in patients suffering from a potentially malignant disease such as OLP [12, 16-18]. Clinical efficacy of formulations after incorporation of TA and FLU in Orabase®for topical treatment of mucosal lesions has been investigated in many studies [9, 19]. Kenacort® A Orabase® is a marketed product containing 0.1 % TA. Although Orabase® enables the solubilisation of poorly water soluble, lipophilic drugs like TA and FLU, the clinical outcomes have been somewhat modest suggesting that the clinical potential of these drugs was not fully utilized [20-22]. The ‘oily’ excipients present in

Orabase® could also make the formulation inconvenient to apply on to the wet lesions in the highly hydrated environment in the mouth.

Polymeric micelles are colloidal particles made of amphiphilic polymers that can self-assemble above a critical micelle concentration (CMC) to form a core shell structure. These nanostructures have been used to prepare aqueous formulations of hydrophobic drugs that are otherwise difficult to formulate for topical delivery to the skin, eye and buccal mucosa [23-26]. Aqueous formulations of TA (434.5 Da, aqueous solubility: 43 µg/mL) and FLU (494.5 Da, aqueous solubility: 29 µg/mL) for OLP would facilitate delivery into the buccal mucosa since release of poorly water soluble drug from the micelle into the external aqueous environment would most likely result in transient supersaturation and the elevated thermodynamic activity would enhance drug partitioning into the mucosa. Formulation of micelles into a hydrogel could be a means to improve mucoadhesion through the formation of hydrogen bonds with saliva and it could also promote patient compliance by being easy to apply and possessing a neutral taste.

D-α-Tocopheryl polyethylene glycol 1000 succinate (TPGS) is an amphiphilic copolymer with a low critical micelle concentration (0.02% w/w) and a hydrophilic-lipophilic balance value of 13.2, prepared by esterification of vitamin E succinate with poly(ethylene glycol) 1000 [27]. It has GRAS status from the US Food and Drug Administration and has been included in formulations approved by European Medicines Agency. These properties make TPGS an interesting biomaterial for preparing micelle formulations for topical use. We have previously used TPGS based micelle formulations to enhance topical delivery of adapalene to the human hair follicle [28]. In light of those promising results, it was decided to explore whether micelles would be able to improve mucosal bioavailability and if so whether the drugs were able to reach the epithelial-lamina propria (LP) junction. Keeping in mind the practical application of the formulation, an occlusive hydroxyethylcellulose film was prepared and its influence on drug delivery investigated. In addition to improving delivery, a protective layer could prevent formulation loss in vivo by saliva flushing and protect the painful lesions against mastication.

The aim of this study was (i) to develop stable TA/FLU loaded TPGS micelle solution and gel formulations for ease of application and controlled dosing, (ii) to compare the topical mucosal delivery of TA/FLU by performing biodistribution studies using micelle formulations, micelle formulation under an occlusive film and their respective marketed formulations (KO for TA and due to lack of an available commercial formulation of FLU for OLP, Novoter® containing 0.1 % FLU was used). Topical mucosal bioavailability was studied by sectioning the full thickness mucosa comprised of the epithelium and lamina propria in fine lamellae with a thickness of 40 µm and the individual lamellae

were extracted and analysed using sensitive ultra-high pressure liquid chromatography coupled with tandem mass spectrometry.

2. Materials and methods

2.1 Materials

TA and sodium carboxymethyl cellulose were purchased from Haenseler AG (Herisau, Switzerland). FLU was purchased from Hangzhou Dayangchem Co. Ltd (Hangzhou, P.R. China). TPGS, phosphate buffer saline (pH 7.4), polyethylene glycol (PEG) (M.W~35000) and Tween 80 were bought from Sigma-Aldrich (Buchs, Switzerland). NATROSOL 250 hydroxyethyl cellulose (HEC) was a generous gift from Hercules Inc. LC-MS grade acetonitrile (ACN), methanol (MeOH) and acetone were purchased from Fisher Scientific (Reinach, Switzerland) and LC-MS grade formic acid was purchased from Brunschwig (Basel, Switzerland). Kenacort Orabase® containing 0.1 %TA) and Novoter® containing 0.05 % FLU (Teofarma, Italy) were purchased from a local pharmacy. Orabase® is a mix of pectin, gelatin, sodium carboxymethyl cellulose in a liquid paraffin polyethylene glycol base [29]. Novoter® contains propylene glycol, citric acid, glycerol (E-422), stearyl alcohol, polyethylene glycol 4000 (Macrogol 4000) and dimethicone.

2.2 Analytical method

2.2.1 Quantification of TA and FLU by UHPLC-UV

TA was quantified using a Waters Acquity® UPLC® H-class system equipped with a TUV Detector. Isocratic separation was accomplished using a Waters XBridge® BEH C18 (100 x 2.1 mm, 2.5 µm) column maintained at 45°C. The mobile phase consisted of a 50:50 ratio of 0.1 % formic acid in water and 0.1 % formic acid in MeOH. The flow rate was 0.3 mL/min and the injection volume was 5 µL. The run time was 2 min. The limit of detection (LOD) and limit of quantification (LOQ) for TA were 0.25 µg/mL and 1 µg/mL, respectively.

FLU was also quantified using the same system. Gradient separation was achieved using a Waters XBridge® BEH C18 (100 x 2.1 mm, 2.5 µm) column maintained at 40°C (details of the gradient separation are provided in the **Supplementary Material**). The mobile phase consisted of 0.1 % formic acid in water and 0.1 % formic acid in ACN. The flow rate was 0.2 mL/min and the injection volume was 5 µL. The run time was 2 min. The LOD and LOQ were 0.25 µg/mL and 0.75 µg/mL, respectively.

2.2.2 Quantification of TA and FLU by UHPLC-MS/MS

Quantification of the TA and FLU biodistribution required the development of a highly sensitive UHPLC-MS/MS method using a Waters Acquity® UPLC® core system coupled to a Xevo® TQ-MS tandem quadrupole detector. Isocratic separation of mucosal matrix and TA was carried out using a Waters XBridge® BEH C18 (50 × 2.1 mm, 2.5 µm) reverse phase column thermostatted at 45°C and the mobile phase comprised a mixture of MeOH and ultrapure water (50:50 v/v) both containing 0.1% formic acid. A flow rate of 0.3 mL/min and an injection volume of 5 µL were used. Mass spectrometric detection was performed by electrospray ionization in positive ion mode (ESI^+) using multiple reaction monitoring (MRM). The parent ion [$M+H^+$] was selected at 435.29 *m*/*z* and product ion was chosen at 415.17 *m*/*z*. TA retention time was 0.78 min and the LOD and LOQ were 1 and 3.9 ng/mL, respectively. Additional information regarding precision and accuracy is given in the **Supplementary Material**.

FLU was separated from the mucosal matrix by using the same Waters XBridge® BEH C18 (50 × 2.1 mm, 2.5 µm) reverse phase column with a column temperature of 40°C. Gradient separation was achieved using a mobile phase comprising a mixture of ACN and ultrapure water both containing formic acid. A flow rate of 0.2 mL/min and an injection volume of 5 µL were used. Mass spectrometric detection was performed by electrospray ionization in positive ion mode (ESI^+) using multiple reaction monitoring (MRM). The parent ion [$M+H^+$] was selected at 495.15 *m*/*z* and daughter ion was chosen at 337.10 *m*/*z*. FLU retention time was 0.81 min and the LOD and LOQ were 0.1 and 0.78 ng/mL respectively. Additional details and validation of the method can be found in the **Supplementary Material**.

2.3 Formulation developmen

2.3.1 TA and FLU micelle preparation

Micelle formulations were prepared using the solvent evaporation method [28, 30]. Briefly, known amounts of drug (TA or FLU) and TPGS were dissolved in 4 mL of acetone. The mixture was added to 4 mL of ultrapure water dropwise under sonication (Branson Digital Sonifier® S-450D; Carouge, Switzerland). Using a rotary evaporator (Büchi RE 121 Rotavapor®; Flawil, Switzerland) acetone was slowly evaporated at 40 °C. After equilibration overnight, the micelle solution was centrifuged at 10 000 rpm for 20 min (Eppendorf Centrifuge 5804; Hamburg, Germany) to remove free drug from the formulation and the supernatant was carefully collected. The higher strength micelle solutions were diluted with ultrapure water to obtain the desired micelle solution of TA (0.1%) and FLU (0.05%).

2.3.2 Effect of TPGS copolymer concentration on drug loading in the micelles

To study the effect of TPGS copolymer concentration on the incorporation efficiency, different copolymer concentrations (25, 50, 75, 100 and 150 mg/mL) were tested and the stability of the resulting

micelles was studied for 60 days. The target concentrations of TA (1.5 mg/mL) and FLU (0.75 mg/mL) were kept fixed to prepare the formulations. The procedure for the preparation of micelle formulation for screening is the same as described above.

2.3.3 Preparation of HEC film

Drug-free HEC film was prepared by adding 3.3 % (w/v) HEC and 3% PEG to 140 mL Milli-Q water. The mixture was stirred for 4 h at room temperature and left for swelling overnight. The next day 40 mL of the polymeric gel was poured into a glass Petri dish (diameter = 77 mm; area = 46.5 cm^2) and dried for 24 h in a ventilated fume hood at room temperature. The Petri dish were covered with a piece of filter paper to avoid contamination. The dried film was carefully peeled off from the bottom of the Petri dish and punched into disks with a diameter of 3.6 cm (area = 10.1 cm^2).

2.4 Characterization of micelle formulations

2.4.1 Size distribution characterization

Micelle formulations were characterized for their hydrodynamic diameter (Z_{av}) and polydispersity index (P.I.) using dynamic light scattering (DLS) with a Zetasizer Nano-ZS (Malvern Instruments Ltd. Malvern, UK). All measurements were performed in triplicate.

2.4.2 Morphology

The surface morphologies of the micelle formulations were studied using transmission electron microscopy (TEM) FEI Tecnai™ G2 Sphera, (Eindhoven, The Netherlands), equipped with a high-resolution 2000 × 2000 pixel digital camera) using the negative staining method. Briefly, 5 µL of the micelle formulation was placed onto an ionized carbon-coated copper grid (0.3 Torr, 400 V for 20 s). The grid was then placed in contact with a 100 µL drop of a saturated uranyl acetate aqueous solution for 5 s and then again in a fresh second 100 µL drop for 30 s. The excess staining solution was blotted and the grid was dried at room temperature prior to recording TEM images.

2.4.3 Determination of drug content in the micelle formulations

Total drug content of TA and FLU in the micelle formulations was determined by UHPLC-UV. TA and FLU present in the micelles were released by diluting the micelles in 1:20 ratio with MeOH and ACN, respectively, and vortexing for 1 min. The following equations were used to calculate drug content, drug loading and incorporation efficiency:

$$\text{Drug content (mg X / mL formulation)} = \frac{mass\ of\ X\ in\ the\ formulation\ (mg)}{Volume\ of\ the\ formulation\ (mL)} \quad (1)$$

$$\text{Drug loading (mg drug/ g copolymer)} = \frac{X \text{ in the formulation } (\frac{mg}{mL})}{TPGS \text{ in the formulation } (\frac{g}{mL})} \quad (2)$$

$$\text{Incorporation efficiency (\%)} = \frac{mass \text{ of } X \text{ incorporated into micelles } (mg)}{mass \text{ of } X \text{ introduced } (mg)} \times 100 \quad (3)$$

Where X = TA or FLU

2.5 Preparation and characterization of micelle-gel formulations

For ease of application and controlled dosing, the optimal micelle solutions of TA and FLU were gellified using CMC. Briefly, 2.5 % CMC was added to the optimal micelle solution of TA (0.1%) or FLU (0.05%) and stirred using a magnetic stirrer at 300 rpm for 3 h to obtain a homogeneous dispersion. The pH of the gels was measured using a pH meter (Mettler-Toledo (Schweiz) GmbH; Greifensee, Switzerland). A short-term stability study was performed for 4 weeks to study the drug incorporation in the micelle gel formulations.

2.6 Evaluation of *in vitro* drug delivery

2.6.1 Mucosa preparation

In vitro studies were performed using porcine esophageal mucosa. The structural similarities and similar lipid compositions between human buccal epithelium and porcine esophageal epithelium have been described previously [31-33]. Porcine esophagus was obtained from a local slaughterhouse (Abattoir de Loëx Sàrl, Bernex, Switzerland) a few hours after slaughter. It was longitudinally dissected and cleaned with isotonic saline. The mucosa was separated from the underlying muscularis mucosae layer with a scalpel. The separated mucosa was cleaned with cold Krebs-Ringer bicarbonate buffer (KRB, pH 7.4). The full thickness mucosa (thickness ~ 0.15 cm) was either used fresh or wrapped in Paraffin® and stored at -20 ºC for up to 3 months.

2.6.2 *In vitro* mucosal drug delivery

2.6.2.1 Franz cell for experiments to compare the micelle formulation to the references without occlussion

Mucosa samples were mounted on two compartmental Franz diffusion cells (Milian SA; Meyrin, Switzerland) with a formulation contact area of 2 cm^2. The receptor compartment was filled with 10 mL of phosphate buffered saline (PBS, pH 7.4) containing 1.5% Tween 80 to maintain sink conditions. After equilibration, 250 mg (or 125 mg/cm^2) of either micellar gel or the commercial formulation i.e. (i) TA micellar gel (0.1%) or Kenacort Orabase® (0.1%) (ii) FLU micellar gel (0.05%) or Novoter®(0.05%)] was applied. To study the effect of gellification, 250 µl of optimal micellar solutions

of TA (0.1%) or FLU (0.05%) were applied in separate studies. To investigate the effect of formulation application time all experiments were performed at 30 and 60 min. Upon completion of the experiment, 1 mL aliquot was withdrawn from the receiver compartment to quantify the permeation of drugs across the mucosa. Samples were centrifuged at 10 000 rpm for 15 min and the supernatant was analysed by UHPLC-MS/MS. The diffusion cells were dismantled and the mucosa surface was carefully washed with 1.5% Tween in order to ensure the removal of the residual formulations from the mucosa surface. Mucosa samples were blotted with a cotton swab.

2.6.2.2 Deposition set up for experiments to compare the micelle formulation to the references under occlussion

A new deposition set up was developed to study the effect of overlaying a blank HEC film over the micellar formulations. We have previously reported a similar set up to study short duration simultaneous iontophoretic delivery of two drugs where the donor area was divided concentrically in two parts and the receptor compartment was absent. The set up used in the current study was a simplified version with a single donor compartment with 5-fold more donor area than the Franz diffusion cells used. In short, the set up consisted of two poly(methyl methacrylate) trays which could be screwed together by wing screws placed at the corners of the trays. A circular disk of mucosa with a diameter of ~ 4.5 cm and an area of ~16 cm^2 was placed on a damp absorbent paper to maintain tissue hydration and placed on the lower tray. The upper tray was placed on the mucosa, which was held in place between the upper and lower trays by fastening the screws. 0.25 g of either TA micellar gel (0.1%) or FLU micellar gel (0.05%) was applied in the centre (2 cm^2) of the exposed donor surface area (~ 10.1 cm^2) and immediately covered with a hydrated blank HEC film (area = 10.1 cm^2). After 30 min, the covering film and the micellar gel were carefully removed. The mucosa was washed with 1.5% Tween 80. More details about the dimensions of the set up are provided in the **Supplementary Material**.

2.6.2.3 Biodistribution sample preparation

Upon completion of the experiments (Franz cell or the deposition set up) mucosal samples were prepared for biodistribution analysis. A 0.5 cm^2 disk in contact with the formulation was punched out and fixed in OCT embedding medium, and flattened using a glass slide. It was subsequently snap-frozen in isopentane cooled by liquid nitrogen and sliced using a Microm HM 560 Cryostat (Thermo Scientific; Walldorf, Germany)into 40 µm thick lamellae from the mucosa surface to a depth of 480 µm. The individual lamellae and the remaining tissue were extracted overnight in 1 mL of 50/50

MeOH/ultrapure water (v/v) for TA samples or 75/25 ACN/ultrapure water for FLU samples. The extracts were centrifuged at 12 000 rpm for 15 min and analysed by UHPLC-MS/MS.

2.6 Data analysis

All data are expressed as mean ± standard deviation. Statistical significance was evaluated by analysis of Student's t-test. Groups were compared using analysis of variance (ANOVA). Student Newman Keuls test was used when necessary as a *post-hoc* procedure. The level of significance was fixed at (α =0.05) for all tests.

3. Results and Discussions

3.1 Development of optimal micelle formulation and characterization

3.1.1 TA

The target drug concentration was 1.5 mg/mL and a series of TA micelle formulations were prepared with different drug to copolymer ratios to study the effect on TA incorporation. At a TPGS concentration of 50 mg/mL, TA concentration in the micelles was 1.3 ± 0.1 mg/mL on Day 0 but the formulation was not stable and after 30 days the TA concentration had decreased by ~50% to only 0.6 ± 0.1 mg/mL. Increasing the TPGS concentration to 75, 100 or 150 mg/mL enabled the target drug concentration to be achieved and the formulations were stable for 30 days. However, only the formulation prepared with a TPGS concentration of 150 mg/mL TPGS was stable for 60 days (**Figure 1**). This concentration of TPGS was used to prepare the optimized formulation, TA_2 by appropriate dilution (**Table 1**). The pH of the diluted formulation was 6.5.

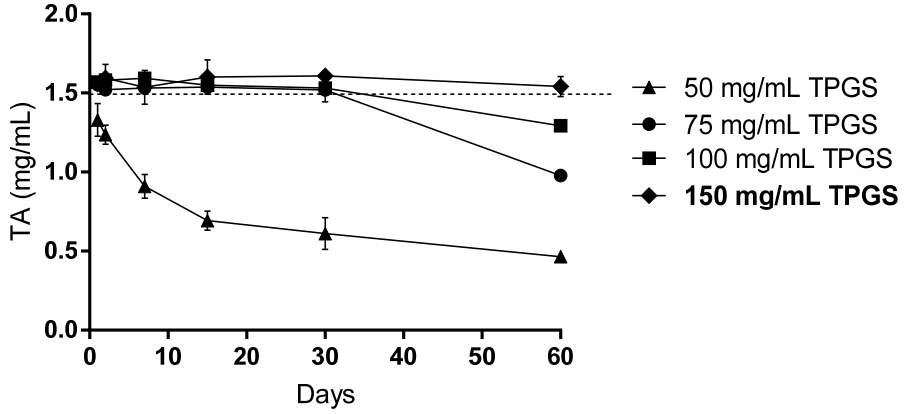

Figure 1: TA drug content in the micelles as a function of time for 2 months stored at 4º C (n=3). Dashed line represents the target drug content of TA i.e. 1.5 mg/mL

Table 1. Drug content of TA micelle formulations

		Drug content		
Formulation	Copolymer content (mg/mL)	Drug loading ± SD (mg_{TA}/g_{copol})	Drug content ± SD (mg_{TA}/mL formulation)	Incorporation efficiency ± SD (%)
TA_1	150	10.3 ± 0.3	1.5 ± 0.0	103.8 ± 3.2
TA_2	110	10.3 ± 0.3	1.1 ± 0.2	103.8 ± 3.2

*Obtained by diluting formulation TA_1

DLS revealed that formulation TA_2 had a hydrodynamic diameter of 10.6 nm. **Figure 2a** shows the size distribution by intensity of formulation TA_2. The polydispersity index was 0.023 ± 0.009. DLS data was confirmed with TEM microscopy (**Figure 2b**). Micelles were spherical in shape with diameters below 20 nm (Z_{av}).

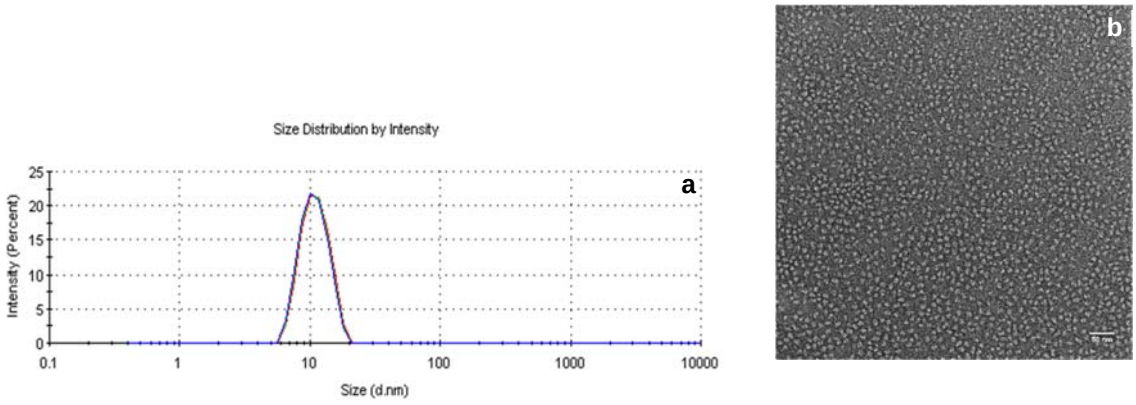

Figure 2. a) Size distribution of TA micelles measured by DLS (in nm) b) TEM micrograph (bar = 50 nm)

Formulation TA_2 was gellified using 2.5% CMC and its stability was studied before using it for transport experiments. The drug content in the gel was stable for 4 weeks and the pH of the micelle gel was 6.28, i.e. suitable for topical application to the mucosa.

3.1.2 FLU

The target concentration for FLU was 0.75 mg/mL. As for TA, TPGS concentrations of 50 and 100 mg/mL did not result in stable micelles and it was decided to use the formulation prepared with 125 mg/mL TPGS as the optimal formulation due to its stability of 2 months (**Figure 3**).

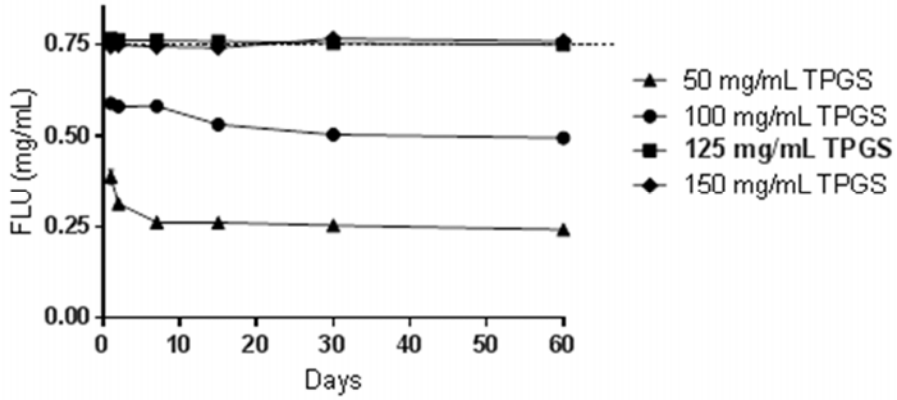

Figure 3. FLU drug content in the micelles as a function of time for 2 months stored at 4º C (n=3). Dashed line represents the target drug content of FLU i.e. 0.75 mg/mL.

The hydrodynamic diameter (Z_{av}) of the optimal micelle solution was 11.8 nm (**Figure 4a**). TEM images confirmed the size and spherical morphology of the micelles (**Figure 4b**).

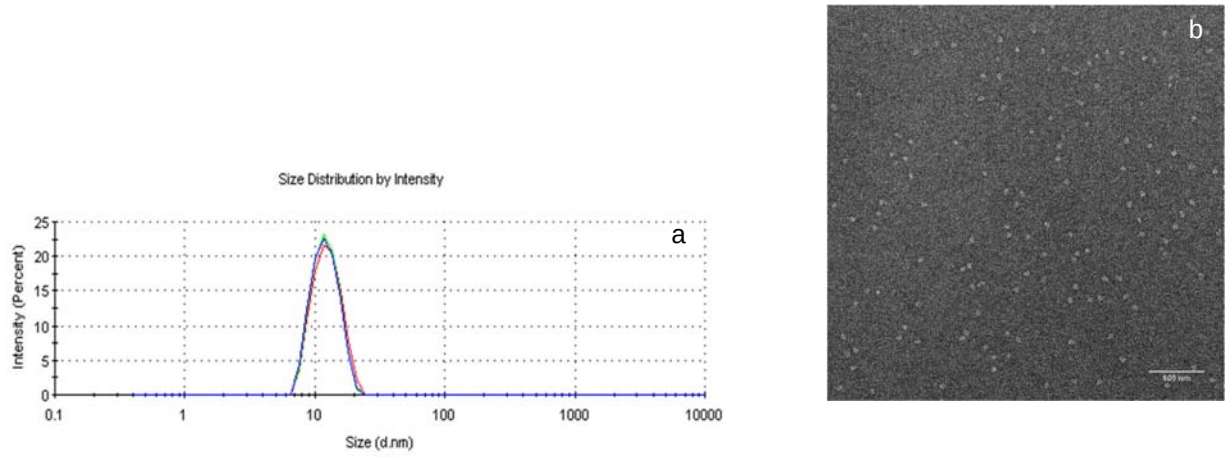

Figure 4: a) Size distribution of FLU micelles measured by DLS (in nm) b) TEM micrograph (bar = 100 nm)

The micelle formulation used for delivery experiments (FLU_2) was prepared by diluting the optimal solution (**Table 2**).

Table 2. Drug content of FLU micelle formulations

		Drug content		
Formulation	Copolymer content (mg/mL)	Drug loading ± SD (mg_{TA}/g_{copol})	Drug content ± SD (mg_{TA}/mL formulation)	Incorporation efficiency ± SD (%)
FLU_1	125	6.0 ± 0.1	0.75 ± 0.0	100.0 ± 1.7
FLU_2*	86.6	6.0 ± 0.1	0.52 ± 0.1	100.0 ± 1.7

*Obtained by diluting formulation FLU_1

A polymeric gel was prepared by adding 2.5 % CMC to FLU_2 solution. The pH of the solution and gel was in the range of 6.6-7.0.

Previously, multiple linear regression analysis of data of a study investigating the nature of incorporation of eighteen drugs into MPEG-hexPLA suggested that the number of hydrogen bond donors of the molecule is a key factor affecting the drug loading. TA and FLU contain a single and two H bond donors respectively, which may explain the resulting relatively low drug loading in the micelles. [34] Other factors affecting the incorporation efficiency in decreasing order of relevance after H bond donor groups were log P, H bond acceptor groups and the aqueous solubility [34].

The formulation and morphology of micelles is highly influenced by the chemical nature and structure of the copolymer used. Especially the nature and relative size of the hydrophobic and hydrophilic chains of the copolymer that determine the size of the resulting micelle. Therefore, the relatively small size of micelles <15 nm was attributed to the relatively small size of TPGS (MW = 1513 Da) copolymer. For topical drug delivery, the smaller size of the micelles may be advantageous since they increase the surface to volume ratio of the formulation making it easier to interact with the environment. A small nanocarrier may also penetrate deeper into the mucosa through the narrow intercellular spaces of less than 20 nm in the epithelium [35]. CMC micelles have previously shear thinning behaviour i.e. the viscosity of the gel decreases upon presentation with shear stress, making it ideal for topical application [28].

The results presented here demonstrate that the amount of copolymer was directly proportional to the consequent drug content and the stability of the micelles. For TPGS content ≤ 25 mg/mL (results not presented here), the incorporation efficiency was less than 50% for both TA and FLU. On increasing the TPGS content to ≥50 mg/mL the incorporation efficiency of the micelles started improving. The optimal copolymer content was chosen by following the stability of the micelles for 2 months. By using TPGS content 75 mg/mL or more it was possible to achieve 100% incorporation efficiency for TA.

However the micelles using 150 mg/mL TPGS were eventually stable at the end of 2 months. Similarly for FLU micelles, 125 mg/mL of TPGS content was able to produce micelles stable upto 2 months. Clearly it was possible to tune the stability of the micelles by tuning the copolymer content, however to maintain formulation stability and to prevent the formation of elongated and hexagonal micelles, the TPGS content was not increased beyond 15% [36].

3.2 In vitro delivery study

3.2.1 TA

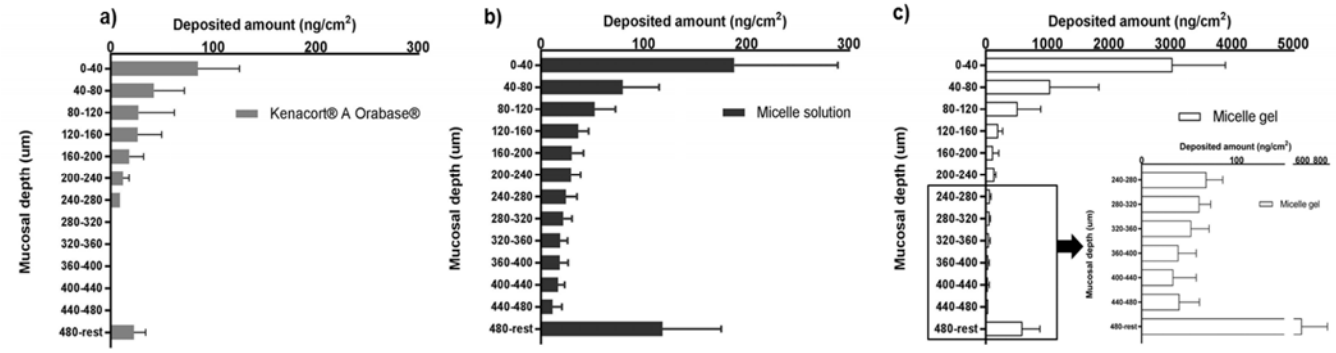

Figure 5. Deposition of TA in the mucosa after 60 min application of a) Kenacort® A Orabase® b) TA Micelle solution c) TA CMC micelle gel

The amounts of TA permeated through the mucosa were below the LOQ (5 ng/mL) for applications times up to 60 min. After application of KO for 60 min [37], TA delivery to the mucosa of was poor. The total deposition of TA in the mucosa was 242.1 ± 68.5 ng/cm^2. Biodistribution data revealed that ~65% of the total deposited amount stayed in the upper 120 µm of the epithelium (**Figure 5a**). The amounts of TA deposited in the epithelial-lamina propria (LP) junction (between 240 – 480 µm) were below the LOQ.

Application of 0.25 mL micellar solution containing the same number of moles of TA as KO for 60 min improved the total delivery 2.5-fold to 644.6 ± 125.9 ng/cm^2 and deposition in the epithelial-lamina propria junction (240 - 480 µm) was 110. 6 ± 1.9 ng/cm^2 (**Figure 5b**).

For ease of application, a micelle gel was formulated. **Figure 5c** shows the delivery from the micelle gel containing the same number of moles of TA as the micelle solution and KO after 60 min. The amounts of TA deposited after application of the gel were much higher than from any other formulation. The total delivery of TA from the gel was 24.5-fold and 9.2-fold higher than KO and micelle solution. The amounts of TA reaching the epithelial-lamina propria junction were also higher (292.7 ± 43.5

ng/cm^2) and TA was more evenly distributed (inset **Figure 5c**). It is worth noting that the polymer matrix used in both KO and micelle gel was the same – CMC however the change in the drug delivery vehicle base from oil based to water based (polymeric micelle) clearly had a significant impact on the delivery of TA in the mucosa.

Following these very promising results, the application time of the gel formulation was reduced to 30 min. To prevent formulation loss and to improve the delivery of TA, it was decided to cover the formulation with a blank HEC film. **Figure 6** shows the effect of occlusion on TA delivery.

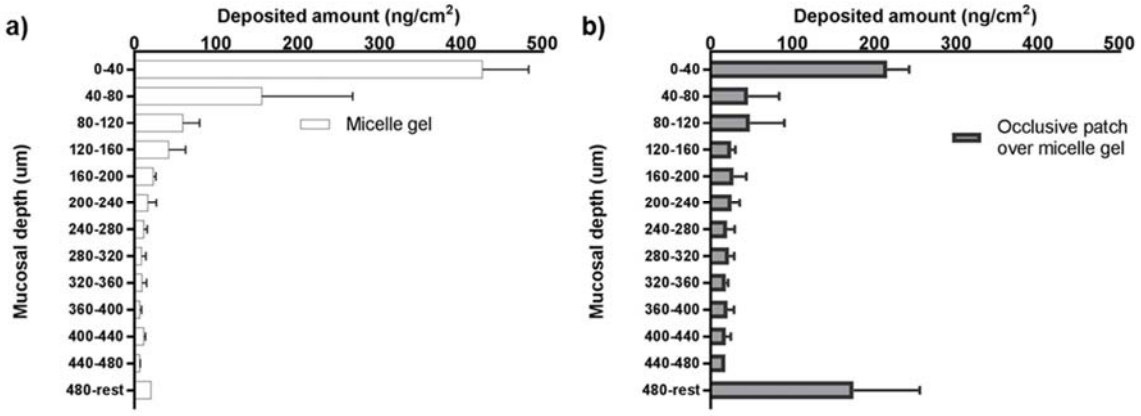

Figure 6. Deposition of TA in the mucosa after 30 min application of a) CMC micelle gel b) Occlusive patch over CMC micelle gel

Total delivery of TA in the mucosa after 30 min with and without occlusionwas not statistically different (799.2 ± 128.8 and 679.96 ± 105.5 ng/cm^2, respectively) (Student's t-test, p = 0.1480). However, the biodistribution of TA was markedly different. In the absence of occlusion, >50% of the total TA delivered remained in the upper 40 µm of mucosa; only 55.0 ± 7.3 ng/cm^2 reached the target therapeutic area. In contrast, under occlusion conditions TA could penetrate deeper into the mucosal layers and similar amounts of TA were found in the first 40 µm and beyond 480 µm (215.6 ± 27.0 and 174.8 ± 80.8 ng/cm^2 respectively). The amounts of TA reaching the epithelial-lamina propria junction (240 - 480 µm) were >2-foldhigher than unoccluded conditions (117.05 ± 15.7 *vs.* 55.0 ± 7.3 ng/cm^2). It is worth noting that the amounts of TA deposited in the mucosa after 30 min of occluded/unoccluded micelle gel application were at least 3 times higher than 60 min of KO application.

TA deposited in the epithelium-lamina propria junction (240-480 µm) after 30 min of application of the occluded hydrogel was ~ 11 * 10^7 folds more than the reported IC_{50} of TA (0.7-1.0 nM) [38].

3.2.2 FLU

There was no statistically significant difference between FLU deposition after application of 250 mg Novoter 0.05% and 0.25 ml of micelle solution (0.05%) for 60 min (617 ± 126.5 and 507.4 ± 68.5 ng/cm^2, respectively; Student's t-test, p=) (**Figure 7**). However, there was a 5-fold increase in deposition upon application of the CMC micelle gel (0.05%; 250 mg) for 60 min (2580.05 ± 285 ng/cm^2) (**Figure 7c**). The amount reaching the epithelial-lamina propria after application of the gel were 3-fold higher than that with Novoter (120.9 ± 33.6 *vs.* 392.9 ± 135.5 ng/cm^2, respectively).

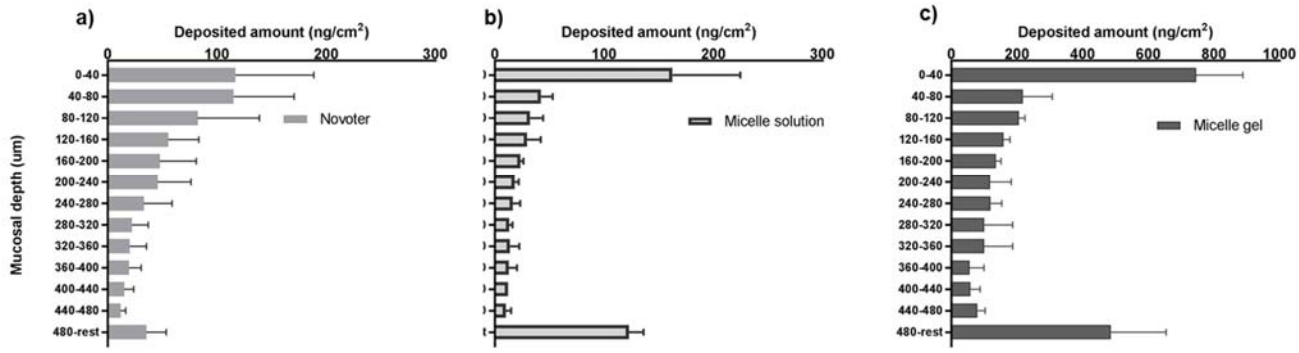

Figure 7. Deposition of FLU in the mucosa after 60 min application of a) Novoter b) FLU Micelle solution c) FLU CMC micelle gel

FLU permeation through the mucosa for all three formulations was below the LOQ.

For the next series of experiments, the application time was reduced to 30 min and the delivery of FLU from the micelle gel under occlusive conditions studied. Total mucosal delivery of FLU from Novoter decreased to 181.9 ± 49.7 ng/cm^2 (**Figure 8a**), and more than 50% of FLU remained in the superficial layers of the epithelium and the amounts deposited below 320 µm were below the LOQ.

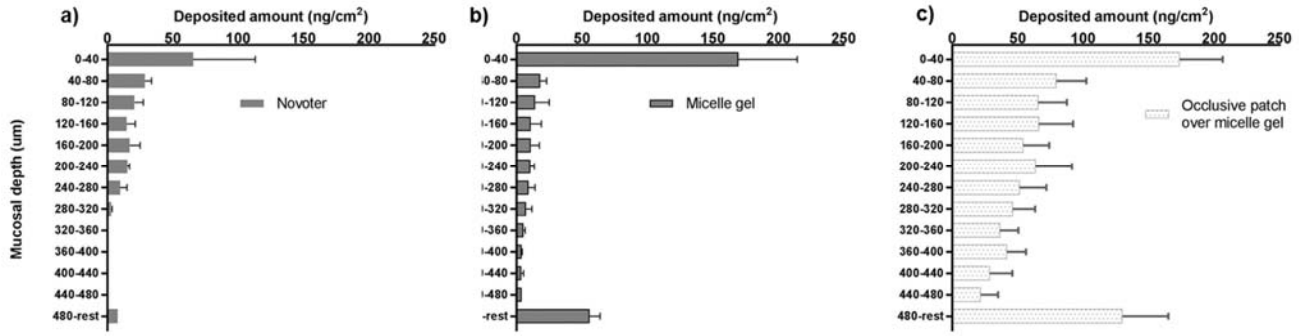

Figure 8. Deposition of FLU in the mucosa after 30 min application of a) Novoter b) FLU CMC micelle gel c) FLU CMC micelle gel under occlusion

The total delivery of FLU improved significantly when FLU CMC micelle gel (without occlusion) was applied for 30 min – 323.6 ± 48.8 ng/cm^2 and 33.3 ± 5.8 ng/cm^2 was able to reach the target therapeutic area (**Figure 8b**). Application of a blank occlusive HEC gel over the gel improved the delivery to 858.1 ± 82.4 ng/cm^2 FLU - 4.7 fold- higher than Novoter and over 2.5-fold higher than in the absence of occlusion. The amount of FLU present in the epithelial-lamina propria (LP) junction after 30 min was 225.6 ± 36.7 ng/cm^2.

Clearly polymeric nanocarriers applied over the mucosa under occlusion significantly improved the delivery of FLU compared to Novoter in the deeper layers of the mucosa. Occlusion can improve the delivery of drugs in the deeper layers of the mucosa by retaining the hydration in the epithelium thereby affecting the interaction of the chemicals present on the surface and the mucosa (**Figure 6b** and **Figure 8c**).[39] Occlusion by a patch may also increase the surface temperature of mucosa and affect the intercellular lipid layer organisation in the mucosa.[40] The synergistic effect of nanocarrier formulation and occlusion techniques resulted in the most superior delivery of TA/FLU compared to unoccluded micelle formulation and commercial formulation.

The amounts of FLU found in the target layers of the mucosa after 30 min of application of the occluded hydrogel was ~19 * 10^7 folds more than the IC_{50} of FLU (10-11 nM).[41] It was concluded that short duration occluded micellar gel application of TA and FLU on the mucosa was able to deposit supratherapeutic concentrations of the drugs in the target area providing a promising therapeutic strategy for OLP patients.

Finally, to understand the improved delivery of TA and FLU offered by the polymeric micelles, it is important to discuss the thermodynamic activity of the system. The nanocarrier assembly of the micelles are an expression of an optimum thermodynamic activity of the whole system. This activity is related to the thermal energy and interaction energies between the copolymer and the solvent and is minimized when factors such as copolymer chains readjustment, interfacial tension and repulsive interactions between the hydrophilic groups are minimized.[42, 43] A lower energy indicates greater thermodynamic stability which can have a significant effect on the formulation stability and consequent delivery of the drug from the carrier. As demonstrated in this study, a hydrophilic formulation of the hydrophobic TA and FLU remarkably improved their delivery in the mucosa compared to the lipophilic formulations of the drug. We hypothesize that this improvement is due to the high thermodynamic activity offered by the micellar systems which forces the drugs to move from the formulation to mucosa and partition. The entropy of the micellar systems were further increased by the addition of another excipient – CMC to form the hydrogels. Therefore after 60 min of application, the total delivery from

the micellar gels were 9.2 folds and 5 folds more than the micellar solution for TA and FLU respectively (**Figure 5** and **Figure 7**).

4. Conclusions

Corticosteroids such as TA and the more potent, FLU are the mainstay in the topical treatment of OLP. Although the disease affects a large population, commercial formulations focused towards OLP patients are scarce. The formulations used are intended for dermal use that are potentially unsafe to be applied in the mouth and ingested. There is an unmet need for a safe, patient friendly and clinically effective formulation. In this study, TPGS copolymer based micelle solution and gel formulations were developed and characterized. To improve the delivery of the drugs an occlusive patch over the formulations was also tested. The biodistribution study demonstrated that the micelle based aqueous formulations were indeed able to deliver superior amounts of drugs in the epithelial-lamina propria (target area) compared to the commercial formulations of TA/FLU. Thus the results suggest that TPGS based micelles of TA and FLU can provide a safe and effective treatment alternative to OLP patients. These promising results must be confirmed in a clinical study.

5. Supplementary information

5.1 Quantification of TA using UHPLC-MS/MS detector

TA was detected using UHPLC-MS/MS. A isocratic chromatographic method was developed using MeOH in 0.1% formic acid and 0.1 % formic acid (50/50 *v/v*). Mass spectrometer settings are provided in **Table S1**.

5.1.1 Specificity

The developed method was considered specific for TA quantification using MRM transition observed for 435.29 → 415.17. TA was eluted at 0.78 min.

5.1.2 Limit of detection and limit of quantification

The limit of detection (LOD) and limit of quantification (LOQ) were 1.0 ng/mL and 3.9 ng/mL respectively.

5.1.3 Linearity

The standards were prepared in the mucosa extract. The mucosa extract was prepared by soaking two cm^2 skin in 10mL of the extraction solvent MeOH:water (1:1) mixture. The method was found to be linear in the concentration range of 3.9-500 ng/mL. ($R^2 = 0.99$)

5.1.4 Accuracy and precision

Intra- and inter-day accuracy and precision was determined using 3.9, 15.6 and 500 ng/mL standards. Table S2 shows the accuracy and precision values for TA quantification method.

Table S1. MS/MS parameters for the detection of TA

Parameters	**Value**
Nature of parent ion	$[M+H]^+$
Parent ion (m/z)	435.29
Daughter ion (m/z)	415.17
MS mode collision energy (V)	2.0
MS/MS mode collision energy (V)	20.0
Cone voltage (V)	34.99
Capillary voltage (kV)	0.5
Source temperature (°C)	150
Desolvation temperature (°C)	350
Desolvation gas flow (L h−1)	658
LM resolution 1	2.8
HM resolution 1	15
Ion energy 1 (V)	0.5
LM resolution 2	2.7
HM resolution 2	14.9
Ion energy 2 (V)	0.6

Table S2. Intra- and inter- day accuracy and precision values for TA quantification

	Intra day			**Inter day 1**		
$[TA]_{theo}$ (ng/mL)	$[TA]_{mean}$ (ng/mL)	RSD (%)	Recovery (%)	$[TA]_{mean}$ (ng/mL)	RSD (%)	Recovery (%)
3.9	3.7 ± 0.3	3.9	95.5	3.8 ± 0.2	2.6	96.9
15.6	15.6 ± 0.3	1.9	100.1	15.3 ± 0.6	2.1	100.1
500	511.2 ± 9.1	4.2	101.2	504.8 ± 6.0	3.8	100.8

5.2 Quantification of TA using UHPLC-TUV detector

TA was detected using UHPLC-TUV detector. An isocratic chromatographic method was developed using MeOH in 0.1% formic acid and 0.1 % formic acid (50/50 *v/v*).

5.2.1 Specificity

The method was specific for TA at 240 nm. TA were eluted at 0.72 min respectively.

5.2.2 Limit of detection and limit of quantification

The LOD and LOQ of TA were 0.25 and 1 µg/mL respectively

5.2.3 Linearity

The method was linear for TA from the concentration range of 1-100 µg/mL ($R^2 = 0.99$).

5.2.4 Accuracy and precision

Intra- and inter-day accuracy and precision was determined using 2.5, 10 and 100 µg/mL standards.

Table S3. Intra- and inter- day accuracy and precision values for TA quantification

	Intra day			**Inter day 1**		
$[TA]_{theo}$ (µg/mL)	$[TA]_{mean}$ (µg/mL)	RSD (%)	Recovery (%)	$[TA]_{mean}$ (µg/mL)	RSD (%)	Recovery (%)
2.5	2.7 ± 0.0	3.8	111.2	2.5 ± 0.0	2.8	105.1
10	10.4 ± 0.4	0.4	98.7	5.0 ± 0.0	0.5	100.0
100	96.6 ± 0.1	0.1	96.6	50.1 ± 0.7	1.5	100.2

5.3 Quantification of FLU using UHPLC-MS/MS detector

FLU was detected using UHPLC-MS/MS. A gradient chromatographic method was developed using ACN in 0.1% formic acid and 0.1 % formic acid. **Table S4** shows the details of the isocratic method. Mass spectrometer settings are provided in **Table S5**.

Table S4. Gradient chromatographic elution method of FLU

Time (min)	Flow rate (mL/min)	Mobile phase A (%)	Mobile phase B (%)
0.00	0.20	10.0	90.0
1.00	0.20	70.0	30.0
2.50	0.20	70.0	30.0
3.00	0.20	10.0	90.0
4.00	0.20	10.0	90.0

5.3.1 Specificity

The developed method was considered specific for FLU quantification using MRM transition observed for 495.15 → 377.1. FLU was eluted at 3.1 min.

5.3.2 Limit of detection and limit of quantification

The limit of detection (LOD) and limit of quantification (LOQ) were 0.1 ng/mL and 0.78 ng/mL respectively.

5.3.3 Linearity

The standards were prepared in the mucosa extract. The mucosa extract was prepared by soaking two cm^2 skin in 10mL of the extraction solvent ACN and water (75/25 *v/v*) mixture. The method was found to be linear in the concentration range of 0.78-500 ng/mL. ($R^2 = 0.99$)

5.3.4 Accuracy and precision

Intra- and inter-day accuracy and precision was determined using 1.5, 6.25 and 250 ng/mL standards. Table S2 shows the accuracy and precision values for FLU quantification method.

Table S5. MS/MS parameters for the detection of FLU

Parameters	**Value**
Nature of parent ion	$[M+H]^+$
Parent ion (m/z)	495.15
Daughter ion (m/z)	377.10
MS mode collision energy (V)	3.0
MS/MS mode collision energy (V)	20.0
Cone voltage (V)	18.5
Capillary voltage (kV)	3.5
Source temperature (°C)	150
Desolvation temperature (°C)	497
Desolvation gas flow (L h−1)	995
LM resolution 1	12.91
HM resolution 1	15.81
Ion energy 1 (V)	0.1
LM resolution 2	11.18
HM resolution 2	14.9
Ion energy 2 (V)	0.1

Table S6. Intra- and inter- day accuracy and precision values for FLU quantification

	Intra day			**Inter day 1**		
$[FLU]_{theo}$ (ng/mL)	$[FLU]_{mean}$ (ng/mL)	RSD (%)	Recovery (%)	$[FLU]_{mean}$ (ng/mL)	RSD (%)	Recovery (%)
1.5	1.7 ± 0.1	5.9	111.8	1.6 ± 0.0	4.6	109.3
6.25	6.0 ± 0.2	3.4	97.5	6.1 ± 0.2	3.1	98.2
250	256.4 ± 5.1	5.8	102.5	252.3 ± 3.4	2.9	101.7

5.4 Quantification of FLU using UHPLC-TUV detector

FLU was detected using UHPLC-TUV detector. A gradient chromatographic method was developed using ACN in 0.1% formic acid and 0.1 % formic acid (Table S4).

5.4.1 Specificity

The method was specific for FLU at 240nm. FLU was eluted at 3.1 min.

5.4.2 Limit of detection and limit of quantification

The LOD and LOQ of FLU were 0.25 and 0.75 µg/mL respectively

5.4.3 Linearity

The method was linear for FLU from the concentration range of 0.75-100 µg/mL ($R^2 = 0.99$).

5.4.4 Accuracy and precision

Intra- and inter-day accuracy and precision was determined using 3.1, 25 and 100 µg/mL standards.

Table S7: Intra- and inter- day accuracy and precision values for FLU quantification

	Intra day			**Inter day 1**		
$[FLU]_{theo}$ (µg/mL)	$[FLU]_{mean}$ (µg/mL)	RSD (%)	Recovery (%)	$[FLU]_{mean}$ (µg/mL)	RSD (%)	Recovery (%)
3.1	3.1 ± 0.0	0.02	99.89	3.1 ± 0.0	0.01	99.9
25	24.8 ± 0.2	1.0	99.3	25.0 ± 0.0	0.8	99.5
100	100.3 ± 0.0	0.03	100.3	100.1 ± 0.0	0.02	100.1

5.5 Deposition set up

The set-up was designed in house and constructed by Elega SA (Le Lignon, Switzerland). The set-up was made of polymethly(methacrylate). The base of the set-up on which the mucosa piece was placed was 10 x 8 cm. The top part of the set-up, which sandwiched the mucosa had the concentric donor compartment was also 10 x 8 cm. The height of the cylinder from the base of the tray was 2 cm. Thickness of both the trays was 1 cm. Figure S1 shows a schematic of the top tray and the bottom of the top tray.

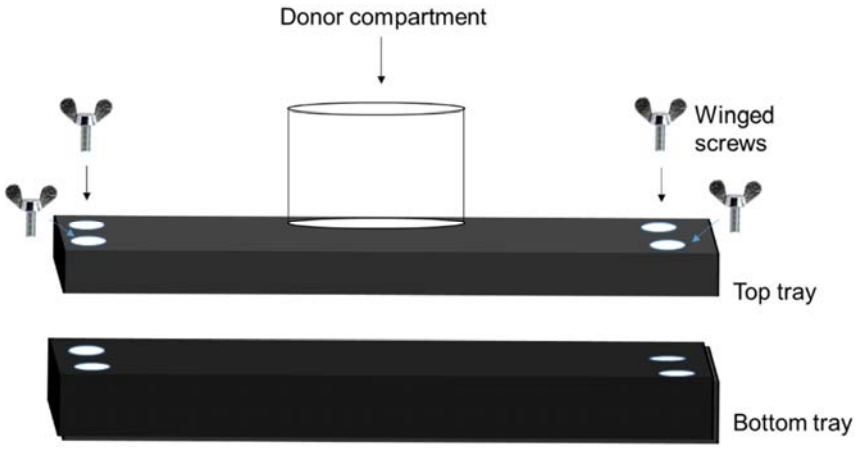

Figure S1. Schematic of the deposition set up

6. Acknowledgment

YNK would like to thank the University of Geneva, for providing financial support to enable the acquisition of the Waters Xevo® TQ-S Micro detector. VT and SK are grateful to the Swiss Federal Commission for Scholarships for Foreign Students for the award of PhD studentships.

7. References

1. Gorouhi F., Davari P. *et al.* Cutaneous and Mucosal Lichen Planus: A Comprehensive Review of Clinical Subtypes, Risk Factors, Diagnosis, and Prognosis. *The Scientific World Journal.* **2014** *2014*: 22.

2. Andreasen J. O. Oral lichen planus: I. A clinical evaluation of 115 cases. *Oral Surgery, Oral Medicine, Oral Pathology.* **1968** *25(1)*: 31-42.

3. Olson M. A., Rogers R. S., 3rd *et al.* Oral lichen planus. *Clinics in Dermatology.* **2016** *34(4)*: 495-504.

4. Di Rosa M., Calignano A. *et al.* Multiple control of inflammation by glucocorticoids. *Agents and Actions.* **1986** *17(3)*: 284-289.

5. Norris D. A., Capin L. *et al.* The effect of epicutaneous glucocorticosteroids on human monocyte and neutrophil migration in vivo. *Journal of Investigative Dermatology.* **1982** *78(5)*: 386-90.

6. Thorburn D. N. and Ferguson M. M. Topical corticosteroids and lesions of the oral mucosa. *Adv. Drug Deliv. Rev.* **1994** *13(1)*: 135-149.

7. Thongprasom K. and Dhanuthai K. Steriods in the treatment of lichen planus: a review. *Journal of oral science.* **2008** *50(4)*: 377-85.

8. Zegarelli E. V., Kutscher A. H. *et al.* Triamcinolone acetonide in the treatment of acute and chronic lesions of the oral mucous membranes: Preliminary report. *Oral Surgery, Oral Medicine, Oral Pathology.* **1960** *13(2)*: 170-175.

9. ZEGARELLI E. V. and KUTSCHER A. H. Triamcinolone Acetonide in the Treatment of Erosive Lichen Planus of the Oral Mucosae: Preliminary Report. *JAMA Dermatology.* **1960** *82(6)*: 1010-1011.

10. Lodi G., Scully C. *et al.* Current controversies in oral lichen planus: report of an international consensus meeting. Part 2. Clinical management and malignant transformation. *Oral surgery, oral medicine, oral pathology, oral radiology, and endodontics.* **2005** *100(2)*: 164-78.

11. Lozada F. and Silverman S., Jr. Topically Applied Fluocinonide in an Adhesive Base in the Treatment of Oral Vesiculoerosive Diseases. *JAMA Dermatology.* **1980** *116(8)*: 898-901.

12. Georgakopoulou E. A., Achtari M. D. *et al.* Oral Lichen Planus as a Preneoplastic Inflammatory Model. *Journal of Biomedicine and Biotechnology.* **2012** *2012*: 8.

13. Sugerman P. B., Savage N. W. *et al.* The Pathogenesis of Oral Lichen Planus. *Critical Reviews in Oral Biology & Medicine.* **2002** *13(4)*: 350-365.

14. Xia J., Li C. *et al.* Short-term clinical evaluation of intralesional triamcinolone acetonide injection for ulcerative oral lichen planus. *J. Oral Pathol. Med.* **2006** *35(6)*: 327-331.

15. Ungphaiboon S., Nittayananta W. *et al.* Formulation and efficacy of triamcinolone acetonide mouthwash for treating oral lichen planus. *American Journal of Health-System Pharmacy.* **2005** *62(5)*: 485-491.

16. Winn D. M., Blot W. J. *et al.* Mouthwash Use and Oral Conditions in the Risk of Oral and Pharyngeal Cancer. *Cancer Research.* **1991** *51(11)*: 3044-3047.

17. Fitzpatrick S. G., Hirsch S. A. *et al.* The malignant transformation of oral lichen planus and oral lichenoid lesions: a systematic review. *J. Am. Dent. Assoc.* **2014** *145(1)*: 45-56.

18. Liu Y., Messadi D. V. *et al.* Oral lichen planus is a unique disease model for studying chronic inflammation and oral cancer. *Medical Hypotheses.* **2010** *75(6)*: 492-494.

19. Kutscher A. H., Zegarelli E. V. *et al.* A new vehicle (Orabase) for the application of drugs to the oral mucous membranes. *Oral Surgery, Oral Medicine, Oral Pathology.* **1959** *12(9)*: 1080-1089.

20. Arunkumar S., Kalappanavar A. N. *et al.* Relative efficacy of pimecrolimus cream and triamcinolone acetonide paste in the treatment of symptomatic oral lichen planus. *Indian J Dent.* **2015** *6(1)*: 14-19.

21. Sivaraman S., Santham K. *et al.* A randomized triple-blind clinical trial to compare the effectiveness of topical triamcinolone acetonate (0.1%), clobetasol propionate (0.05%), and tacrolimus orabase (0.03%) in the management of oral lichen planus. *Journal of pharmacy & bioallied sciences.* **2016** *8(Suppl 1)*: S86-S89.

22. Cheng S., Kirtschig G. *et al.* Interventions for erosive lichen planus affecting mucosal sites. *The Cochrane database of systematic reviews.* **2012** *(2)*: Cd008092.

23. Lapteva M., Mignot M. *et al.* Self-assembled mPEG-hexPLA polymeric nanocarriers for the targeted cutaneous delivery of imiquimod. *Eur. J. Pharm. Biopharm.* **2019**.

24. Kandekar S. G., Singhal M. *et al.* Polymeric micelle nanocarriers for targeted epidermal delivery of the hedgehog pathway inhibitor vismodegib: formulation development and cutaneous biodistribution in human skin. *Expert Opin. Drug Deliv.* **2019**: 1-8.

25. Yu Y., Chen D. *et al.* Improving the topical ocular pharmacokinetics of lyophilized cyclosporine A-loaded micelles: formulation, in vitro and in vivo studies. *Drug delivery.* **2018** *25(1)*: 888-899.

26. Lv Q., Shen C. *et al.* Mucoadhesive buccal films containing phospholipid-bile salts-mixed micelles as an effective carrier for Cucurbitacin B delivery. *Drug delivery.* **2015** *22(3)*: 351-358.

27. Zhang Z., Tan S. *et al.* Vitamin E TPGS as a molecular biomaterial for drug delivery. *Biomaterials.* **2012** *33(19)*: 4889-4906.

28. Kandekar S. G., Del Rio-Sancho S. *et al.* Selective delivery of adapalene to the human hair follicle under finite dose conditions using polymeric micelle nanocarriers. *Nanoscale.* **2018** *10(3)*: 1099-1110.

29. Burgess J. A., van der Ven P. F. *et al.* Review of over-the-counter treatments for aphthous ulceration and results from use of a dissolving oral patch containing glycyrrhiza complex herbal extract. *The journal of contemporary dental practice.* **2008** *9(3)*: 88-98.

30. Lapteva M., Möller M. *et al.* Self-assembled polymeric nanocarriers for the targeted delivery of retinoic acid to the hair follicle. *Nanoscale.* **2015** *7(44)*: 18651-18662.

31. Diaz Del Consuelo I., Pizzolato G. P. *et al.* Evaluation of pig esophageal mucosa as a permeability barrier model for buccal tissue. *J. Pharm. Sci. (Philadelphia, PA, U. S.).* **2005** *94(12)*: 2777-88.

32. Telo I., Tratta E. *et al.* In-vitro characterization of buccal iontophoresis: the case of sumatriptan succinate. *Int. J. Pharm. (Amsterdam, Neth.).* **2016** *506(1-2)*: 420-8.

33. Diaz Del Consuelo I., Falson F. *et al.* Transport of fentanyl through pig buccal and esophageal epithelia in vitro: influence of concentration and vehicle pH. *Pharm. Res.* **2005** *22(9)*: 1525-9.

34. Bachhav Y. G., Mondon K. *et al.* Novel micelle formulations to increase cutaneous bioavailability of azole antifungals. *J. Control. Release.* **2011** *153(2)*: 126-32.

35. Landay M. A. and Schroeder H. E. Differentiation in normal human buccal mucosa epithelium. *J. Anat.* **1979** *128(Pt 1)*: 31-51.

36. Duhem N., Danhier F. *et al.* Vitamin E-based nanomedicines for anti-cancer drug delivery. *J. Control. Release.* **2014** *182*: 33-44.

37. Creeth J., Bosma M. L. *et al.* How much is a 'pea-sized amount'? A study of dentifrice dosing by parents in three countries. *International dental journal.* **2013** *63 Suppl 2*: 25-30.

38. JAFFUEL D., DEMOLY P. *et al.* Transcriptional Potencies of Inhaled Glucocorticoids. *American Journal of Respiratory and Critical Care Medicine.* **2000** *162(1)*: 57-63.

39. Zhai H. and Maibach H. I. Effects of skin occlusion on percutaneous absorption: an overview. *Skin pharmacology and applied skin physiology.* **2001** *14(1)*: 1-10.

40. Matsumura H., Oka K. *et al.* Effect of occlusion on human skin. *Contact dermatitis.* **1995** *33(4)*: 231-5.

41. Epstein E. H. and Bonifas J. M. Glucocorticoid Receptors of Normal Human Epidermis. *Journal of Investigative Dermatology.* **1982** *78(2)*: 144-146.

42. Feng H., Lu X. *et al.* Block Copolymers: Synthesis, Self-Assembly, and Applications. *Polymers (Basel).* **2017** *9(10)*: 494.

43. Owen S. C., Chan D. P. Y. *et al.* Polymeric micelle stability. *Nano Today.* **2012** *7(1)*: 53-65.

CONCLUSIONS

Conclusions

The buccal epithelium remains the major barrier to all foreign substances from entering the body including therapeutic molecules. Yet another challenge to the delivery of these therapeutic molecules is the location of the buccal mucosa, which demands that the contact time of the formulations be short to ensure patient comfort. In this study, different strategies to improve the local buccal delivery of therapeutic molecules depending on their physicochemical properties were studied.

The delivery kinetics of hydrophilic ionic molecules was improved by the application of low current densities (iontophoresis). A detailed investigation into the feasibility of using this technique to improve the delivery of buflomedil hydrochloride (BUF) for oral submucous fibrosis was performed. Iontophoresis significantly enhanced the delivery of BUF compared to the passive controls where no current was applied. For convenience of application, hydrogel and fast dissolving film of BUF was developed. Biodistribution data confirmed that 10 min of current application from the fast dissolving film resulted in therapeutically relevant concentrations of BUF at the target site.

Further, a simultaneous delivery of BUF and the oppositely charged dexamethasone disodium phosphate (DEX-P) was studied as a multi action therapy for the management of oral submucous fibrosis. A special apparatus equipped with concentric donor compartments was developed in house to study the simultaneous delivery of the two ions. Compared to no current application, 5 min of iontophoretic application improved the delivery of both molecules under their own application area as well as the neighbouring areas. Moreover, the concentrations of both molecules achieved in the entire area under investigation were sufficient to produce the required therapeutic response. The delivery efficiencies of the drugs were found to be highly dependent on the physicochemical properties of the molecules and the buccal mucosa.

For the next part of the work, an unprecedented investigation employed iontophoresis to transport rituximab (RTX) – an antibody in the mucosa for the management of oral pemphigus vulgaris. It was confirmed that the presence of an electric current did not deform the structure of the antibody. Compared to the amounts of RTX deposited in the absence of current application, 10 min ofelectro transport deposited significantly higher amounts into the mucosa which were therapeutically relevant. An examination into the mechanism of the electrotransport revealed that unlike small ions, which are primarily transported by electromigration, RTX was delivered by electroosmosis. The study also suggested that RTX did not neutralize the mucosa and therefore was unable to influence the direction of solventflow.

It is reasonable to conclude that different mechanisms of iontophoresis are able to efficiently deliver small and high molecular weight hydrophilic molecules into the mucosa.

The limitations for lipophilic molecules are different. Compared to hydrophilic molecules, it is easier for lipophilic molecules to partition in the lipid rich epithelium. However, it is more challenging to develop patient friendly formulations of these molecules that are able to perform in the highly aqueous environment in the mouth. The aim for the final part of the work was to develop aqueous formulations of poorly water-soluble drugs – triamcinolone acetonide (TA) and fluocinonide (FLU). Micelle based nanocarrier systems of TA and FLU were developed using TPGS diblock copolymer leading to an enhancement of an aqueous solubility of ~ 35- and ~26-fold, respectively. Compared to the currently marketed formulations of these drugs, 30 min of micellar hydrogel application delivered significantly more amounts at the target site in the mucosa. The delivery of the drugs further improved when the hydrogel(s) were occluded by thin water-soluble film(s) – providing a promising approach to manage the lesions induced from oral lichen planus.

In conclusion, this study demonstrates the importance of choosing appropriate drug delivery enhancement techniques depending on the physicochemical properties of the drug molecules. Given the rapid replenishing nature of the oral mucosa, the needs of patients suffering from local buccal diseases are often ignored. Innovative drug delivery strategies can improve the delivery of existing drug and ultimately advance the therapy options for oromucosal diseases.

Major limitations in this study were the absence of vascularization of the mucosa and saliva, which can influence the delivery of the drugs. It must be acknowledged that results obtained *in vitro* are most certainly an overestimation of the in vivo scenario, but the valuable information is provided on the extent and the pattern of overcoming the physical static barrier – buccal mucos

APPENDIX I

Iontosomes: Novel electroresponsive liposomes for targeted local chemotherapy of oral cancers using buccal iontophoresis

Kiran Sonaje, Vasundhara Tyagi, Yogeshvar N. Kalia

School of Pharmaceutical Sciences,
University of Geneva & University of Lausanne,
Rue Michel-Servet 1,
1206 Geneva, Switzerland

Manuscript in preparation

Abstract

The targeted local delivery of anticancer therapeutics would offer an alternative to systemic chemotherapy for oral cancers not amenable to surgical excision. However, epithelial permeability remains a challenge for the topical/buccal delivery of these molecules. The iontosomes described here are able to overcome this barrier via a combination of the electrical potential gradient imposed by iontophoresis and their shape deforming characteristics. Cisplatin (CDDP) and docetaxel (DTX) were co-encapsulated in cationic iontosomes comprising DOTAP and Lipoid-S75. The entrapment of CDDP was improved by formulating it in anionic reverse micelles of DPPG prior to loading in the iontosomes. Cryo-TEM imaging clearly demonstrated the electro-responsive shape deformation characteristics of the iontosomes. The *in vitro* transport study using porcine esophagus indicated that iontosomes did not enter the mucosa without an external driving force. However, after anodal iontophoresis, significantly greater amounts of co-encapsulated CDDP and DTX were deposited in the mucosa, without any noticeable increase in their transmucosal permeation. Confocal microscopy confirmed that the iontosomes penetrated the mucosa through the intercellular spaces and the penetration depth could be controlled by varying the duration of iontophoresis. Overall, the results suggested that the application of topical iontophoresis with a suitable carrier system could be used to deliver multiple chemotherapeutics selectively to oral cancers while decreasing the extent of systemic absorption and associated risk of side-effects.

Keywords*:* Iontophoresis; deformable liposomes; oral cancer; drug delivery; buccal mucosa

1. Introduction

A major challenge in treating any cancer is achieving a high cure rate while preserving vital functions of the affected tissue. This is especially important for oral cancers, where the affected regions are essential for regular human activities such as speaking and eating.[1] Surgical resection of such cancers can permanently affect the normal functioning of affected organs; moreover the outcome of radiotherapy alone can be disappointing, particularly for advanced stage cancer. As a consequence, systemic chemotherapy has been increasingly incorporated into treatment protocols in recent years.[1, 2] However, the high rates of off-site adverse events induced by systemic chemotherapy can compromise the overall success of such treatments. Given this scenario, a topical system providing local delivery of chemotherapeutic agents for oral cancer could be a non-invasive and patient-friendly alternative to intravenous chemotherapy. However, the oral mucosa represents a significant barrier to the transport of drugs with unfavorable physicochemical properties. Another difficulty in topical buccal treatment is to achieve therapeutically significant drug levels in the affected tissue quickly, since only short duration applications are practical in the oral cavity due to obvious anatomical constraints.[3]

Iontophoresis, a non-invasive technique involving application of mild electric current to enhance the penetration of water-soluble, ionizable drugs offers a simple and effective method to deliver chemotherapeutics into the buccal mucosa.[4] The electrical potential acts as a second driving force in addition to the concentration gradient and results in increased drug delivery rates as compared to passive drug diffusion alone. The amount of drug delivered can be controlled by modulating the electric field, making personalized dosing feasible.[5] It has been shown to effectively deliver a variety of drugs across the skin and buccal mucosa. Previously we demonstrated successful concurrent delivery of 5-fluorouracil (5-FU) and leucovarin (LV; folinic acid) to buccal mucosa using short duration iontophoresis for the treatment of head and neck (H&N) cancers.[4] However, one drawback in delivering free-form chemotherapeutics using this technique is the possibility of their systemic clearance and exposure to associated side effects. Moreover, not all chemotherapeutic agents are suitable for iontophoretic delivery; e.g. molecules that are non-polar, display poor aqueous solubility and do contain ionizable functional groups, are unsuited for this technique.[5] Therefore, a carrier system is needed to encapsulate chemotherapeutics with diverse physicochemical properties and provide sustained release after iontophoretic delivery to buccal mucosa.

The oral mucosa is composed of several layers of tightly packed epithelial cells that form the primary barrier to drug permeation.[6-8] The intercellular space in these layers is believed to be narrower than

20 nm.[6] Hence, traditional nanocarriers such as polymeric nanoparticles or conventional liposomes are unlikely to cross this barrier by passive diffusion. In recent years, various deformable vesicles such as Transferosomes®, niosomes or ethosomes have been introduced for transdermal drug delivery.[9-12] Transferosomes® and niosomes are composed of an edge activator, a surfactant that destabilizes the lipid bilayer and provides elasticity to the liposomes. In the case of ethosomes, ethanol imparts flexibility to vesicles via its interdigitation into the lipid bilayers. It has been assumed that the elastic nature of such deformable vesicles allows them to squeeze between the corneocytes and traverse across the epidermis. However, the precise mechanism that drives their penetration remains unclear. It has been hypothesized that Transferosomes® utilize the transdermal osmotic gradient resulting from differences in the hydration levels of outer stratum corneum and inner viable epidermis to spontaneously penetrate the skin. However, unlike the skin, oral mucosa is uniformly hydrated due to the presence of saliva and this mechanism is unlikely to work for buccal delivery.

The present investigation describes novel cationic liposomes called 'iontosomes' for the effective iontophoretic delivery of chemotherapeutics across the buccal mucosa. Docetaxel (DTX) and cisplatin (CDDP), which are widely prescribed in combination for the treatment of head and neck cancers, were loaded in these carriers for simultaneous iontophoretic delivery. The iontosomes were engineered to undergo shape deformation in response to the applied electric field, which facilitates their penetration through the narrow intercellular spaces of mucosal epithelium. They were formulated by combining a cationic lipid film with reverse micelles of an anionic lipid. The iontosomes were characterized in terms of size, zeta potential, electro-responsive shape deformation and *in vitro* drug release behavior. Their anti-tumoral activity was evaluated *in vitro* using HeLa cells. Finally, the mucosal iontophoretic delivery of these iontosomes was investigated in the porcine esophageal mucosa, a widely used model to study buccal permeation.[13]

2. Materials and methods

2.1 Materials

The different lipids used to formulate iontosomes, namely, 1,2-dioleoyl-3-trimethylammonium-propane chloride (Lipoid-DOTAP), soybean phosphatidylcholine (Lipoid-S75) and 1,2-Dipalmitoyl-sn-glycero-3-phospho-rac-glycerol sodium (Lipoid-DPPG) were generous gifts from Lipoid AG (Steinhausen, Switzerland). The chemotherapeutic agents, DTX and CDDP were obtained from Alfa Aesar GmbH (Karlsruhe, Germany) and Strem Chemicals, Inc. (Kehl, Germany), respectively. All other chemicals were of analytical reagent grade.

2.2 Formulation development

2.2.1 Preparation of conventional liposomes

The conventional cationic liposomes encapsulating DTX were prepared by a lipid film hydration method as described previously.[14] First, DOTAP (0.1 mmol), Lipoid-S75 (0.09 mmol), and DTX (0.01 mmol) were added to 15 mL of chloroform in a round-bottomed flask. The mixture was gently warmed to 40°C for 15 min and the solvent was evaporated using a rotary evaporator (Rotavapor R-124, Buchi; Flawil, Germany) until a thin lipid film was formed. Solvent traces were removed by desiccating the film for 60 min at high vacuum. The lipid film was hydrated with an aqueous solution of CDDP (1 mg/mL, 10 mL) in 0.9% (w/v) NaCl. Large multilamellar liposomes were spontaneously formed upon addition of the CDDP solution. The lipid suspension was left overnight to allow swelling of the liposomes and partitioning of CDDP in the liposomes. The uniformly sized liposomes were then obtained by extruding the initial suspension through a series of polycarbonate membrane filters of decreasing pore sizes (400 nm, 200 nm and 100 nm, five cycles each) using a mini-extruder (Avanti Polar Lipids, Inc.; Alabaster, Alabama, USA) maintained at 40°C. Finally, the formulated liposomes were purified using a Zeba™ spin desalting column (Life Technologies Europe B.V.; Zug, Switzerland) to remove the unentrapped drugs.

2.2.2 Preparation of iontosomes

The iontosomes were obtained by mixing the aforementioned cationic lipid film with the CDDP-loaded reverse micelles of DPPG (**Fig. 1**). The preparation of reverse micelles was based on Lipoplatin™, a successful liposomal formulation of cisplatin.[15] Briefly, DPPG (0.1 mmol) and CDDP (0.1 mmol) were added to 6 mL of Tris buffer (pH 7.5, 0.1 M) containing 30 % ethanol (v/v) and the mixture was heated at 50°C for 15−30 min. The heating step converted the suspended CDDP powder into a colloidal gel form. The reverse micelles were obtained by diluting the colloidal gel with 5% glucose solution (w/v) to a CDDP concentration of 2 mg/mL.

The formulated CDDP-DPPG reverse micelles were used to hydrate the DTX-loaded cationic lipid film described above. Three kinds of formulations were prepared using increasing volumes of reverse micelles (2.5, 5.0 and 10 mL) (**Table 1**). After overnight hydration, the volume of the formulation was adjusted to 10 mL with glucose solution (5% w/v) where necessary and large clumps of hydrated lipids were dispersed using a micropipette tip to obtain a homogenous suspension of lipid vesicles. The uniformly sized iontosomes were then obtained by extrusion through polycarbonate membrane filters as described above.

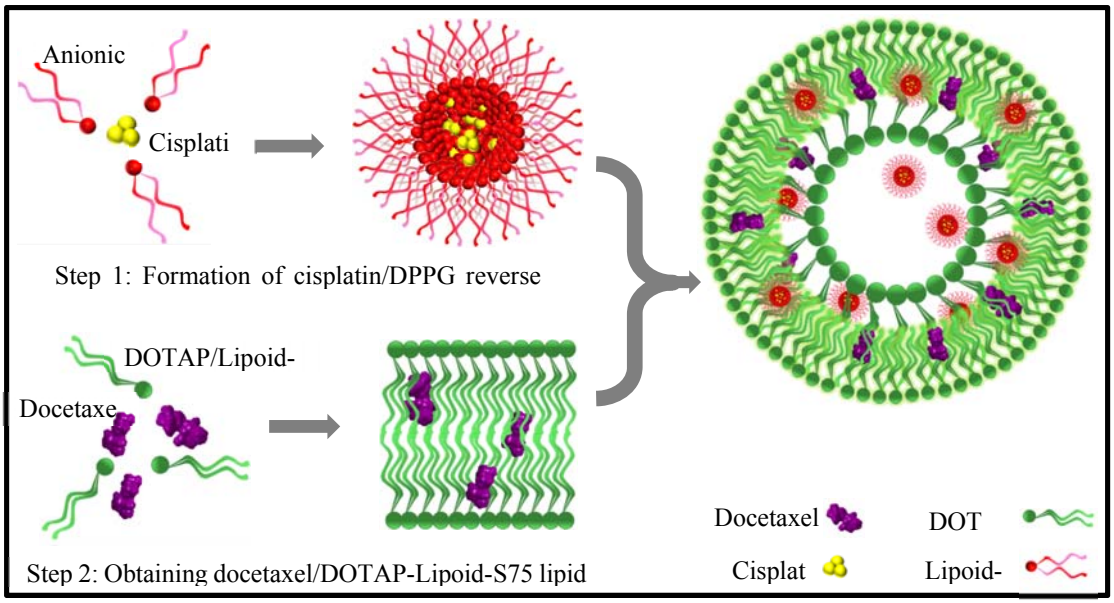

Figure 1. Formulation of electro-responsive iontosomes; cisplatin (CDDP) was formulated into the anionic reverse micelles using the DPPG (red) and docetaxel (DTX) was loaded in the cationic lipid bilayer of DOTAP-Lipoid-S75 (green). The iontosomes were then obtained by hydrating the cationic lipid bilayer with the CDDP-DPPG reverse micelles.

Table 1. Composition, mean diameter, polydispersity index (PDI), zeta potential, loading efficiency and drug content of formulated iontosomes.

Formulation	Vol. R.M. (mL)	Particle size (nm)	PDI	Zeta Pot. (mV)	EE (%)		Content ratio
					CDDP	DTX	
Lip-1	0.0	120.3 ± 13.9	0.29	52.8 ± 2.1	6.3 ± 0.8	87.3 ± 4.1	0.1 ± 0.0
Lip-2	2.5	107.5 ± 15.5	0.21	42.3 ± 4.6	91.1 ± 3.1	84.2 ± 4.9	0.7 ± 0.0
Lip-3	5.0	109.8 ± 12.4	0.25	34.3 ± 3.6	84.4 ± 4.9	81.7 ± 3.7	1.3 ± 0.1
Lip-4	10.0	120.4 ± 17.1	0.35	8.6 ± 2.4	51.8 ± 6.5	48.8 ± 8.2	2.7 ± 0.8

Note: Vol. RM: volume of reverse micelles used, PDI: polydispersity index; EE: entrapment efficiency; CDDP: cisplatin, DTX: docetaxel, Content ratio: the ratio of CDDP:DTX amounts present in final formulation. Lip-1 comprises conventional liposomes prepared using CDDP solution.

2.2.3. Preparation of fluorescent iontosomes

To prepare fluorescent iontosomes, Lipoid-S75 was labeled with an amine-reactive dye, NHS-fluorescein (Thermo Scientific), as described previously.[16] Briefly, Lipoid-S75 (1 mmol) was reacted with NHS-fluorescein (0.1 mmol) in 10 mL of tetrahydrofuran containing 0.2 mL of triethylamine at room temperature for 4 h. The reaction mixture was dried under vacuum and the product was dissolved in 100 mL of chloroform. The fluorescent lipid was purified to remove the unreacted dye by liquid-liquid extraction with MilliQ water until no fluorescence was observed in the aqueous phase. The purity of the fluorescein-labeled lipid was confirmed using reversed phase HPLC.[17] The fluorescent iontosomes were prepared as per the method described above except half of the Lipoid-S75 was substituted with its fluorescent derivative.

2.2.4. Preparation of solution formulations

The solution formulations of CDDP and DTX were used as controls in the subsequent studies. Although CDDP is slightly soluble in water (solubility ~2.5 mg/mL), it isomerizes into the inactive *trans*-form in chloride free medium.[18] Therefore, a stock solution of CDDP at 1 mg/mL was prepared in normal saline (0.9% NaCl w/v). The availability of excess chloride ions prevents the isomerization of CDDP in saline and provides stable solutions that retain CDDP activity for at least 30 days.[19, 20]

The preparation of DTX solution was based on its commercial formulation, Taxotere®. Briefly, 20 mg DTX was added to 0.5 mL of Tween 80 (520 mg) and vortexed until a clear solution was obtained. The resulting DTX solution was then mixed with 1.5 mL of 13% ethanol in PBS (pH 7.4) resulting in a 1% w/v stock solution of DTX. Both stock solutions were stored in the dark at 2–8°C for no longer than four weeks. These stock solutions were diluted to the required working concentrations for respective experiments using appropriate vehicles.

2.3 Characterization of liposomes

2.3.1 Physicochemical characteristics and drug content

The particle sizes and zeta potentials of the formulated iontosomes were analyzed by dynamic light scattering (DLS) using a Zetasizer Nano-ZS (Malvern Instruments, UK) at 25 °C. All measurements were made in triplicate.

To determine the drug content, purified liposomes or iontosomes were disrupted by 0.1% Triton X-100 and amounts of DTX and CDDP were quantified using the validated HPLC-UV method (**Supplementary Information**).

The encapsulation efficiency (EE) was calculated using the following equation:

$$Encapsulation\ efficiency\ (\%) = \frac{Amount\ of\ drug\ incorporated\ in\ iontosomes \times 100}{Intial\ mass\ of\ the\ drug}$$

2.3.2. Cryo-transmission electron microscopy (Cryo-TEM)

The shape and morphology of the formulated reverse-micelles, liposomes and iontosomes were studied using transmission electron microscopy at cryogenic temperature (Cryo-TEM) as per a previously reported protocol.[21] Briefly, 5 µL of each formulation was applied to a copper grid precoated with perforated carbon film. After blotting the excess formulation, the grid was immediately immersed in liquid ethane container cooled using liquid nitrogen. Cryo-TEM images were recorded at -170°C using a Philips CM12 transmission electron microscope (Eindhoven, The Netherlands) operating at 100 kV and equipped with a cryo-specimen holder Gatan 626 (Warrendale, PA). Digital images were recorded with a Gatan MultiScan CCD camera and processed using the Gatan Digital Micrograph.

2.3.3. Effects of iontophoresis on drug release and iontosome characteristics

Drug release from the iontosomes was tested using a dialysis membrane with 6–8 kDa molecular weight cut-off (Spectrapor® 3, Spectrum Laboratories, USA) mounted between the donor and receptor compartments of Franz diffusion cells. The donor cell was filled with 0.5 mL of formulation and the receptor cell contained 4.5 mL of 0.1% (w/v) Tween 80 in phosphate-buffered saline (PBS, pH 7.4). The positive electrode (anode) was connected to the donor compartment via a salt bridge assembly (3% agarose with 100 mM NaCl). Constant current (0.5 mA/cm^2) was applied using Ag/AgCl electrodes connected to a power supply (Kepco® APH 1000 M, Flushing, NY). The electric current was applied for 20 min followed by passive release *in vitro* for 12 h.

Aliquots (500 µL) of the receptor medium were withdrawn at predetermined intervals and immediately replaced with an equal volume of fresh buffer. In addition, the amounts of unreleased drug were determined in the residual formulation and dialysis membranes after the experiment. The amounts of CDDP and DTX in the samples were determined using the respective HPLC-UV analytical methods. Finally, the size and morphology of iontosomes after exposure to the iontophoretic conditions were determined using the zetasizer and Cryo-TEM, respectively.

2.4. Evaluation of in vitro anti-tumoral activity of iontosomes

A human cervical cancer cell line (HeLa cells) was employed for the evaluation of the anti-tumoral activity of the formulated iontosomes *in vitro*. The cells were cultured in Dulbecco's modified Eagle

medium (DMEM, high glucose, GlutaMAX™) supplemented with 10% fetal calf serum, 100 U/mL penicillin and 100 µg/mL streptomycin (all from Invitrogen Life Technologies; Basel, Switzerland) in a humidified atmosphere with 5% CO_2 at 37°C.

The cells were seeded in 96-well plates at a density of 10^4 cells (100 µL) per well and incubated for 24 h to allow cell attachment. After 24 h, the medium in the wells was replaced with DMEM containing drug-loaded iontosomes, solution formulations of CDDP and DTX or their combination and incubated for 24 h. The concentrations of drugs in the solution formulations were equivalent to those in the iontosomes. The blank iontosomes were also tested to evaluate whether the lipids exhibited any cytotoxic activity on the HeLa cells. After the 24 h treatment, DMEM containing MTT (20 µL, 5 mg/mL) was added and cells were incubated for an additional 4 h. Finally, the medium containing MTT was aspirated and formazan crystals formed by viable cells were dissolved by addition of DMSO (100 µL). Absorbance was measured at 570 nm using a microplate reader (Synergy™ MX, BioTek Instruments, Luzern, Switzerland). Untreated cells were considered as control representing 100% viability.

2.5. Visualization of cellular uptake studies using confocal microscopy

To visualize the cellular uptake of iontosomes, the cells were seeded on glass coverslips in twelve well plates (10^5 cells/well). After incubating the cells for 24 h, the medium was replaced with fluorescent iontosomes and incubated for a further 4 h. After the treatment, cells were washed thrice with PBS and fixed using paraformaldehyde (PFA, 4% w/v) in PBS at room temperature for 15 min. The fixed cells were counterstained with Hoechst 33258 and the coverslips were mounted on glass slides with 60% glycerol a mounting medium. Cells were scanned and images were recorded with a CLSM microscope (Zeiss LSM700, Carl Zeiss Microscopy GmbH, Jena, Germany).

2.6. Mucosal transport studies

2.6.1. Mucosa source

The mucosal transport of iontosomes was evaluated in porcine esophageal mucosa, which has been reported to possess a similar structure and lipid composition as that of buccal mucosa.[13] The porcine esophagus was obtained from a local abattoir (Abattoir de Loëx Sàrl, Bernex, Switzerland) and transported to the laboratory in ice cold Krebs-Ringer bicarbonate buffer (KRB, pH 7.4). Esophagus was longitudinally dissected and rinsed with isotonic saline. The mucosa was separated from the underlying muscular layer with a scalpel. The full-thickness mucosa was cut into 2 cm^2 circular pieces and immediately used for the transport studies.

2.6.2. Iontophoretic transport study

The iontophoretic set-up used for evaluation of the mucosal iotophoresis was similar to that described in our earlier studies.[4, 22] The mucosal tissue was clamped in vertical Franz diffusion cells (diffusion area 0.6 cm^2). After equilibrating the mucosa for 30 min with PBS (pH 7.4), 0.5 ml of free-form drug solutions or drug-loaded iontosomes were placed in the donor compartment. The receiver compartment was filled with 4.5 mL of PBS containing 0.1% Tween 80. The positive electrode (anode) was connected to the donor compartment via a salt bridge assembly (3% agarose with 100 mM NaCl), while the receptor compartment contained the negative electrode (cathode). Constant current (0.5 mA/cm^2) was applied using Ag/AgCl electrodes connected to a power supply (Kepco® APH 1000 M, Flushing, NY). After iontophoresis for either 10 or 20 min, a 1 mL aliquot was withdrawn from the receptor compartment to quantify the amount of drug permeated across the mucosa. Passive permeation experiments using a similar set-up but without current application served as controls. The deposited amounts of DTX and CDDP were extracted by cutting the mucosa samples into small pieces and soaking in 10 mL of extraction media for 12 h. DTX was extracted using a 30:70 mixture of ammonium acetate (5 mM) and methanol; CDDP was extracted using the PBS (pH 7.4) containing 1 % (w/v) Triton X-100 at 45°C. The extraction methods were validated by spiking mucosa samples with known amounts of drugs. The extracts were filtered using 0.22 µm PTFE filters (Simplepure-PTFE, BGB Analytik SA) and processed for HPLC-UV analysis as described in the **Supporting Information**.

2.6.3. CLSM microscopy

The mucosal transport of iontosomes was also visualized using confocal microscopy to determine the penetration pathways for such carrier systems in the oral mucosa. For this, the iontophoretic transport study was performed using the fluorescent iontosomes as described above. At the end of the experiment, the mucosa was washed under running tap water and fixed using 4% PFA in PBS. Transverse sections (10–20 µm thick) of the PFA-fixed tissue were obtained using a cryomicrotome (Leica Microsystems GmbH, Nußloch, Germany). The sections were mounted on glass slides, counterstained for nuclei with Hoechst 33258 and scanned using a Zeiss LSM700 microscope (Carl Zeiss Microscopy GmbH; Jena, Germany).

2.7. Statistical analysis

Data were expressed as mean ± SD. Outliers were determined using the Grubbs test. Results were statistically evaluated using Student's t-test. The level of significance was fixed at $\alpha = 0.05$.

3. Results and Discussions

3.1 Preparation and characterization of iontosomes

Liposomes are versatile carriers enabling encapsulation of both lipophilic and hydrophilic drugs, the former are held within the lipid bilayer, while the latter are entrapped inside the aqueous core of the liposomes.[23] Here, we report the successful co-encapsulation of a hydrophilic-lipophilic drug combination (CDDP and DTX) in cationic liposomes. Initially, the liposomes were prepared by the conventional lipid film hydration method, wherein DTX containing lipid film was hydrated with an aqueous solution of CDDP. However, the entrapment of CDDP in these liposomes was inadequate (6.3 ± 0.8 %). The aqueous volume entrapped within such liposomes is generally less than 10% of the total volume; consequently, a large amount of CDDP remained unentrapped in the liposomes.[24] Hence, a modified method was employed to improve CDDP entrapment (**Fig. 1**).

In the modified method, CDDP was first formulated into reverse micelles using an anionic lipid, DPPG. Formation of reverse micelles was driven by the aquation of CDDP, a process involving hydrolysis of the chloride atoms in CDDP and their replacement by water molecules. The aquated CDDP carries two positive charges due to which it instantaneously forms reverse micelles with the DPPG in 30% ethanol.[15] The reverse micelles obtained displayed a Z-average size of 15.6 ± 5.2 nm and exhibited a negative zeta potential of −32.8 ± 8.6 mV (**Fig. 2a** and **2b**). The cryo-TEM images displayed uniformly distributed micelles in a similar size range (**Fig. 2c**). The presence of an electron dense core in the micelles further confirmed that the CDDP had been successfully loaded. The cryo-TEM micrographs also indicated that some of the reverse micelles aggregated into strings and larger particles, which explained the relatively broad size distribution observed during DLS measurements (**Fig. 2a**). The rationale for using anionic CDDP-DPPG reverse micelles was that they could provide higher CDDP loading in the liposomes via electrostatic interaction with the cationic lipid film.

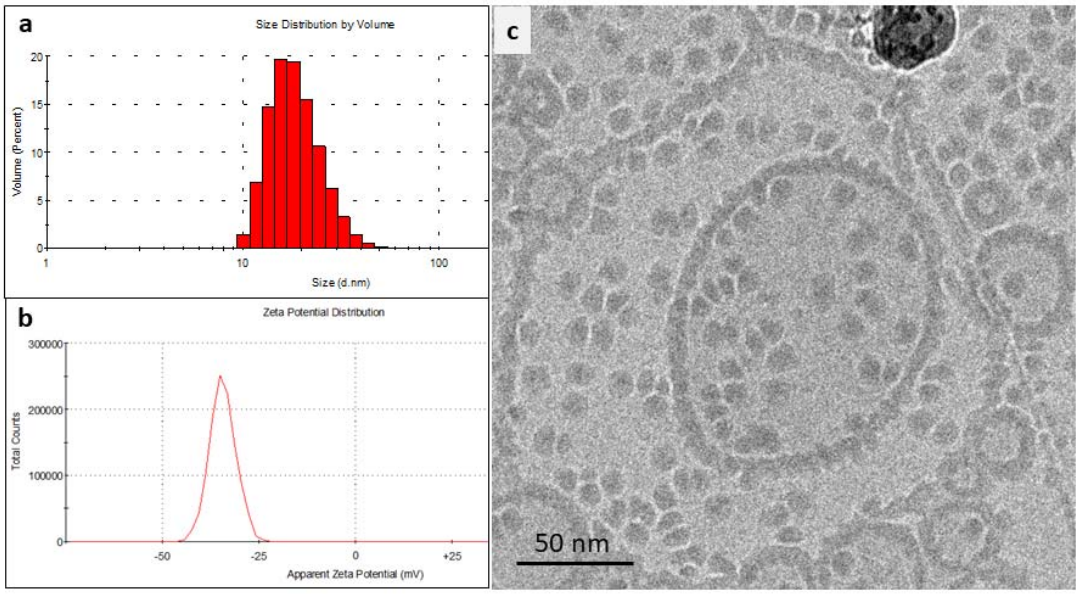

Figure 2. [a] The particle size distribution, [b] zeta potential distribution and [c] the cryo-TEM images of the formulated CDDP-DPPG reverse micelles.

In the next step, the DTX-loaded cationic lipid film was hydrated with the CDDP-DPPG reverse micelles to obtain the iontosomes. A series of formulations were prepared by adding varying volumes of the reverse micelles (Table 1). As shown, the formulated iontosomes displayed similar Z-average diameters with positive zeta potential. The cationic zeta potential was provided by DOTAP as it carries a positively charged head group. Increasing the volume of CDDP-DPPG reverse micelles added from 2.5 mL to 10 mL lowered the zeta potential of formulated iontosomes from 42.3 ± 4.6 mV to 8.6 ± 2.4 mV, indicating the neutralization of cationic charge on lipid bilayers by the anionic reverse micelles.

As expected, the addition of reverse micelles also increased the amount CDDP entrapped in the iontosomes, as indicated by the ratio of CDDP:DTX content in the iontosomes (**Table 1**). The content ratio increased linearly from 0.7 in Lip-2 to 2.7 in Lip-4 when the volume of reverse micelles was increased from 2.5 mL to 10 mL. However, this adversely affected the content and EE of DTX, especially in Lip-4. It is possible that some of the reverse micelles were also incorporated in the lipid bilayer of the iontosomes, displacing DTX from the lipid bilayer. Lip-3 with a CDDP:DTX content ratio of 1.28 was selected for further studies due to the positive zeta potential it offered with a relatively high EE for both drugs. In addition, the CDDP:DTX ratio was similar to that of the clinical doses of these drugs when used in combination chemotherapy of head and neck cancers.[25, 26] The combination

regimen with similar dose ratio (75–100 mg/kg CDDP with 75 mg/kg DTX) has been shown to offer higher tumor response and survival rates relative to the standard regimen of CDDP/5-FU in treatment of recurrent head and neck cancer. The selected formulation had a mean diameter of 109.8 ± 12.4 nm with a polydispersity index (PDI) of around 0.25 and displayed a positive zeta potential of 37.3 ± 1.9 mV. The CDDP and DTX contents in the selected formulation were 0.84 ± 0.05 mg/mL and 0.66 ± 0.03 mg/mL, respectively.

3.2 Cryo-TEM analysis of the co-encapsulated iontosomes

The cryo-TEM micrographs clearly demonstrate the structural differences between the conventional liposomes and the iontosomes (**Fig. 3**). The conventional DOTAP/Lipoid-S75 liposomes prepared without CDDP-DPPG reverse micelles were predominantly spherical and unilamellar (**Fig. 3a**). On the other hand, majority of the iontosomes had bilamellar structures (**Figs. 3b** and **3c**). This was expected, as the liposomes with highly flexible lipid bilayers are known to undergo vesicle deformation and bilayer invaginations. The otherwise rigid DOTAP/Lipoid-S75 bilayers were made flexible by the small amount of ethanol present in the CDDP-DPPG reverse micelles. Ethanol is known to cause membrane fusion and interdigitation in the phosphatidylcholine based bilayers leading to the formation highly deformable liposomes (ethosomes).[27, 28] However, unlike the previously reported ethosomes, the formulated iontosomes were uniform in size, shape and lamellarity. This can be explained by the electrostatic interactions between the cationic lipid bilayer and anionic reverse micelles in the iontosomes. It is possible that the anionic reverse micelles were sandwiched between multiple cationic vesicles during the hydration step. The extrusion process then causes the inversion of larger vesicles and results in complete invagination of the smaller vesicle with the sandwiched reverse micelles leading to the formation of bilamellar vesicles. A similar mechanism has been reported for the DOTAP liposomes encapsulating DNA.[29] Some of the iontosomes also showed interlamellar attachments (indicated by white arrows) resulting in semi-toroidal structures. These structures are the intermediates formed during the process of membrane fusion and are commonly observed during the formation of bilamellar vesicles.[30] The mean size of all formulations was in the range 100 – 125 nm which was in good agreement with the DLS data (Table 1).

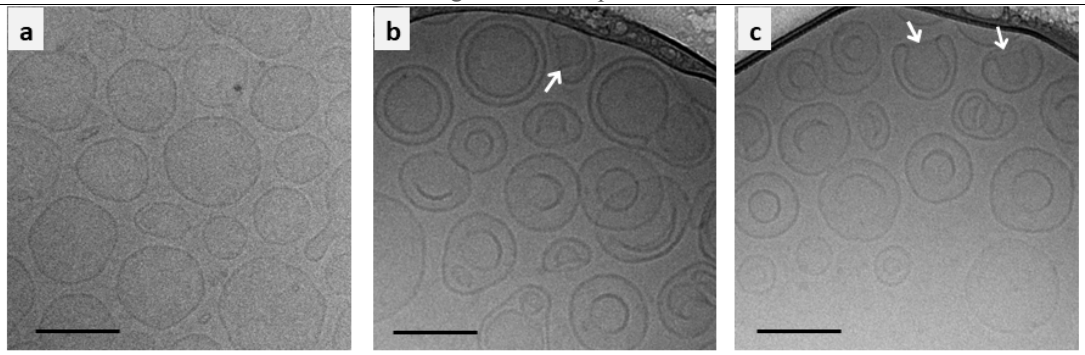

Figure 3. The cryo-TEM images of [a] the conventional liposomes and [b,c] the iontosomes co-encapsulating cisplatin and docetaxel. The scale bars represent 100 nm. The white arrows indicate the interlamellar attachments, a defect commonly observed during the formation of bilamellar vesicles.

3.3. Iontophoretic stability and in vitro drug release

The iontosomes containing co-encapsulated CDDP and DTX were examined for their ability to undergo shape deformation under the iontophoretic conditions (0.5 mA/cm^2 for 20 min). The cryo-TEM micrographs clearly show the shape deformation of iontosomes after the iontophoretic treatment (**Fig. 4**). The untreated iontosomes had a spherical bilamellar structure before being exposed to the electric current (**Fig. 4a**). However, after iontophoresis, most of the iontosomes had an elongated shape (**Fig. 4b**). We postulated that this shape deformation was due to the differences in the charge distribution within the iontosomes. During anodal iontophoresis (as used in this case), the positively charged molecules electromigrate from the electrode compartment towards the adjoining membrane, simultaneously the anionic species are attracted towards the anode.[5] Therefore, when the iontosomes are exposed to the electric current, the cationic lipids electromigrate towards the receiver compartment; whereas, the anionic micelles are attracted to the electrode. The opposing movements of components within the same vesicle possibly results in the elongation of the flexible iontosomes.

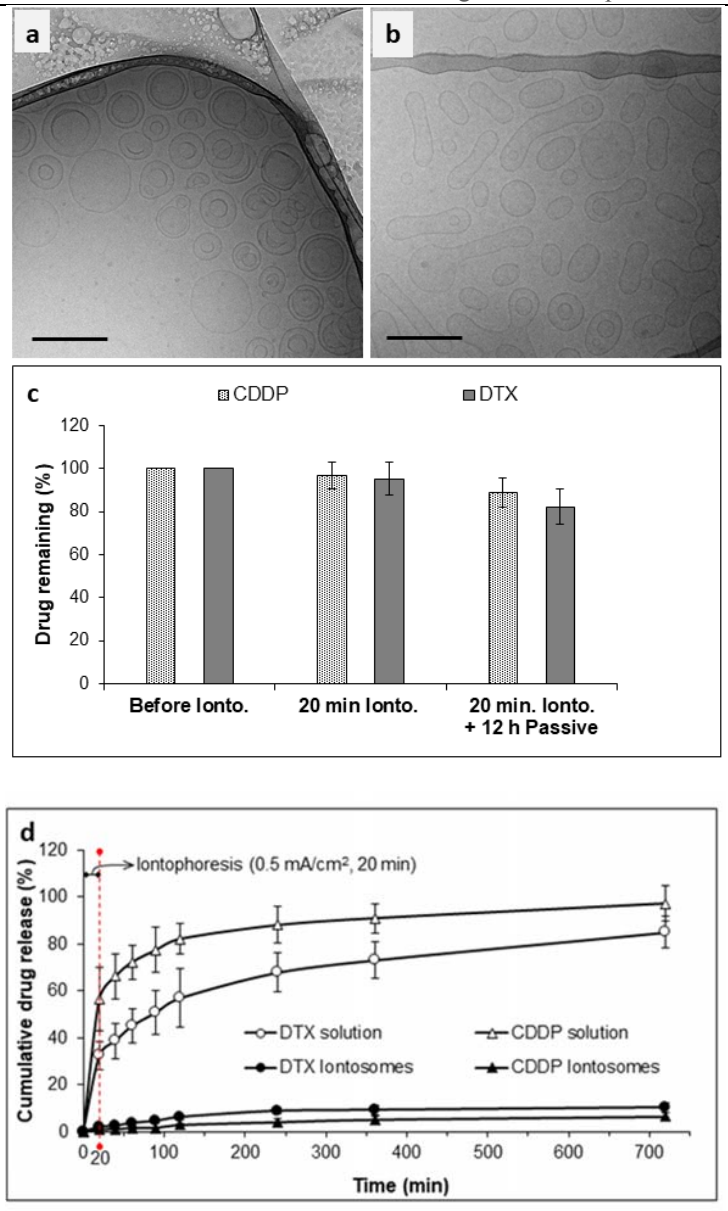

Figure 4. Effects of iontophoresis on the stability of iontosomes; [a,b] the cryo-TEM images (scale bars represent 100 nm), [c] drug contents and [d] in vitro release behavior of the iontosomes before and after iontophoresis.

The cryo-TEM images indicated that the diameters of the elongated iontosomes were between 40 to 50 nm. However, the DLS results indicated that the mean particle sizes and PDI of the test iontosomes slightly increased after the iontophoresis (**Table 2**). This disparity could be due to the elongated shapes of the iontosomes, since the hydrodynamic diameter reported by the DLS is influenced by the shape of particles. It is well-known that DLS measures the Brownian motion of the particles and relates it to

their size.[31] The larger the particle, the slower the Brownian motion; however, this holds true only if the particles are spherical, the diffusion speeds of the rod shaped particle are slower and hence the hydrodynamic sizes calculated by DLS were higher.

Table 2. Effect of iontophoresis on the characteristics of formulated iontosomes.

Condition	Particle size (nm)	PDI	Zeta Pot. (mV)
Before ionto.	109.8 ± 12.4	0.25	42.3 ± 4.6
10 min ionto.	125.8 ± 24.5	0.29	40.3 ± 7.2
20 min.ionto.	139.8 ± 27.4	0.37	41.7 ± 5.5

Next, the ability of iontosomes to retain the loaded drugs under the iontophoretic conditions was evaluated (**Fig. 4c**). The amounts of CDDP and DTX remaining in the formulation after iontophoresis (0.5 mA/cm^2 for 20 min) were similar to those observed in the untreated iontosomes. DOTAP is known to improve the physical stability of phosphatidylcholine based liposomes by increasing lipid bilayer fluidity, thereby efficiently retaining the bulky hydrophobic drugs such as DTX in the lipid domains of the liposomes.[32] Similarly, the electrostatic attraction between cationic lipid bilayer and anionic CDDP-DPPG reverse micelles helped in retaining CDDP inside the liposomes during the 20 min iontophoresis. Further, only small amounts of DTX and CDDP were released from the formulations during the subsequent *in vitro* release study.

After the iontophoretic treatment, the *in vitro* release behavior of the iontosomes was evaluated for 12 h. The CDDP and DTX solutions were used as controls to confirm that the experimental set up did not hinder the diffusion of drugs across the selected dialysis membrane. As expected, the solution formulations of both CDDP and DTX easily diffused across the dialysis membrane into the receiver chamber of Franz diffusion cells, releasing over 50% of the drug content within 2 h. Faster release of CDDP could be attributed to its smaller size and cationic charge, which enables its iontophoretic transport during the initial 20 min. In contrast, sustained release was observed from the co-encapsulated iontosomes. The cumulative amounts of CDDP and DTX released into receiver chambers after 12 h were 6.7 ±1.7 % and 10.4 ± 1.9%, respectively. These findings clearly demonstrated the potential of the iontosomes as carriers to enable the sustained release of chemotherapeutics into cancerous tissue.

3.4. Evaluation of cytotoxic activity in vitro

In order to verify that the DTX and CDDP co-encapsulated in iontosomes still retained their bioactivity, cytotoxicity assays were performed *in vitro* using HeLa cells. The solution formulations of DTX and CDDP were used as the reference. Before incubation with HeLa cells, the formulations were sterilized by aseptic filtration to exclude the possibility of any contamination. The formulations were diluted to achieve predetermined DTX and CDDP concentrations between 0.5-10 μg/mL. Figure 6a shows the effect of the co-encapsulated iontosomes, DTX solution and CDDP solution at equivalent drug concentrations on cell viability *in vitro*. The percentage of viable cells was quantitatively assessed via the MTT assay, a widely used method for determination of cytotoxicity. The results indicated that the blank iontosomes were non-toxic to the cells as no significant cytotoxicity was observed even at the highest iontosome concentration. The HeLa cells appeared less sensitive to the CDDP in comparison to DTX, even at the highest CDDP concentration tested (34.4 nmol/mL) over 85% cells were still viable. On the other hand, formulations containing DTX exhibited a dose dependent cytotoxicity on HeLa cells. In addition, the drug-loaded iontosomes exhibited a slightly better cytotoxicity than the free-form DTX or its combination with the CDDP.

Fig. 5b shows the confocal imaging demonstrating cellular uptake of fluorescent iontosomes. The images showed that the iontosomes were successfully internalized by the HeLa cells and were transported to the nuclei (white arrows). Some of the iontosomes also appeared to adhere to the cell surfaces due to their cationic zeta potential. These results clearly indicated that the formulated iontosomes retained the chemotherapeutic potential of DTX and CDDP.

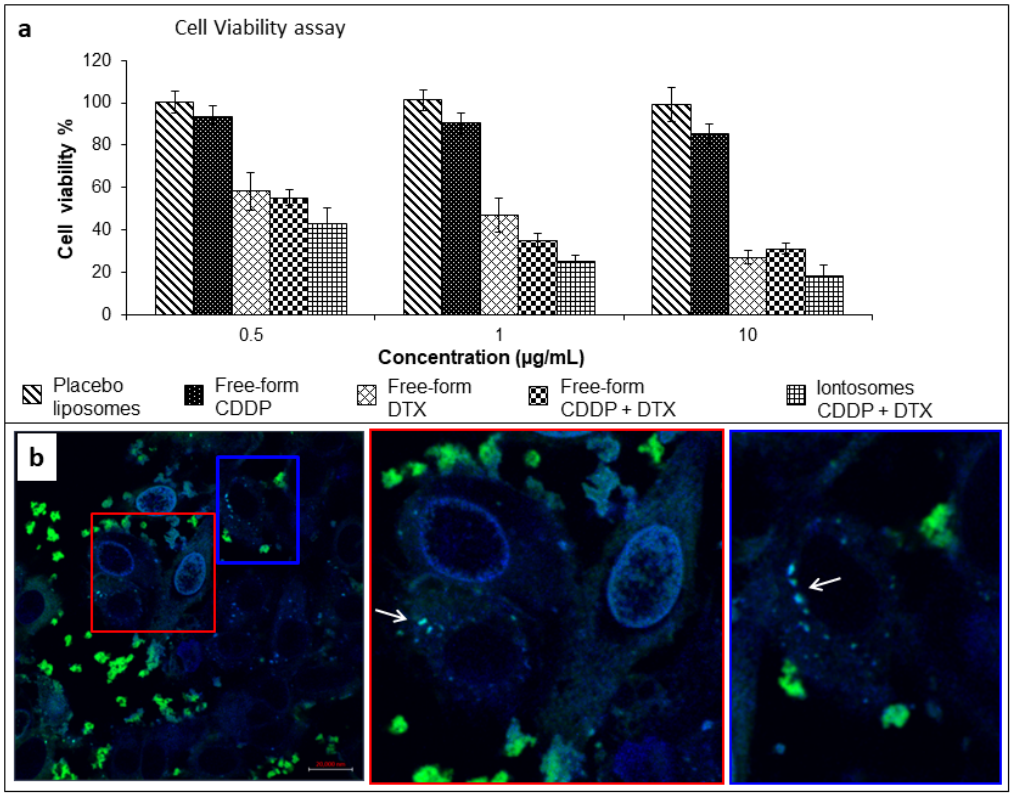

Figure 5. [a] Viability of HeLa cells incubated with placebo iontosomes, free-form cisplatin (CDDP), free-form docetaxel (DTX), their combinations in solution formulation or co-encapsulated iontosomes. The CDDP and DTX concentrations used in solution formulations were similar to those observed in the iontosomes; the DTX concentration ranged from 0.01 to 10 µg/ml, the corresponding CDDP concentrations were 0.013 to 12.8 µg/ml. Cell viability was determined by the MTT assay. Untreated cells were used as controls. The results are expressed as mean ± standard deviation of 5 measurements. [b] Confocal images showing the adhesion and uptake of fluorescent iontosomes by HeLa cells. The white arrows in the magnified views show the transport of iontosomes to the nuclei of the cells.

3.6. Buccal delivery of iontosomes

Porcine buccal mucosa is generally considered to be a good model to predict permeation in human oral mucosa.[4, 13] However, limited availability of this tissue prompted the use of porcine esophageal mucosa, which has been shown to possess similar structure, composition and barrier properties to the buccal tissue.[33] Furthermore, the permeabilities of small molecule drugs such as carbamazepine and fentanyl citrate across the two epithelial barriers were reported to be comparable.[13, 34] Hence, the

iontophoretic buccal delivery of the CDDP and DTX formulated in iontosomes was tested using porcine esophageal mucosa and solution formulations of CDDP and DTX containing equivalent concentrations were used as reference.

The passive delivery of CDDP and DTX solutions or co-encapsulated iontosomes for 10 or 20 min resulted in receiver concentrations that were below the detection limit.. Furthermore, the results indicated that only the CDDP in solution form permeated (0.92 ± 0.13 μg/cm^2) across the mucosal tissue following iontophoresis (0.5 mA/cm^2, 20 min).

The amounts of each drug deposited in the mucosa are shown in **Fig. 6**. After passive delivery for 10 or 20 min, ~2–4 μg/cm^2 of free-form CDDP was deposited in the mucosa (**Fig. 6a**). Application of an electric current resulted in a 4.5- and 3.4-fold increase in its deposition after application for 10 and 20 min, respectively. In contrast to the CDDP solution, the passive delivery or iontophoresis of DTX solution resulted in negligible mucosal deposition (**Fig. 6b**). As described earlier, CDDP is positively charged under physiologic conditions due to the aquation process, which favors its anodal iontophoretic delivery. DTX being a large molecule does not penetrate the mucosa easily in such short time periods.

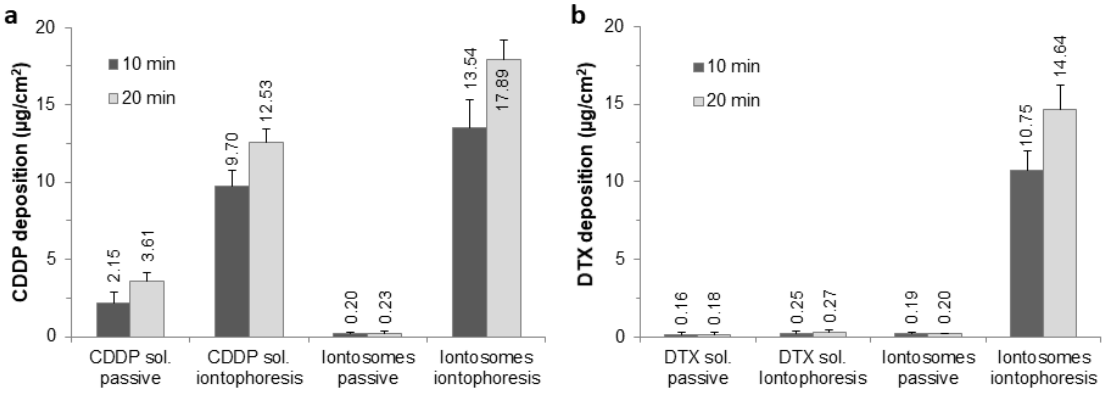

Figure 6. Mucosal deposition of [a] CDDP and [b] DTX following passive diffusion or co-iontophoresis (at 0.5 mA/cm2) for either 10 or 20 min using their aqueous solutions (at pH 7.0) or co-encapsulated iontosomes. The CDDP and DTX concentrations were 0.84 and 0.66 mg/mL, respectively. The results are expressed as mean ± standard deviation of 4 measurements.

The deposition of CDDP and DTX loaded in the iontosomes was also compared following passive and iontophoretic delivery for 10 and 20 min. The mucosal deposition of both drugs after the iontophoretic delivery of iontosomes was significantly higher in comparison to the passive delivery of the same formulation. Iontophoretic delivery for 10 and 20 min lead to 68- and 77-fold increases in the deposited amounts of CDDP, respectively. Similarly, for DTX, the improvements in deposition following

iontophoresis for similar 10 and 20 min duration were 55- and 75-fold, respectively. Interestingly, the CDDP:DTX deposition ratios (1.26 and 1.22) after the iontophoretic delivery of iontosomes were similar to their initial content ratio (1.28), suggesting that the deposited CDDP and DTX were still associated with iontosomes and the iontosomes remained intact during the transport. The disintegration of iontosomes and/or release of loaded drugs during the iontophoretic transport would have led to a reduced deposition of DTX or improved deposition of CDDP as seen during the iontophoretic transport of their solution formulations. To demonstrate the therapeutic relevance of local iontosomal delivery in oral cancers, the CDDP and DTX amounts deposited in the mucosa samples were converted into the approximate tissue levels in μM (Table 3). These levels were found to be higher by multiple orders of magnitude than the reported IC_{50} values for CDDP (670 nM) and DTX (70 nM) in TE-2 cells, a human esophageal squamous cell carcinoma cell line. Unfortunately, it was not possible to make a similar extrapolation for intratumoral levels of CDDP and DTX, to our knowledge, there are no available data on the intratumoral levels of these drugs.

Table 3. Therapeutic relevance of the CDDP and DTX amounts deposited in the mucosa.

Drug	Iontophoresis duration	Deposition ($\mu g/cm^2$)	Approx. mucosal conc. (μM)*	X-fold higher than IC_{50}
CDDP	10 min	13.5 ± 1.8	835.8 ± 109.7	1247.45
	20 min	17.9 ± 1.3	1104.6 ± 079.1	1648.62
DTX	10 min	10.8 ± 1.3	246.5 ± 028.7	3521.10
	20 min	14.6 ± 1.5	335.6 ± 035.3	4794.55

*These amounts were calculated by considering that the mucosa samples had an average thickness of ~0.9 mm and that the area was 0.6 cm^2, meaning the mucosal volume was 0.054 cm^3.

3.7. Visualization of mucosal transport of iontosomes

The incorporation of fluorescent Lipoid-S75 in iontosomes allowed their visualization during iontophoretic transport across the mucosal tissue using the CLSM. Confocal images of mucosa treated with the fluorescent iontosomes for different durations (**Fig. 7**), show that at a macroscopic level, iontophoresis led to a yellowish staining of mucosal surfaces with fluorescent iontosomes as compared to passive delivery. This was more pronounced with increased duration of iontophoresis indicating that more iontosomes were adhering to mucosal surfaces(**Fig. 7a**, upper panels). The iontosomes also appeared to accumulate at certain dense spots on the mucosa following iontophoresis for 20 min (**Fig.**

7a, white arrows). These spots were possibly the low resistance regions in the mucosa that allowed enhanced passage of charged species during iontophoresis. In the case of transdermal iontophoresis, the charged species follow an appendageal pathway through the sweat glands and/or pilosebaceous units as the diffusional resistance of the skin is lowest in such regions.[35] However, experiments with cell-culture based living skin equivalents have pointed that these appendages are not essential for the successful iontophoresis.[36] Furthermore, it also suggested that transient pores may be created through lipid reorganization by the applied electric field.[37, 38] Transdermal iontophoretic transport of several compounds has been shown to occur through the intercellular route, it was claimed that the application of electrical current makes the stratum corneum lipid lamellae more accessible to water and ions. We hypothesized that, the iontosomes also enter the epithelium through intercellular pathways owing to their flexible structures. To confirm this, transverse section of the mucosa samples were observed using the CLSM (**Fig. 7a**, lower panels).

After the passive treatment, most of the iontosomes were present on the mucosal surfaces. In contrast, iontophoresis led to a visually significant improvement in mucosal penetration of iontosomes. Magnified sections of the confocal images clearly indicated that the major pathway for penetration of iontosomes was through the intercellular spaces. As discussed earlier, these intercellular spaces are known to be narrower than 20 nm; hence, without iontophoresis the iontosomes remain on the surface of the mucosa. However, during iontophoresis, the iontosomes undergo shape deformation and are carried into the mucosa due to their cationic surface charge. The penetration depths appeared similar for either 10 or 20 min iontophoresis (~40-50 μm). This was surprising, so an additional study was performed with longer duration iontophoresis (120 min) (**Fig. 7b**). The macroscopic examination indicated that the number of dense spots was increased. Similar activation of low resistance pores has been shown to occur during the transdermal iontophoresis in hairless mice, it was shown that the spatial density of current-carrying pores increased from 0 to 100–600 pores/cm^2 during the first 30–60 min of iontophoresis.[39] Our findings suggested that the buccal mucosa behaved to skin and that iontophoresis created low resistance pores that resulted in the accumulation of iontosomes as spots on the epithelial surfaces. The confocal images of transverse section through these spots displayed the penetration of iontosomes through the epithelium and into the submucosa. Overall, the results pointed that the permeation depths of the iontosomes can be controlled by varying the duration of the iontophoresis.

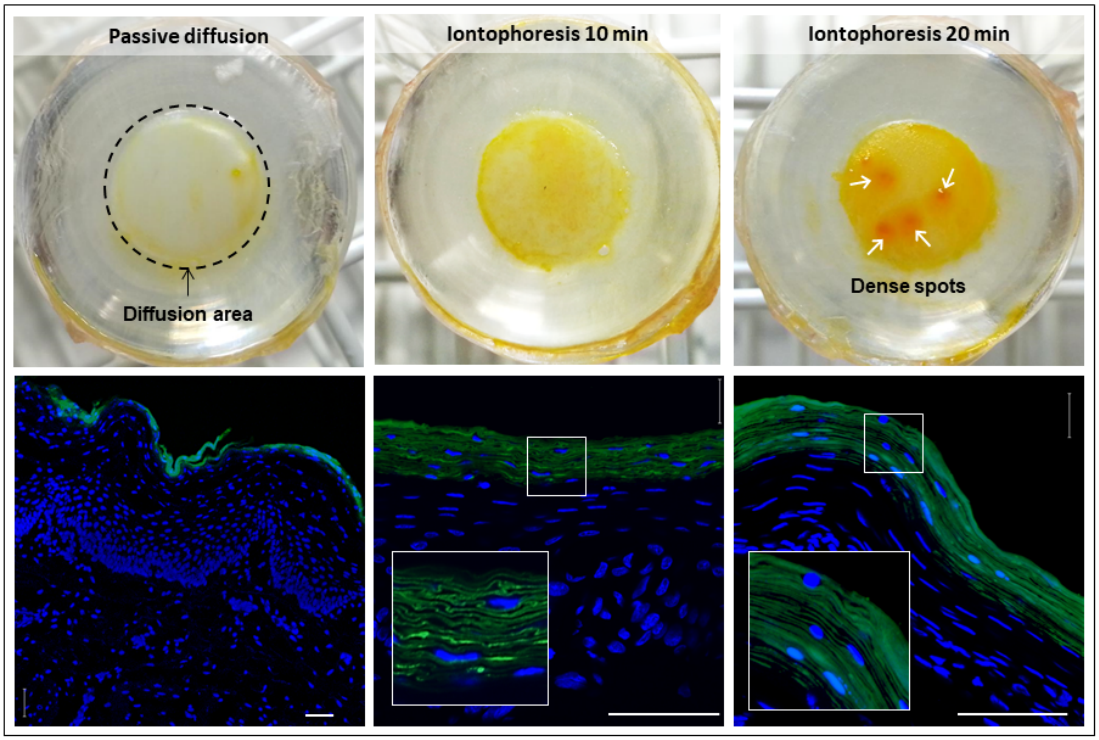

Figure 7. [a] The photographs and confocal images showing the deposition and mucosal transport of iontosomes following passive (20 min) or iontophoretic delivery (10 or 20 min). The insets show the magnified views of the white squares in respective images. The formation of dense spots (white arrows) due to accumulation of iontosomes can be clearly seen after iontophoresis for 20 min

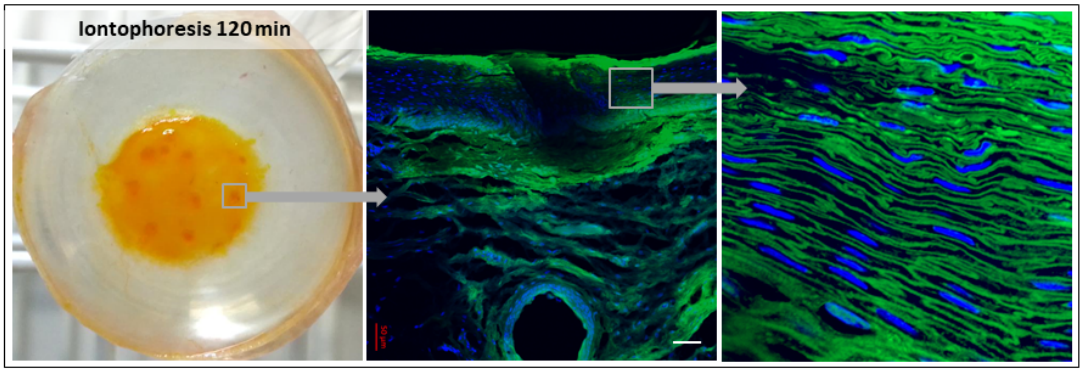

Figure 7 [b] The mucosal transport of iontosomes after iontophoretic delivery for 120 min. A transverse section through the dense spot (confocal images) show the iontosomes can be penetrate into the deeper layers of mucosa through intercellular spaces.

4. Conclusions

The formulated iontosomes were suitable for co-encapsulating CDDP and DTX at high entrapment efficiencies. The iontosomes carried a cationic surface charge with flexible lipid bilayers; however these properties were not sufficient for their spontaneous penetration in the mucosa. Application of iontophoresis led to shape deformation of iontosomes and significantly enhanced their mucosal penetration through the intercellular spaces between epithelial cells. In conclusion, the combination of iontosomes with electrical delivery appears promising for delivering multiple chemotherapeutics selectively to the oral cancers without increasing their systemic absorption and associated risk of side-effects.

5. Supplementary information

5.1 Validation of HPLC-UV method for quantification of DTX in mucosa samples

5.1.1 Specificity

The method was specific for DTX quantitative analysis at 227 nm. DTX was eluted at 9.3 ± 0.3 min. Fig SI1 presents the chromatogram for mucosa matrix, DTX extraction solvent (70:30 mix of methanol and ammonium acetate) and DTX 10 µg/mL standard. DTX stock solution (1 mg/mL) was prepared in methanol and further diluted in the extraction solvent to prepare working solutions. The volume of injection was 50 µL.

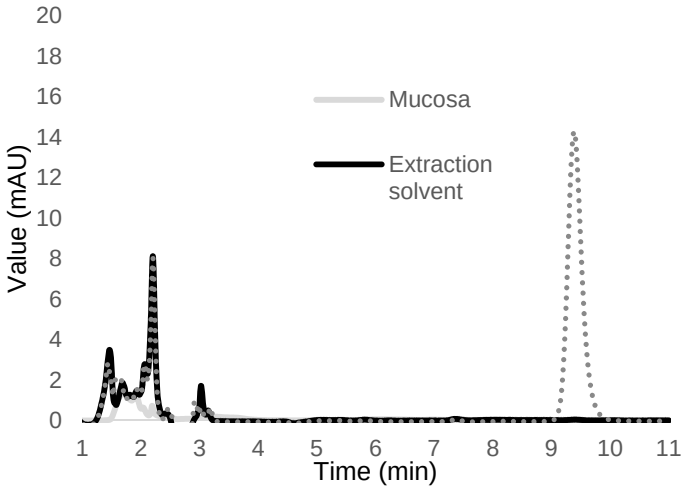

Figure SI1: Chromatograms of mucosa, extraction solvent and DTX standard (10 µg/mL)

5.1.2 Limit of detection and limit of quantification

The lower limit of detection (LOD) and limit of quantification (LOQ) were 0.05 µg/mL and 0.2 µg/mL.

5.1.3 Linearity

The method was linear in the concentration range of 0.2 – 20 µg/mL with a R^2 of 0.99.

5.1.4 Accuracy and precision

Intra- and inter-day accuracy and precision were calculated using 0.5, 1 and 10 µg/mL standard solutions. Table SI1 shows the intra- and inter-day accuracy and precision values for DTX quantification method.

Table SI1: Intra- and interday accuracy and precision values for DTX quantification method

	Intra day			**Inter day 1**			**Inter day 2**		
$[DTX]_{theo}$ (µg/mL)	$[DTX]_{mean}$ (µg/mL)	RSD (%)	Recovery (%)	$[DTX]_{mean}$ (µg/mL)	RSD (%)	Recovery (%)	$[DTX]_{mean}$ (µg/mL)	RSD (%)	Recovery (%)
0.5	0.48 ± 0.00	1.18	96.79	0.46 ± 0.00	2.4	93.42	0.51 ± 0.01	2.34	98.64
1	1.02 ± 0.10	0.66	102.4	0.97 ± 0.01	1.15	97.27	0.92 ± 0.01	1.07	92.8
10	9.95 ± 0.06	1.18	99.51	10.0 ± 0.04	0.53	100.17	10.1 ± 0.21	2.08	101.2

The method was accurate and precise according to the validation guidelines [1].

5.2 Validation of HPLC-UV method for the quantification of CDDP in mucosa samples

5.2.1 Derivatization of CDDP

Due to the low molar absorptivity of CDDP alone, indirect measurement of CDDP was performed via derivatization using diethyldithiocarbamate (DDTC). Aqueous CDDP readily reacts with the sulphur groups in DDTC to form the derivative DDTC-CDDP (Figure SI2)

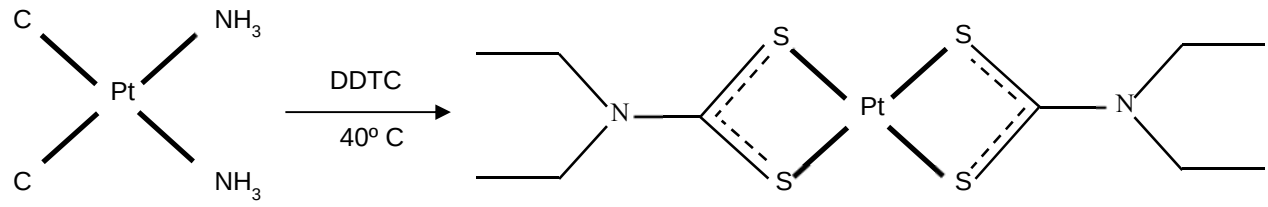

Figure SI2 : Formation of the derivative of CDDP with DDTC to form CDDP-DDTC

Briefly, the extracted samples were centrifuged at 10,000 rpm for 15 minutes to separate the mucosa matrix. The supernatant was collected. After the addition of appropriate amount of 1% w/v DDTC in 0.1M NaOH, the mix was incubated at 40 degrees for 30 mins. The mix was then centrifuged at 10,000 rpm for 15 minutes. The supernatant was separated and reconstituted with acetonitrile. The sample was ready to be injected in HPLC-UV.

5.2.2 Specificity

The method was specific for CDDP-DDTC quantitative analysis at 254 nm. CDDP-DDTC was eluted at 7.0 ± 0.2 min. Fig SI3 presents the chromatogram for mucosa matrix, CDDP-DDTC 12.5 µg/mL standard and only DDTC. CDDP-DDTC stock solution (1 mg/mL) was prepared in dimethylsulfoxide (DMSO) and further diluted acetonitrile to prepare working solutions. The volume of injection was 50 µL.

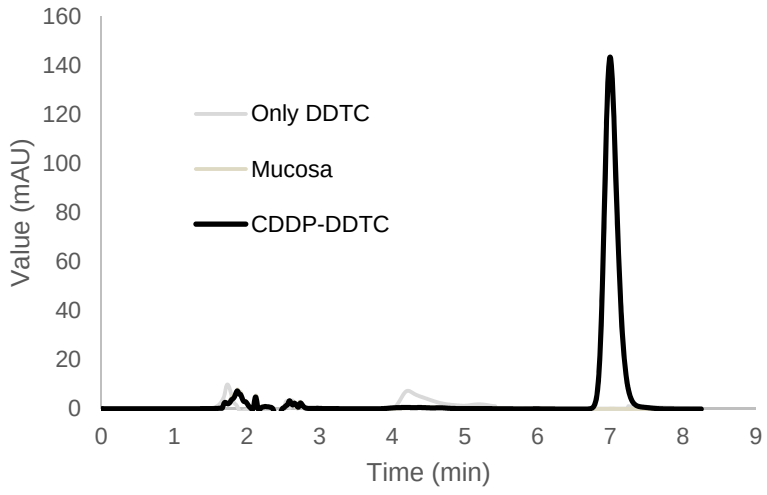

Figure SI3: Chromatograms of mucosa, DDTC alone, complex CDDP-DDTC standard (12.5 µg/mL)

5.2.3 Limit of detection and limit of quantification

The lower limit of detection (LOD) and limit of quantification (LOQ) were 0.05 µg/mL and 0.3 µg/mL.

5.2.4 Linearity

The method was linear in the concentration range of 0.3 – 25 µg/mL with a R^2 of 1.

5.2.5 Accuracy and precision

Intra- and inter-day accuracy and precision were calculated using 1.5, 6.25 and 12.5 µg/mL standard solutions. Table SI2 shows the intra- and inter-day accuracy and precision values for CDDP-DDTC quantification method.

Table SI2: Intra- and interday accuracy and precision values for CDDP-DDTC quantification method.

	Intra day			**Inter day 1**			**Inter day 2**		
[CDDP-DDTC]$_{theo}$ (µg/mL)	[CDDP-DDTC]$_{mean}$ (µg/mL)	RSD (%)	Recovery (%)	[CDDP-DDTC]$_{mean}$ (µg/mL)	RSD (%)	Recovery (%)	[CDDP-DDTC]$_{mean}$ (µg/mL)	RSD (%)	Recovery (%)
1.5	1.48 ± 0.01	0.58	95.46	1.43 ± 0.00	0.17	91.95	1.41 ± 0.01	0.72	90.74
6.25	6.30 ± 0.08	1.21	100.76	6.30 ± 0.00	0.1	101.04	6.45 ± 0.00	0.12	103.44
12.5	12.5 ± 0.21	1.28	100.61	12.9 ± 0.01	0.15	103.66	12.4 ± 0.05	0.42	99.94

The method was accurate and precise according to the ICH validation guidelines

6. Acknowledgment

KS thanks the University of Geneva and the Swiss Commission for Technology Innovation for financial support (CTI 13933.2). VT is grateful to the Swiss Federal Commission of Scholarships for Foreign Students for the award of a PhD studentship. We thank Dr. Davide Demurtas, Interdisciplinary Centre for Electron Microscopy, EPFL for assistance in Cryo-TEM characterization. We also acknowledge the UNIGE Bioimaging platform for access to the confocal imaging facilities.

7. References

1. Neville B. W. and Day T. A. Oral cancer and precancerous lesions. *Ca-Cancer J. Clin.* **2002** *52(4)*: 195-215.

2. Haddad R. I. and Shin D. M. Recent advances in head and neck cancer. *N. Engl. J. Med.* **2008** *359(11)*: 1143-54.

3. Senel S. and Hincal A. A. Drug permeation enhancement via buccal route: possibilities and limitations. *J. Control. Release.* **2001** *72(1-3)*: 133-44.

4. Gratieri T. and Kalia Y. N. Targeted local simultaneous iontophoresis of chemotherapeutics for topical therapy of head and neck cancers. *Int. J. Pharm. (Amsterdam, Neth.).* **2014** *460(1-2)*: 24-7.

5. Kalia Y. N., Naik A. *et al.* Iontophoretic drug delivery. *Adv. Drug Deliv. Rev.* **2004** *56(5)*: 619-658.

6. Landay M. A. and Schroeder H. E. Differentiation in normal human buccal mucosa epithelium. *J. Anat.* **1979** *128(Pt 1)*: 31-51.

7. Harris D. and Robinson J. R. Drug delivery via the mucous membranes of the oral cavity. *J. Pharm. Sci. (Philadelphia, PA, U. S.).* **1992** *81(1)*: 1-10.

8. Swartzendruber D. C., Manganaro A. *et al.* Organization of the intercellular spaces of porcine epidermal and palatal stratum corneum: a quantitative study employing ruthenium tetroxide. *Cell Tissue Res.* **1995** *279(2)*: 271-6.

9. Benson H. A. Transfersomes for transdermal drug delivery. *Expert Opin. Drug Deliv.* **2006** *3(6)*: 727-37.

10. Schreier H. and Bouwstra J. Liposomes and niosomes as topical drug carriers: dermal and transdermal drug delivery. *J. Control. Release.* **1994** *30(1)*: 1-15.

11. Muzzalupo R., Tavano L. *et al.* A new approach for the evaluation of niosomes as effective transdermal drug delivery systems. *Eur. J. Pharm. Biopharm.* **2011** *79(1)*: 28-35.

12. Dubey V., Mishra D. *et al.* Dermal and transdermal delivery of an anti-psoriatic agent via ethanolic liposomes. *J. Control. Release.* **2007** *123(2)*: 148-54.

13. Diaz Del Consuelo I., Pizzolato G. P. *et al.* Evaluation of pig esophageal mucosa as a permeability barrier model for buccal tissue. *J. Pharm. Sci. (Philadelphia, PA, U. S.).* **2005** *94(12)*: 2777-88.

14. C. Mundus C. W., O. Schramel, H. Haas, T. Fichert, B.Schulze, T. Peymann, U. Michaelis, M.Teifel, F. Gruber, G. Winter Method of producing a cationic liposomal preparation comprising a lipophilic compound. 2011.

15. Boulikas T. Therapy for human cancers using cisplatin and other drugs or genes encapsulated into liposomes. 2003.

16. Struck D. K. and Pagano R. E. Insertion of fluorescent phospholipids into the plasma membrane of a mammalian cell. *J. Biol. Chem.* **1980** *255(11)*: 5404-10.

17. Meyer O., Roch O. *et al.* Direct lipid quantitation of cationic liposomes by reversed-phase HPLC in lipoplex preparation process. *Eur. J. Pharm. Biopharm.* **2000** *50(3)*: 353-6.

18. Buntrock R. E. The Merck Index: An Encyclopedia of Chemicals, Drugs, and Biologicals, Fourteenth Edition Edited by Maryadele J. O'Neil, Patricia E. Heckelman, Cherie B. Koch, and Kristin J. Roman. Merck & Co., Inc.: Whitehouse Station, New Jersey, 2006. xiv + 1756 pp. + tables and indexes; includes CD and Internet access. ISBN 978-0-911910-00-1. Hardcover. U.S. $125.00. *J. Chem. Inf. Model.* **2007** *47(2)*: 703-704.

19. Berners-Price S. J. and Appleton T. G., The Chemistry of Cisplatin in Aqueous Solution. In *Platinum-Based Drugs in Cancer Therapy*, ed.; Kelland, L. R.; Farrell, N. P., Humana Press, Totowa, NJ, 2000.

20. Karbownik A., Szalek E. *et al.* The physical and chemical stability of cisplatin (Teva) in concentrate and diluted in sodium chloride 0.9%. *Wspolczesna Onkol.* **2012** *16(5)*: 435-9.

21. Bonnaud C., Vanhecke D. *et al.* Spatial SPION Localization in Liposome Membranes. *IEEE Trans. Magn.* **2013** *49(1)*: 166-171.

22. Dubey S. and Kalia Y. N. Understanding the poor iontophoretic transport of lysozyme across the skin: when high charge and high electrophoretic mobility are not enough. *J. Control. Release.* **2014** *183*: 35-42.

23. Allen T. M. and Cullis P. R. Liposomal drug delivery systems: from concept to clinical applications. *Adv. Drug Deliv. Rev.* **2013** *65(1)*: 36-48.

24. Çağdaş M., Sezer A. D. *et al.*, Liposomes as potential drug carrier systems for drug delivery. In *Application of nanotechnology in drug delivery*, ed.; Sezer, A. D., InTech, London, UK, 2014.

25. Glisson B. S., Murphy B. A. *et al.* Phase II Trial of docetaxel and cisplatin combination chemotherapy in patients with squamous cell carcinoma of the head and neck. *J. Clin. Oncol.* **2002** *20(6)*: 1593-9.

26. Schoffski P., Catimel G. *et al.* Docetaxel and cisplatin: an active regimen in patients with locally advanced, recurrent or metastatic squamous cell carcinoma of the head and neck. Results of a phase II study of the EORTC Early Clinical Studies Group. *Annals of oncology : official journal of the European Society for Medical Oncology / ESMO.* **1999** *10(1)*: 119-22.

27. Komatsu H. and Okada S. Ethanol-induced aggregation and fusion of small phosphatidylcholine liposome: participation of interdigitated membrane formation in their processes. *Biochim. Biophys. Acta.* **1995** *1235(2)*: 270-80.

28. Cortesi R., Ravani L. *et al.* Ethosomes for the delivery of anti-HSV-1 molecules: preparation, characterization and in vitro activity. *Die Pharmazie.* **2010** *65(10)*: 743-9.

29. Templeton N. S. and Senzer N. Reversible masking using low-molecular-weight neutral lipids to achieve optimal-targeted delivery. *J. Drug Delivery.* **2012** *2012*: 173465.

30. Carboni M., Falchi A. M. *et al.* Physicochemical, cytotoxic, and dermal release features of a novel cationic liposome nanocarrier. *Adv. Healthcare Mater.* **2013** *2(5)*: 692-701.

31. Bootz A., Vogel V. *et al.* Comparison of scanning electron microscopy, dynamic light scattering and analytical ultracentrifugation for the sizing of poly(butyl cyanoacrylate) nanoparticles. *Eur. J. Pharm. Biopharm.* **2004** *57(2)*: 369-75.

32. Campbell R. B., Balasubramanian S. V. *et al.* Influence of cationic lipids on the stability and membrane properties of paclitaxel-containing liposomes. *J. Pharm. Sci. (Philadelphia, PA, U. S.).* **2001** *90(8)*: 1091-105.

33. Diaz-Del Consuelo I., Jacques Y. *et al.* Comparison of the lipid composition of porcine buccal and esophageal permeability barriers. *Arch. Oral Biol.* **2005** *50(12)*: 981-7.

34. Caon T. and Simoes C. M. Effect of freezing and type of mucosa on ex vivo drug permeability parameters. *AAPS PharmSciTech.* **2011** *12(2)*: 587-92.

35. Alvarez-Roman R., Naik A. *et al.* Visualization of skin penetration using confocal laser scanning microscopy. *Eur. J. Pharm. Biopharm.* **2004** *58(2)*: 301-16.

36. Hager D. F., Mancuso F. A. *et al.* Evaluation of a cultured skin equivalent as a model membrane for iontophoretic transport. *J. Control. Release.* **1994** *30(2)*: 117-123.

37. Gratieri T. and Kalia Y. N. Mathematical models to describe iontophoretic transport in vitro and in vivo and the effect of current application on the skin barrier. *Adv. Drug Deliv. Rev.* **2013** *65(2)*: 315-329.

38. Curdy C., Kalia Y. N. *et al.* Post-iontophoresis recovery of human skin impedance in vivo. *Eur. J. Pharm. Biopharm.* **2002** *53(1)*: 15-21.

39. Scott E. R., Laplaza A. I. *et al.* Transport of Ionic Species in Skin: Contribution of Pores to the Overall Skin Conductance. *Pharm. Res.* **1993** *10(12)*: 1699-1709.

CONFERENCE COMMUNICATION

Conference communications/ oral presentations

Poster presentations

1. **Targeted iontophoretic delivery of buflomedil hydrochloride for oral submucosal fibrosis**
   Vasundhara Tyagi, Sergio Del Rio-Sancho, Yogeshvar N. Kalia
   Swiss Pharma Science Day – Bern (Switzerland), August 2017

2. **Targeted iontophoretic delivery of buflomedil hydrochloride for oral submucosal fibrosis**
   Vasundhara Tyagi, Sergio Del Rio-Sancho, Yogeshvar N. Kalia
   8th APS International PharmSci Conference – Hertfordshire (United Kingdom), September 2017

3. **Buccal iontophoretic delivery of buflomedil hydrochloride for oral submucous fibrosis**
   Vasundhara Tyagi, Sergio Del Rio-Sancho, Yogeshvar N. Kalia
   11th World Meeting on Pharmaceutics, Biopharmaceutics and Pharmaceutical Technology – Granada (Spain), March 2018

Oral presentations

1. **Targeted drug delivery to the buccal mucosa**: ***Development of new techniques and therapeutic strategies***
   Vasundhara Tyagi, Yogeshvar N. Kalia
   La Journée des boursiers d'excellence de la Confédération – Geneva (Switzerland), September 2017

2. **Targeted drug delivery to the buccal mucosa**: ***Development of new techniques and therapeutic strategies***
   Vasundhara Tyagi, Yogeshvar N. Kalia
   PhD day – Geneva (Switzerland), June 2018

ACKNOWLEDGMENTS

Acknowledgments

This thrilling journey was only possible because one fine day Prof. Yogeshvar Kalia decided to write back to an overly enthusiastic master's student. A tale he likes to tell. I will always be grateful to Prof Kalia for this wonderful opportunity and the transformational time I have spent under his guidance. He has been an incredible teacher who always told me where to look but rarely mentioned what to look at.

Many thanks to Dr Valerie Suter for all the insightful discussions and your willingness to travel to Geneva to meet us.

A major highlight of the journey has been to meet all the wonderful people on my way. A huge thank you to all the former and current FAPER and FABIP members I had the opportunity of working and being friends with. I have learned something from each of you that I will forever cherish. Thank you to Kiran sir for your valuable scientific guidance and for lending me that blanket on my first day in Geneva when I was highly ill prepared. Thank you Mayank and Somnath for being wonderful colleagues and loving friends that I call my family now. Thank you Cesar for sharing your exceptional technical knowledge and being a trustworthy friend. I would also like to express my gratitude to Sergio for his patience and his indispensable contribution to this work. To my fantastic ladies club – thank you Julie for proving that language is no barrier to a heartfelt friendship, Francesca for all the chats, smiles and positivity that I direly needed, Marta for being a heart-warming friend, Elinam for understanding my humour when no one else did, Ece for her hugs, Maria S for being the Spanish sunshine and Si for her warmth and quirky sense of humor. I am truly fortunate to have found a true friend in Maria, a brilliant scientist and a loving friend I laugh and cry (and both) with. And to the special one who has looked out for me since day one – Verena, thank you for being you. You have made me a better scientist and a person, I don't know what would I do without you.

Thank you to Naoual, Whitney, Gisela, Jonathan and Yvonne who contributed to this work and to the person I have become today. To the newcomers – Aditya, Laeticia and Phedra I wish you the very best as you embark on this journey.

Thank you to my first friend in Geneva, Nonhlanhla, who just always gets it. To Chandana, Sujata and Ridima for bringing home far from home. Then there are those who are close no matter how far, thank you Rasamrit, Jasmeet, Anjali, Navtha, Vibha, Nikita, Isha and Kashish for always being there even if it meant 3 am on a Tuesday night.

None of this would have been possible without the constant support from my family who have been my rock – Mummy, Papa, Didi and Jij. Thank you didi for bringing the greatest joy of my life – Sasha. When I see her, I know it will all be okay. Thank you for your boundless love, your trust and for making my dreams your own. A huge thank you to the family I chose – Veronique, Olivier, Camille and Paul for the love and consistent encouragement.

Finally to my best friend, my lover, my biggest cheerleader, my confidante – Florian. Words fall short to describe how grateful I am to the universe for you. Thank you for always keeping your promises and loving me – in sickness and in health.